Studies on the enhancement of *Sorghum bicolor* (L.) Moench as a biomass crop through sustainable nutrient management

Reza Ramdan Rivai

2022

Contents

General Introduction

Utilization of sustainable and renewable resources for energy is critical to achieve the sustainable development goals (SDGs) in 2030 (Griggs et al., 2013). As of 2018, renewable energy accounted for approximately 14% of the global primary energy supply (World Bioenergy Association, 2020), and this share is expected to grow further (Morrison, 2007). Bioenergy is a sector of renewable energy that includes municipal waste, industrial waste, solid biofuels, biogases, and liquid biofuels, and it accounts for approximately 67% of the current renewable energy mix (World Bioenergy Association, 2020). Hence, increased production of bioenergy feedstocks would be significant to facilitate the shift to renewable energy, in turn, stimulating the demand for biomass as the feedstock for bioenergy. To meet the ever-increasing demand for biomass energy, the availability of source biomass also needs to be increased. However, the expansion of arable land area is becoming difficult, while the lands remaining available often have marginal status, that is, they have certain limitations, such as low water availability, poor soil fertility, or pollution. Thus, growing stress-tolerant biomass crops in marginal lands would be a plausible option.

Sorghum [*Sorghum bicolor* (L.) Moench] is a multipurpose crop grown for food, feed, and fiber production (Blümmel et al., 2003; Reddy & Yang, 2015; Xiong et al., 2019). Recently, it has received attention as a biomass energy feedstock (Dahlberg, 2019; Wiloso et al., 2020). Potential applications of sorghum in biomass energy production include utilization as feedstock for ethanol production, either as the starch in the seeds of grain sorghum or the sugars accumulated in the stalks of sweet sorghum (Tang et al., 2018; Wang et al., 2008). Bagasse, the plant residue left after extracting the sugars, can also be used as a source of fermentable sugars via saccharification. Another resource obtained from sorghum is lignocellulose biomass. Compared on per area and year basis, the production of lignocellulose biomass by certain types of sorghum can be higher than that of trees (Umezawa, 2018). The lignocellulose biomass of sorghum is a promising material for use in the production of solid fuels, such as biopellets and biochar (Dahlberg, 2019; Ferreira et al., 2019; Wahyuni et al., 2019; Wiloso et al., 2020), and lignocellulose-derived chemicals (Cheng et al., 2020; Kshirsagar et al., 2017). Sorghum is relatively tolerant to environmental stresses and is capable of maintaining yield under unfavorable conditions, such as drought and salinity (Tari et al., 2013). This trait is particularly important given that the availability of arable lands is becoming limited worldwide and the lands remaining are often in marginal status with some sort of obstruction. Hence, growing

sorghum in such marginal lands would be a viable way to secure biomass energy feedstock. It has been actually considered as a candidate crop for the exploitation of currently unused deteriorated lands in Indonesia (Susilowati & Saliem, 2013).

Proper management of nutrient supply is critical in such trials, as sufficient amounts of nutrients need to be provided to achieve good yields, while an excess application of fertilizers can cause environmental problems such as eutrophication and greenhouse gas emission. Since nitrogen (N) significantly affects the plant biomass production, diagnosing the N status of sorghum during its growth would be significant. Therefore, I firstly investigated the changes in several physiological parameters of sorghum in response to N limitation, with the aim of identifying candidates of N status biomarkers in this species. Parameters responding early and sensitively to N deficiency were searched in hydroponically cultured seedlings, and their applicability to field conditions were examined (Chapter 1). In addition, nutrient availability may affect the properties of sorghum biomass, thereby possibly affecting its quality as the feedstock for bioenergy and other purposes. While it is obvious that N supply significantly affects sorghum growth and biomass accumulation, the information is still limited regarding the effect of N on the biomass quality of sorghum, such as the contents and structures of lignin and other cell wall components. Hence, in the Chapter 2, I investigated the effects of N supply on the structure and composition of sorghum cell walls. As a plant nutrient, silicon (Si) may also influence cell wall composition, including lignin content and structure, as both Si and lignin are involved in plant mechanical strength. I then comprehensively analyzed the lignin and other cell wall components of sorghum seedlings cultured hydroponically with or without Si supplementation using chemical, two-dimensional (2D) heteronuclear single quantum coherence (HSQC) nuclear magnetic resonance (NMR), histochemical, gene expression, mechanical properties, and calorific value analyses (Chapter 3). Lastly, the interaction between N and Si and their effect on the quality of sorghum biomass as fodder were also examined (Chapter 4). Overall, this study proved that the nutrient management is an important factor affecting the value of sorghum biomass.

Chapter 1

Search for nitrogen status biomarkers in *Sorghum bicolor*

1.1 Introduction

Nitrogen (N) is required at the highest level among the plant essential elements that are taken up from the soil. Plants take up N in the form of nitrate and ammonium. Although these inorganic N can be provided for plants through a mineralization of soil organic matters, the process is rather slow and cannot meet the amounts required by rapidly growing plants. Hence, application of N fertilizer is essential for agricultural production (Masclaux-Daubresse et al., 2010). This is particularly the case when sorghum as the high-biomass plants are to be grown in marginal lands with less fertile soil. At the same time, however, an excessive application of fertilizers should be avoided, in order to prevent various problems including increased cost, plant toxicity, and environmental pollution (Duan et al., 2019). In general, only approximately 30 - 40% of N applied as the fertilizer is taken up by plants during the season (Raun and Johnson, 1999; Krapp, 2015), and a significant part of the rest can be lost through runoff, leaching, or denitrification. The nitrate leaced into ground water can cause eutrophication. Denitrification leads to the emission of dinitrogen monoxide, a green house gas, into the atmosphere (Savci, 2012).

Thus, it is important to supply plants with necessary and sufficient amounts of N fertilizer but not in excess. Currently, numerous studies have been undertaken to know the exact amounts of the nutrients required in several crops, especially using morphological and physiological parameters such as total N and nitrate content, chlorophyll content, and gene expression analyses (Wiedenfeld et al., 2009; Munoz-Huerta et al., 2013; Ali et al., 2016; Awada, 2016; Singh et al., 2017). Nevertheless, evaluating the internal nutritional status of crop plants during their growth is still not an easy work. Then, it is necessary to found and develop the proper biomarkers which highly reflect the N status with considering several characters include specificity, reproducibility, robustness, effectiveness, and quickly detected.

Therefore, in this chapter, I searched for N status biomarkers in sorghum plants, as a requirement for the development of methods to monitor the N sufficiency of sorghum plants during their growth. Firstly, the biomarker candidates were explored in the controlled environment using hydroponically cultured plants. The promising biomarker candidates indentified were then examined for the usability in the field conditions.

1.2 Materials and Methods

1.2.1 Plant growth condition and treatment using hydroponic culture

Seeds of *Sorghum bicolor* (L.) Moench BTx623 were germinated and grown on vermiculite for a week in the controlled room condition. Seedlings were transferred to the full strength Yoshida B hydroponic culture medium (1 mM KCl, 0.25 mM $(NH_4)_2 HPO_4$, 0.5 mM $MgSO_4$ $7H_2O$, 1 mM $Ca(NO_3)_2$, 0.1 mM Fe(III)-EDTA, 0.5 ppm B, 9 μM $MnCl_2$ $4H_2O$, 0.3 μM $CuSO_4$ $5H_2O$, 0.8 μM $ZnSO_4$ $7H_2O$, 0.1 μM $(NH_4)_2Mo_7O_{24}$ $4H_2O$) and cultured for a week. The 3-week-old sorghum plants were then transferred to low N or control medium, and subjected to the analysis of various physiological parameters in the following period. The control medium was the Yoshida B culture solution. For low N treatment, N was limited to 1/10 of control (0.05 mM NH_4^+ + 0.2 mM NO_3^-), while Ca and K were maintained at the same concentration as the control using $CaCl_2$ and KH_2PO_4, respectively.

1.2.2 Plant growth condition and treatment using soil culture

1.2.2.1 Kitashirakawa Experimental Farm

A field experiment using 1-m^2 containers was carried out in Kitashirakawa Experimental Farm, Graduate School of Agriculture, Kyoto University. Containers were given 133 g of chemical fertilizer (14-15-5, as P_2O_5-K_2O-Mg) and 43 g urea for control treatment, 133 g of chemical fertilizer (14-15-5, as P_2O_5-K_2O-Mg) and 4.3 g urea for low N treatment. The dose corresponded to 200 kg N ha^{-1}, 200 kg P_2O_5 ha^{-1} and 200 kg K_2O ha^{-1} for the control and 20 kg N ha^{-1}, 200 kg P_2O_5 ha^{-1} and 200 kg K_2O ha^{-1} for low N. At 3, 4 and 5 weeks after germination, the SPAD values were measured and the leaves were sampled for gene expression analysis. The chemical fertilizer and urea were given at the half amount of initial application as topdressing at 9 weeks after germination. Following 4 sorghum genotypes were used for the analysis; BTx623, G247, Tanshaku (commercial dwarf sorghum), and Koutoubun-DH (commercial sweet sorghum). Two seeds per hole were directly planted in the field with 5 replicates for each genotype. There were 20 plants from two different sorghum genotypes per container with a row spacing of 45 cm between each genotype.

1.2.2.2 Uji Campus

A pot experiment (approximately 40 cm in diameter) was carried out using sorghum BTx623 in Uji Campus, Kyoto University. Nitrogen was given at three levels including N0 (0 kg N ha^{-1}), N60 (60 kg N ha^{-1}) and N200 (200 kg N ha^{-1}). All treatments were given 200 kg

P_2O_5 ha^{-1} and 200 kg K_2O ha^{-1}. The SPAD values were recorded and the leaves were sampled for gene expression analysis at 3, 4 and 5 weeks after germination.

1.2.2.3 Shugakuin

A field experiment using a commercial sorghum genotype was conducted in Shugakuin Villa Field, Kyoto. Methane fermentation waste fluid (MFWF) containing 2.2 g kg^{-1} N ammonium-N and 1.4 g kg^{-1} organic-N (Matsubara et al. 2016) was used as N fertilizer. The MFWF was applied at 0, 2.5, 5 and 10 liter m^{-2}. The area of cultivation was ca. 1-m^2 for each treatment. The SPAD values were recorded and the leaves were sampled for gene expression analysis at 3, 4 and 5 weeks after germination.

1.2.3 Morphological analysis

Several morphological parameters were measured include plant height, stem diameter, leaf number, leaf length, leaf width, and roots length at 0, 3, 6, 9 day after treatment. Fresh and dry weight of aboveground parts were recorded at 9 day after treatment.

1.2.4 Total nitrogen and nitrate content analyses

Total N and nitrate content of hydroponically cultured seedlings were determined using whole shoots (0 d after the onset of low-N treatment) or shoots without stem (3–9 d), whereas those of soil-grown plants were determined using the third fully expanded leaves. Plant tissues were dried in an oven and pulverized to a fine powder. Total N content was analyzed using a nitrogen and carbon (NC) analyzer (Sumigraph NC-22F, Sumika Chemical Analysis Service, Osaka, Japan). For nitrate analysis, approximately 20 mg of samples were suspended in 1 mL of distilled water, boiled for 10 min, and centrifuged at 12 000 × *g* for 5 min. The supernatants were filtered through a 0.2-μm membrane filter and analyzed by ion chromatography (HIC-6A, Shimadzu, Kyoto, Japan) equipped with a Shim-pack IC-A1 column eluted with a mobile phase containing 2.5 mM phthalic acid and 2.4 mM Tris at a flow rate of 1.0 mL min^{-1} at 40°C.

1.2.5 Chlorophyll content analysis

Chlorophyll content was measured in the third-youngest fully expanded leaves using the soil-plant analysis development (SPAD)-502 plus chlorophyll meter (Konica Minolta, Tokyo, Japan). Within the leaves, the measurement was performed at a position half the distance from the leaf base to the tip, unless otherwise stated. The measurement was conducted

in average of 15 times (5 individual leaves x 3 times readings). The light intensity in the field was measured using a photosynthetically active radiation meter (Spectromaster C-7000; Sekonic, Tokyo, Japan).

1.2.6 Gene expression analyses

1.2.6.1 RNA sequencing analysis

Tips of fully expanded uppermost leaves were used for RNA sequencing analysis. The leaves from two seedlings were pooled, frozen in liquid nitrogen, and stored at –80°C until use. Total RNA was extracted from the frozen leaves using the Total RNA Extraction Kit Mini (Plant) (RBC Bioscience, New Taipei City, Taiwan) according to the manufacturer's instructions with on-column deoxyribonuclease treatment. After confirming the integrity of RNA by electrophoresis on an Agilent 2100 Bioanalyzer (Agilent, Santa Clara, CA, USA), mRNA libraries were constructed using the Illumina TruSeq RNA Sample Prep Kit v2 (Illumina, San Diego, CA, USA). Equal volumes of individual libraries were pooled after purification and equalization using an Agencourt AMPure XP system (Beckman Coulter, Brea, CA, USA), according to the manufacturer's instructions. The paired-end sequences in the pooled library were determined using an Illumina MiSeq sequencer with the MiSeq Reagent Kit v3 (150 cycles) (Illumina). For each sample, 3–4 million paired-end reads were obtained. The short-read data sets were deposited in the DNA Data Bank of Japan (DDBJ) Sequence Read Archive under accession number DRA010070. The sequence analysis was carried out using the Galaxy web tool available at https://usegalaxy.org/ (Afgan et al., 2016). The sequences were quality-checked using FastQC version 0.69 (https://www.bioinformatics.babraham.ac.uk/projects/fastqc/). The reads were mapped to the *S. bicolor* gene model Sbi1 (http://www.phytozome.net) using TopHat version 2.1.0 (Kim et al., 2013) with Bowtie2 version 2.2.5, and transcript abundances were estimated using Cufflinks version 2.2.1 (Trapnell et al., 2010). The count data from three biological replicates for each treatment were used to estimate differential gene expression using Cuffdiff version 2.2.1 with quartile normalization, and a false discovery rate (FDR) of ≤ 0.05 was set as the significance threshold. Gene ontology (GO) enrichment analysis of the differentially expressed genes (DEGs) was performed by singular enrichment analysis method using the AgriGO webtool (http://bioinfo.cau.edu.cn/agriGO/analysis.php) (Zhou et al., 2010).

1.2.6.2 Reverse transcription-quantitative PCR analysis

Total RNA was prepared from the fully expanded uppermost leaves as described for RNA sequencing. For the analysis of the pot-grown (in Uji) or field-grown (in Shugakuin) plants, leaf samples were immersed in the RNA stabilization solution (RNA*later*, Invitrogen, Carlsbad, CA, USA) immediately after sampling and kept on ice until use. The first-strand cDNA was synthesized from approximately 1 µg of total RNA in a 10-µl reaction using ReverTra Ace DNA polymerase (Toyobo, Osaka, Japan) with $(dT)_{18}$ as a primer according to the manufacturer's instructions, diluted 10-fold with the buffer containing 10 mM Tris-HCl (pH 8.0) and 1 mM EDTA, and stored at –20°C until use.

Reverse transcription-quantitative PCR analysis (RT-qPCR) was conducted on a TaKaRa PCR Thermal Cycler Dice Real Time System II TP 960 (Takara Bio, Shiga, Japan) using the KOD SYBR qPCR mix (Toyobo), with 0.2 µM primers and 0.2 µl template cDNA in 10-µl reactions. The temperature program for the analysis included initial denaturation at 95°C for 30 s, followed by 40 cycles of 95°C for 5 s and 60°C for 30 s. The amounts of the targets were estimated based on the comparative gene expression (ΔΔCt) method, and the expression of the corresponding genes was calculated as relative to that of the 18S rRNA gene (Aglawe et al., 2012). Expression levels of the candidate biomarkers were then used to calculate composite expression value (CEV) (Yang et al., 2011) as shown below, where "intensity_induced" and "intensity_suppressed" refer to the expression levels of low N-inducible and suppressive genes, respectively.

Composite expression value (CEV)

$$= \frac{\sum \log_2(\text{intensity induced}) - \sum \log_2(\text{intensity suppressed})}{\text{number of genes}}$$

1.3 Results

1.3.1 Selection of N status biomarkers in hydroponically cultured seedlings

1.3.1.1 Morphology of plants

In order to find the physiological parameters indicative of the internal N status of sorghum plants, I analyzed the responses of hydroponically cultured sorghum seedlings to N limitation. Nitrogen deficiency causes morphological changes such as leaf chlorosis or dwarfism. In this study, plant appearance and several morphological parameters including plant height, stem diameter, leaf length, and leaf width became different between low N and control plants 9 days after treatment (**Figure 1.1-2**).

Figure 1.1. The appearance of hydroponically grown sorghum seedlings at 9 days after low-N treatment, scale bar = 3 cm.

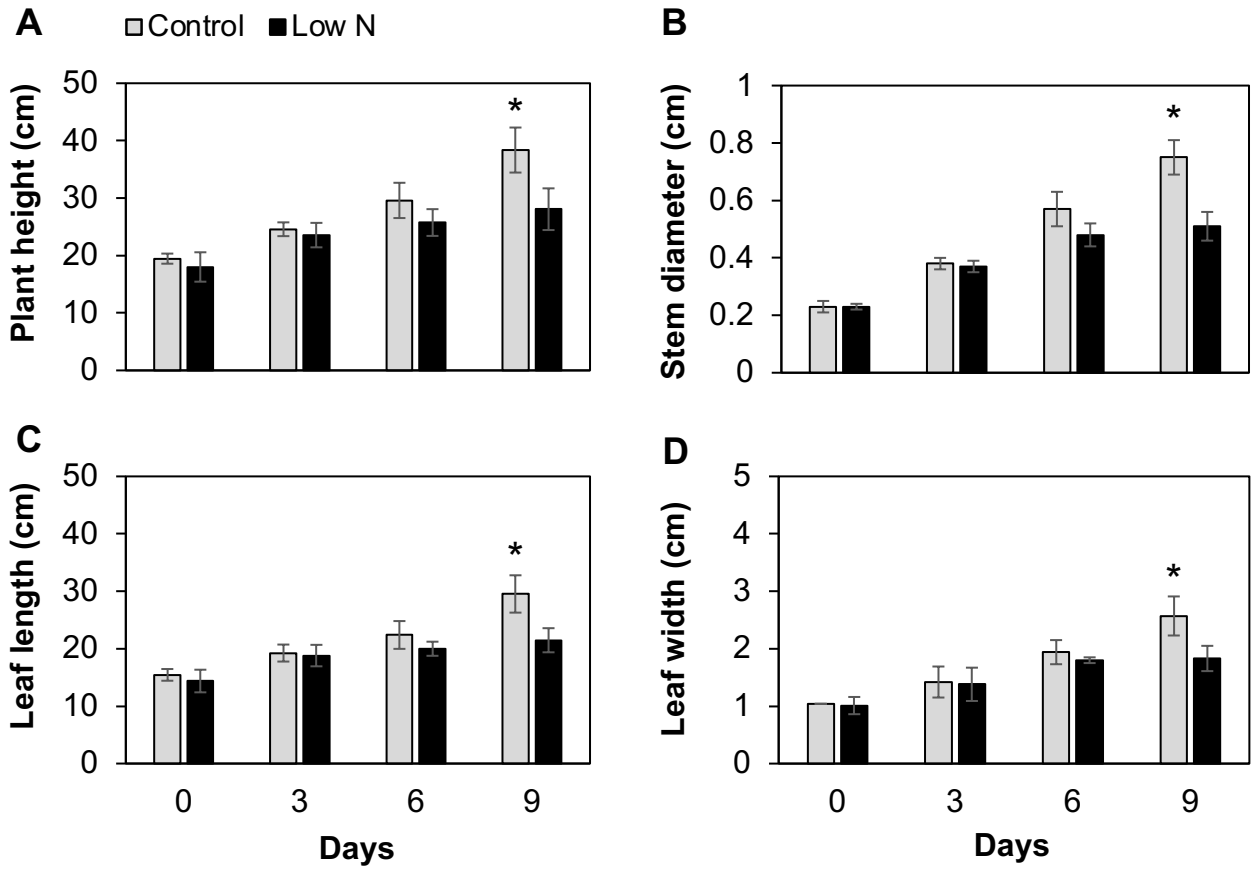

Figure 1.2. Effect of low nitrogen (N) treatment on the (**A**) plant height, (**B**) stem diameter, (**C**) leaf length, and (**D**) leaf width of hydroponically cultured sorghum seedlings. Values are means ± SD (n = 3). Asterisks indicate significant differences between low-N and control plants (Student's *t*-test, $p < 0.05$).

1.3.1.2 Total nitrogen and nitrate content

Total N content in leaves of low N seedlings was significantly lower than that of control seedlings (**Figure 1.3A**). The difference could be seen as early as 3 days after treatment. The difference between treatment got larger as the plants developed.

Nitrate content measured by HPLC was significantly different between treatments, as early as 3 days after treatment (**Figure 1.3B**). However, still detectable amounts were present in low N plants even after 9 days after treatment. Nitrate contents were measured using nitrate ion meter as well. However, for some unknown reason, the results of measurements were not reproducible even with the same samples.

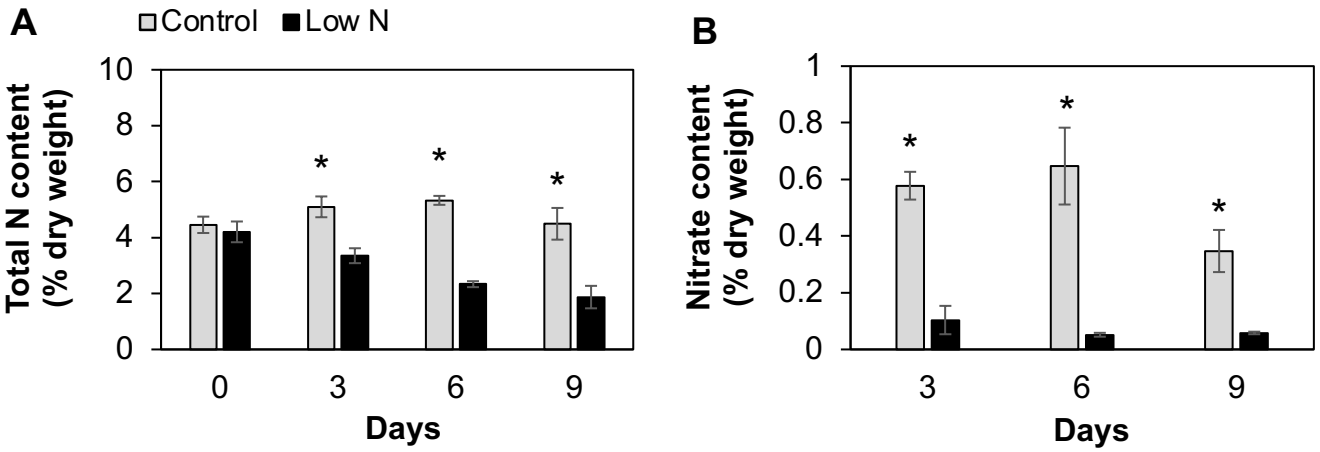

Figure 1.3. Effect of low nitrogen (N) treatment on (**A**) total N and (**B**) nitrate content in shoots of hydroponically cultured sorghum seedlings. The content values were measured using whole shoot for the 0-day sample and combined leaves without stem for the 3-, 6-, and 9-day samples. Values are means ± SD (n = 3). Asterisks indicate significant differences between low-N and control plants (Student's *t*-test, $p < 0.05$).

1.3.1.3 Chlorophyll content

Leaf N and chlorophyll content correlate with each other (Makino and Osmond, 1991; Uchino et al., 2013). Previously, SPAD values have been used as an index of leaf chlorophyll content in several crops, including sorghum (Adams et al., 2015; Loh et al., 2002; Maranville and Madhavan, 2002; Parry et al., 2014; Uddling et al., 2007). Thus, I examined the SPAD values of sorghum seedlings with low-N and control treatments. The SPAD values of the third-youngest fully expanded leaves were significantly different between the treatment groups by 6 d (**Figure 1.4**), indicating that these values could reflect the N sufficiency of sorghum seedlings earlier than the changes in morphological parameters. I then examined the leaf position that best reflected the plant N status, based on the correlation between the SPAD value of each leaf and shoot N content. As shown in **Figure 1.5**, the two parameters seemed correlated in low-N plants, whereas the SPAD values were saturated in control plants. Therefore, the degree of correlation was compared in low-N plants. In the first leaves, the correlation was not statistically significant ($p = 0.05$), whereas in the second and third leaves, the two parameters showed a significant correlation with coefficients of 0.533 and 0.792, respectively. Thus, the highest correlation was obtained in the third fully expanded leaves. I accordingly measured the SPAD values with the third-youngest fully expanded leaves in the following experiments.

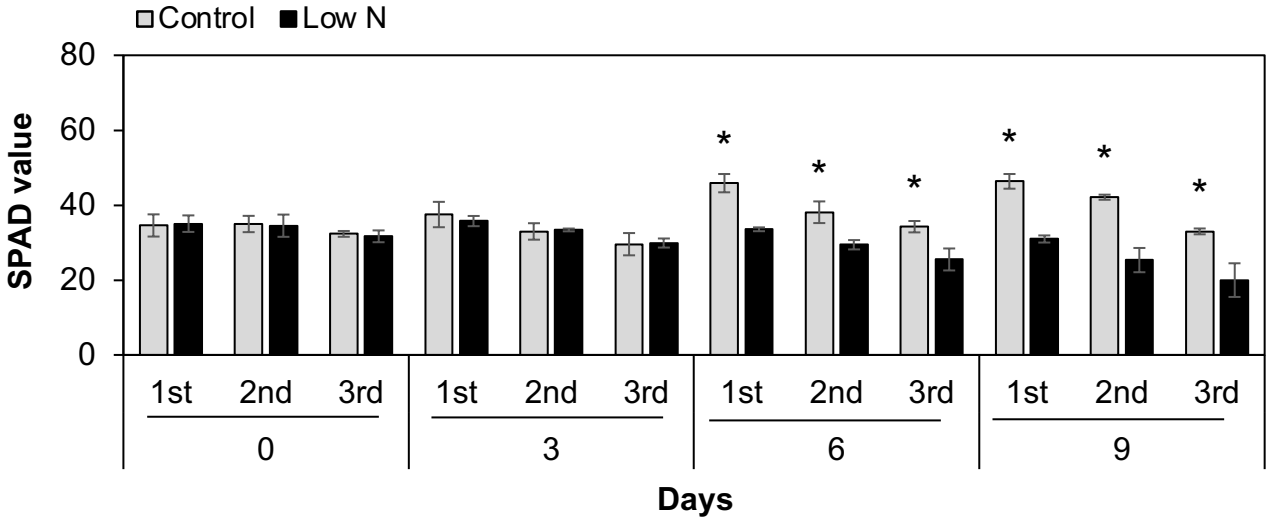

Figure 1.4. Effect of low nitrogen (N) treatment on soil-plant analysis development (SPAD) values of the leaves of hydroponically cultured sorghum seedlings Measurements were done at the first-, second-, and third-youngest fully expanded leaves. Values are means ± SD (n = 3). Asterisks indicate significant differences between low-N and control plants (Student's *t*-test, $p < 0.05$).

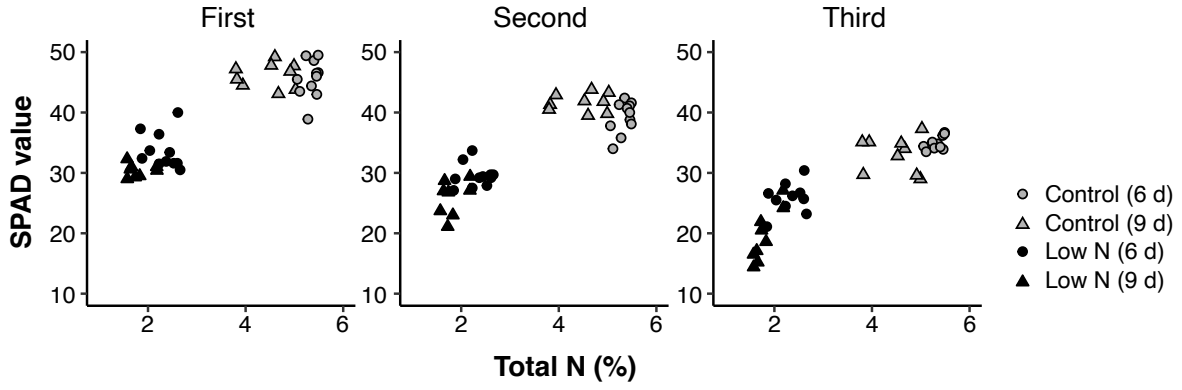

Figure 1.5. Relationship between shoot total nitrogen (N) content and soil-plant analysis development (SPAD) values in the first-, second-, and third-youngest fully expanded leaves of hydroponically cultured sorghum seedlings. The total N content was measured using combined leaves without stem sampled 9 d after starting the treatment. The SPAD values are those measured at 6 and 9 d. Each point represents the data from one individual.

1.3.1.4 Gene expression

1.3.1.4.1 Expression of homologs of maize nitrogen status marker genes

Modulation of gene expression precedes morphological or metabolic changes. Hence, the expression of certain genes may serve as early biomarkers for N shortage in plants, but only a limited amount of information is available regarding the early changes in gene expression in sorghum under low-N conditions. To find such genes in sorghum, I firstly examined if the sorghum homologs of N-responsive genes in maize (Yang et al., 2011) were also applicable for other grasses such as sorghum. Yang et al. (2011) have listed eight genes that accurately reflect nitrogen status of maize (**Table 1.1**). Through a TBLASTN search using the 8 sequences as the query, 13 genes were picked up as their close homologs (several maize genes hit with multiple sequences of sorghum). Expression of the genes in low N and control sorghum seedlings were then examined using RT-qPCR. Primers used for the analysis are listed in Table **Table 1.1**. Six out of 13 sequences were successfully amplified by RT-qPCR, indicating that these genes were expressed in sorghum seedlings (**Figure 1.6A**). Yang et al. (2011) reported that the expression of the 8 maize biomarker genes were downregulated by N deficiency. However, in this study, four out of the six sorghum genes were rather low N-inducible. I then calculated composite expression value (CEV) from the expression values (relative transcript abundance to 18S rRNA) of all these N-responsive genes. The CEV seemed higher in low N than in control seedlings, but the difference was not statistically significant (**Figure 1.6B**).

Table 1.1. List of primers used for quantitative reverse transcription-PCR analysis (the candidate target genes from the homolog N-responsive maize biomarker genes).

Maize genes probeset	UniRef ID (Maize/ Rice)	GenBank ID of sorghum homolog	Primers	Functional annotation
A1ZM006239_at	Q10C31	**XM_002466252.1***	F: GCTCTAAAGGGTTTGGTGCAGA	Uncharacterized plant-specific domain TIGR01615
			R: GCCCTTGCCGCACTTATCG	
A1ZM011316_s_at	Q6Z5C8	**XM_002445909.1***	F: TGATCCATCTGGTGGCGAAC	POZ domain protein family-like
			R: GTGAGGATGTCCTCGTGCAG	
A1ZM058664_at	Q69NI4	**XM_002460573.1***	F: TCCACGCATAAAGTTCAGCAC	Putative nodule inception protein
			R: CTTGTTGAGCGCATGTGACC	
A1ZM019982_at	Q851M9.1	XM_002466087.1	F: TACAAGCTGGTACCTGGAGA	Ammonium transporter 3 OsAMT3;2
			R: GAGAATATTGCACACAGGGCT	
		XM_002456661.1	F: CCGGCGCAGGTCTGGT	
			R: GCACCACCATCATCGTGAAC	
		XM_002452204.1	F: ACAGCTGCTTATCGGGGATG	
			R: TCATCATGGCGGGTTACGTC	
A1ZM019124_at	Q9M4D6	XM_002440703.1	F: CTCCCCTACTACGCCAAACAC	Putative acid phosphatase
			R: CCGAGCGAGATCAGCTTCTTG	
		XM_002439367.1*	F: ATCAAGCCGGTGATCCTGAC	
			R: GTCCTGAGGCTTGAGCAGC	
A1ZM001292_s_at	Q2V8D7	XM_002452118.1	F: AGTTCGACGTCCAGGTCACT	Glycerophosphoryl diester phosphodisterase
			R: GGCCCATACTGGAGGAAGTC	
		XM_002446281.1	F: CCCAACAAGACGGCGAAATC	
			R: CTTCCGGAAAAGTGGCTTGC	
A1ZM016678_at	Q0NZY1	**XM_002455975.1***	F: GTGAAGGACGTGGAGCACAT	AtRL1
			R: CGATCGATTCTGTCGGCGTC	
A1ZM004474_at	Q10R45	**XM_002468376.1***	F: AACATTCCAGGGTGTCGGAG	Alanine-glyoxylate aminotransferase 2
			R: TGCCAGTACGACCAAAACCA	
		XM_002467846.1	F: AGGAGAAGCACGACATCATCG	
			R: TCTTTCGCCGGTGTCTTGAG	

Asteriks mean the primers were successfully amplified by RT-qPCR in sorghum samples

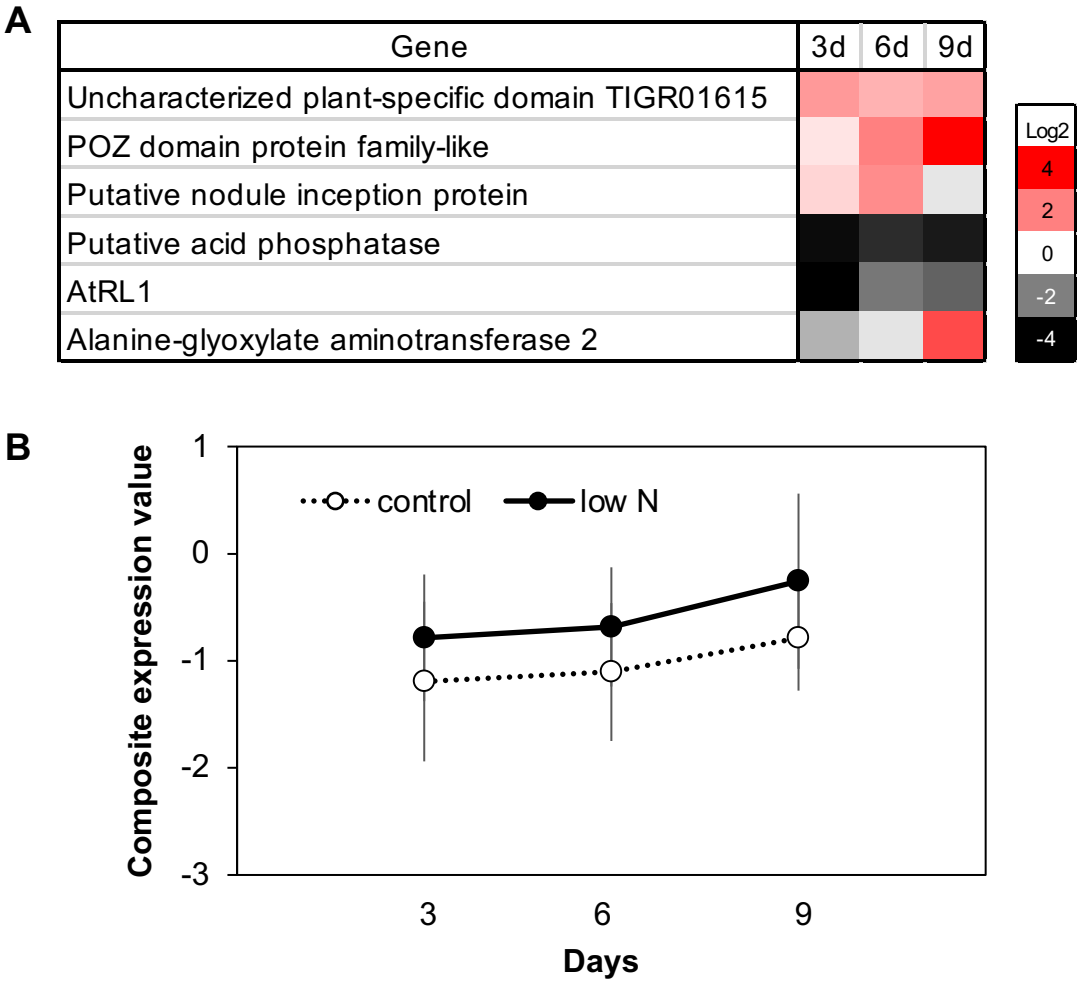

Figure 1.6. Changes in the expression of the sorghum homologs of N-responsive genes in maize. (**A**) heatmap showing fold changes in the expression of the sorghum homologs of N-responsive genes in maize and (**B**) time-course change of the composite expression value calculated from those genes expressed in low-N and control sorghum seedlings. Values are means ± SD (n = 3).

1.3.1.4.2 Expression of genes screened by RNA sequencing

As another approach to identify low N-responsive genes in sorghum, genes differentially expressed in low N and control plants were searched by RNA sequencing, followed by validation with RT-qPCR. The process of selection is shown in **Figure 1.7**. Of the 206 982 expressed genes identified by RNA sequencing, 127 were differentially expressed between low-N and control seedlings at both 3 and 6 days after starting the treatment (data not shown); 40 or 85 DEGs were consistently up- or down-regulated by low N treatment at both 3 and 6 days, respectively, whereas the remaining two DEGs were up-regulated at 3 day but down-regulated at 6 day in low N plants. A GO enrichment analysis of the 127 DEGs revealed significant overrepresentation of the terms denoting the involvement in N compound metabolic process in biological process category (**Table 1.2** and **Table 1.3**). The GO terms related to

response to stress, chemical, and hormone stimulus and N compound metabolism, including cellular nitrogen compound metabolic process (GO: 0034641), cellular amine metabolic process (GO: 0044106), and cellular amino acid metabolic process (GO: 0006520) were enriched among the DEGs both up- and down-regulated by low N treatment (**Table 1.2** and **Table 1.3**, respectively). In cellular component category, significant enrichment of GO terms was associated with the DEGs that were down-regulated by low N treatment. Most of the enriched terms were related to plastid or chloroplast (**Table 1.4**). These results suggest that the sorghum plants tried to adopt to the N-limitation by enhancing the recycling of N compounds from the cellular components including chloroplast proteins.

Among the DEGs, those exhibiting more than 3-fold change in expression (either induced or suppressed) upon low-N treatment at either 3 or 6 days were subjected to validation with RT-qPCR. Several genes that did not fulfill the criteria because of the errors between trials but appeared promising in preliminary experiments were also included in the validation analysis. Out of 57 candidate genes examined, 11 genes were thus confirmed to be responsive to low-N treatment, but not significantly modulated by low phosphorus (P) or low potassium (K) treatment (**Table 1.5**, **Figure 1.8A**). The 11 genes included those possibly involved in amino acid metabolism (e.g., a branched-chain aminotransferase, a tryptophan/tyrosine permease, and a glutamine synthetase), and stress-responsive proteins (e.g., a MYB family protein, a BTB/POZ domain-containing protein, and a chitinase).

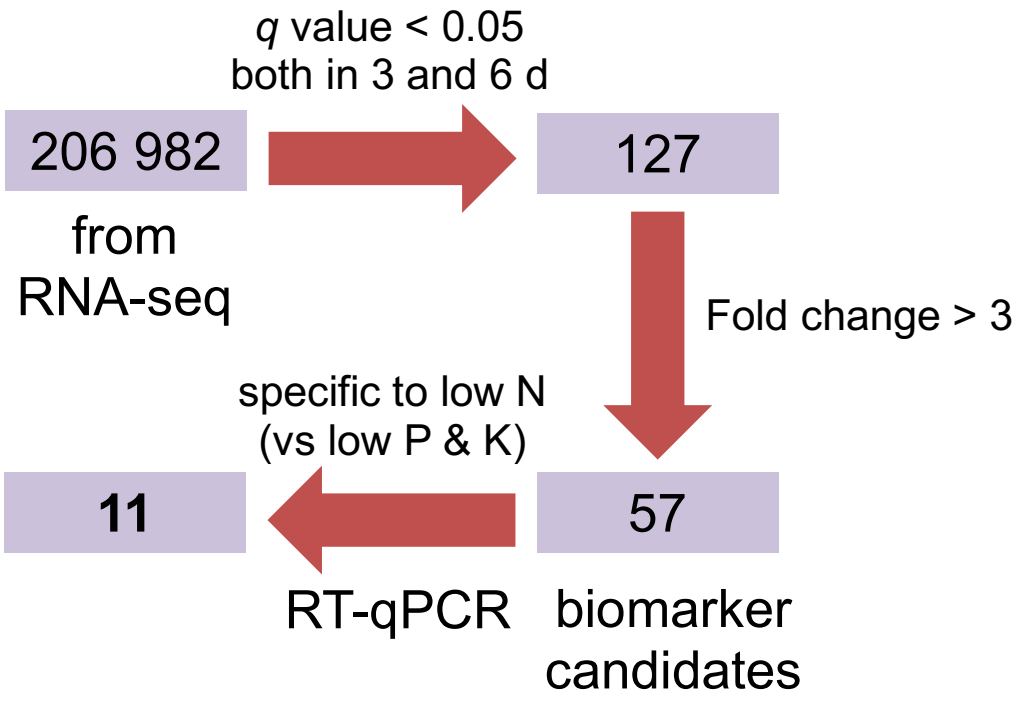

Figure 1.7. The selection process of N status biomarker genes from RNA sequencing screening in hydroponically sorghum seedlings. The numbers inside the box indicate the number of genes.

Table 1.2. Gene ontology (GO) term enrichment in the Biological Process category of the differentially expressed genes (DEGs) induced by low-N reatment of sorghum seedlings at 3 days after treatment.

GO term	Description	Number of genes	*p* value	*q* value
GO:0042221	Response to chemical stimulus	10	3.E-03	3.E-02
GO:0010033	Response to organic substance	8	3.E-03	3.E-02
GO:0009719	Response to endogenous stimulus	8	8.E-04	1.E-02
GO:0009725	Response to hormone stimulus	7	2.E-03	3.E-02
GO:0042180	Cellular ketone metabolic process	7	7.E-04	1.E-02
GO:0006082	Organic acid metabolic process	7	7.E-04	1.E-02
GO:0019752	Carboxylic acid metabolic process	7	7.E-04	1.E-02
GO:0006519	Cellular amino acid and derivative metabolic process	6	2.E-03	3.E-02
GO:0009308	Amine metabolic process	6	4.E-04	1.E-02
GO:0034641	Cellular nitrogen compound metabolic process	6	2.E-04	1.E-02
GO:0006520	Cellular amino acid metabolic process	5	8.E-04	1.E-02
GO:0044106	Cellular amine metabolic process	5	8.E-04	1.E-02

The overrepresentation was tested by web-tool (http://bioinfo.cau.edu.cn/agriGO/analysis.php) (Fisher and Yekutieli tests, q value < 0.05).

Table 1.3. Gene ontology (GO) term enrichment in the Biological Process category of the differentially expressed genes (DEGs) repressed by low-N reatment of sorghum seedlings at 3 days after treatment.

GO term	Description	Number of genes	*p* value	*q* value
GO:0006950	Response to stress	24	5.E-05	4.E-03
GO:0034641	Cellular nitrogen compound metabolic process	14	1.E-08	5.E-06
GO:0009308	Amine metabolic process	12	4.E-06	4.E-04
GO:0044271	Cellular nitrogen compound biosynthetic process	11	2.E-07	4.E-05
GO:0044106	Cellular amine metabolic process	9	7.E-05	4.E-03
GO:0006520	Cellular amino acid metabolic process	8	4.E-04	2.E-02
GO:0009309	Amine biosynthetic process	7	2.E-05	2.E-03
GO:0016052	Carbohydrate catabolic process	6	7.E-04	3.E-02
GO:0008652	Cellular amino acid biosynthetic process	6	8.E-05	4.E-03

The overrepresentation was tested by web-tool (http://bioinfo.cau.edu.cn/agriGO/analysis.php) (Fisher and Yekutieli tests, q value < 0.05).

Table 1.4. Gene ontology (GO) term enrichment in the Cellular Component category of the differentially expressed genes (DEGs) repressed by low-N reatment of sorghum seedlings at 3 days after treatment.

GO term	Description	Number of genes	*p* value	*q* value
GO:0005737	Cytoplasm	39	1.E-03	1.E-02
GO:0044444	Cytoplasmic part	35	8.E-04	1.E-02
GO:0009536	Plastid	28	1.E-12	2.E-10
GO:0009507	Chloroplast	26	2.E-12	2.E-10
GO:0044435	Plastid part	15	6.E-09	4.E-07
GO:0044434	Chloroplast part	12	1.E-06	4.E-05
GO:0009579	Thylakoid	10	3.E-06	8.E-05
GO:0034357	Photosynthetic membrane	10	1.E-06	4.E-05
GO:0031984	Organelle subcompartment	9	1.E-05	1.E-04
GO:0044436	Thylakoid part	9	9.E-06	1.E-04
GO:0031976	Plastid thylakoid	9	8.E-06	1.E-04
GO:0009534	Chloroplast thylakoid	9	8.E-06	1.E-04
GO:0042651	Thylakoid membrane	9	4.E-06	8.E-05
GO:0055035	Plastid thylakoid membrane	9	3.E-06	8.E-05
GO:0009535	Chloroplast thylakoid membrane	9	3.E-06	8.E-05
GO:0009526	Plastid envelope	5	2.E-04	3.E-03

The overrepresentation was tested by web-tool (http://bioinfo.cau.edu.cn/agriGO/analysis.php) (Fisher and Yekutieli tests, q value < 0.05).

I then examined if the expressions of the 11 genes could distinguish the control and low-N plants. The primers of 11 selected genes used for the analysis are listed in **Table 1.6**. Since many factors other than the nutrient availability can affect the gene expression, judgement based on the expression of single gene may lead to wrong conclusion. To reduce such risk, the evaluation was made with CEV, the index representing the average of multiple genes' expression values. The CEV calculated for the 11 genes was different between the treatments at 0 d, which corresponded to 4 h after transferring the plants to low-N or control medium. The difference became more remarkable at 3 d (**Figure 1.8B**). These results show that gene expression can be modulated according to the internal N status of sorghum seedlings, with higher sensitivity and rapidity than the other physiological parameters.

Table 1.5. Genes selected as candidate nitrogen status biomarkers in sorghum.

Gene ID	Functional annotation[a]	day	*p* value	*q* value	Log_2 (fold change)
Sb01g007130	MYB family transcription factor	3	5.E-05	1.E-03	–1.96
		6	5.E-05	1.E-03	–2.69
Sb01g010270	Glutamine synthetase	3	5.E-05	1.E-03	–1.99
		6	5.E-05	1.E-03	–2.64
Sb01g040410	Unknown protein	3	5.E-05	1.E-03	3.50
		6	5.E-05	1.E-03	4.29
Sb01g040820	Tryptophan/tyrosine permease	3	5.E-05	1.E-03	2.47
		6	5.E-05	1.E-03	2.66
Sb01g042040	Branched-chain aminotransferase 3	3	5.E-05	1.E-03	3.19
		6	5.E-05	1.E-03	3.21
Sb01g048140	Chitinase	3	3.E-04	6.E-03	–1.29
		6	5.E-05	1.E-03	–2.03
Sb03g003550	2-Oxoglutarate-dependent dioxygenase	3	5.E-05	1.E-03	2.04
		6	5.E-05	1.E-03	2.27
Sb04g023820	Loricrin-related protein	3	5.E-05	1.E-03	3.19
		6	5.E-05	1.E-03	3.44
Sb06g005000	Flowering promoting factor 1	3	3.E-03	4.E-02	1.79
		6	3.E-03	3.E-02	2.25
Sb07g028630	BTB/POZ domain-containing protein	6	5.E-05	1.E-03	2.65
Sb09g022260	Unknown protein	3	5.E-05	1.E-03	–2.52
		6	5.E-05	1.E-03	–2.22

[a]According to the MOROKOSHI sorghum transcriptome database.

Table 1.6. List of primers used for quantitative reverse transcription-PCR analysis (the eleven selected candidate biomarker genes screened by RNA sequencing analysis).

Gene ID	Forward primer (5′→3′)	Reverse primer (5′→3′)
Sb01g007130	AGAGTGAAATCACCTCGCCG	TAGATGCCGGCGATACCAAC
Sb01g010270	CTCGGGCCATCTTCAGAGAC	GTTGCTCGGAATCGGCTTTC
Sb01g040410	CGTCGCTTTTCGTTTGGGAG	TACGGACGACGACGTTACAC
Sb01g040820	TATGGTGTCCTCCCTCCGTT	CATCCCAACCAGAACAGGCT
Sb01g042040	TACCTGGAGGAGGTGTCGTC	TCAACCTTGTATCCGCGGTC
Sb01g048140	ACACCTACGACGCGTTCATC	ATCCACCGGTAGTTTCGTGG
Sb03g003550	CTACAGGCGGGGTCAACTAC	CAGGATCTGGATGGTGTCGC
Sb04g023820	GTTTGGCCAGAGCTTCTCCT	AAGGAGATGATGGTTCCGGC
Sb06g005000	AGAAACGATGTCGGGTGTGT	GTACGACGTCACCACCTCTC
Sb07g028630	TGATCCATCTGGTGGCGAAC	GTGAGGATGTCCTCGTGCAG
Sb09g022260	TGTTGGGACTGTTGATGCGA	CACCGACCGGATGGATGTAG

A

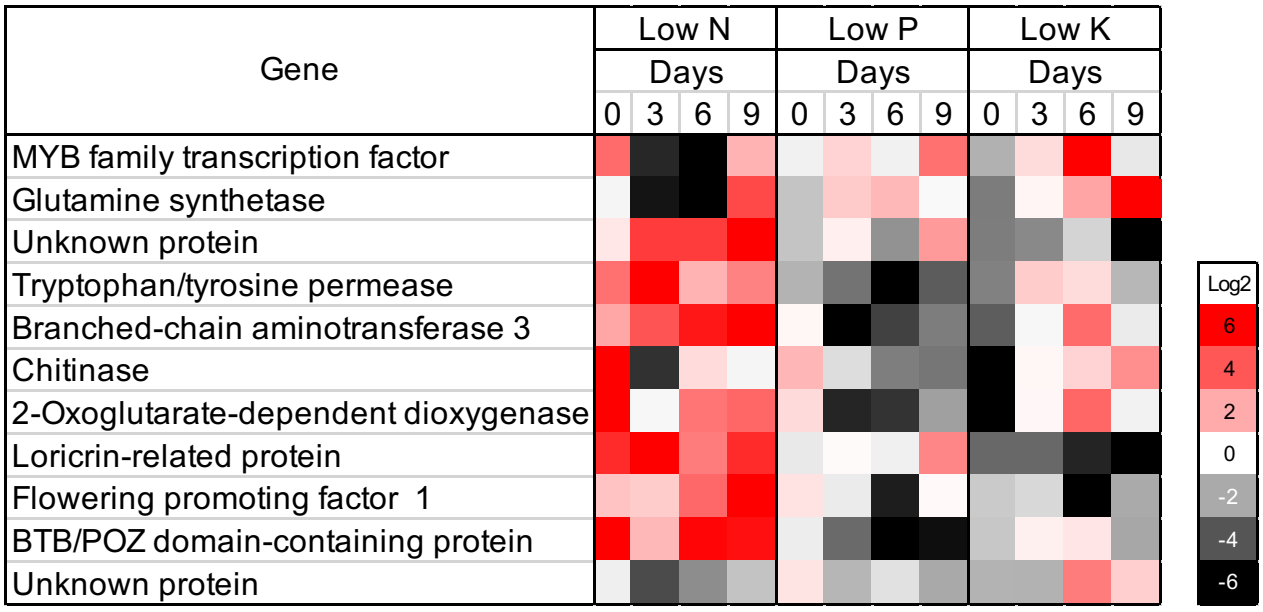

B

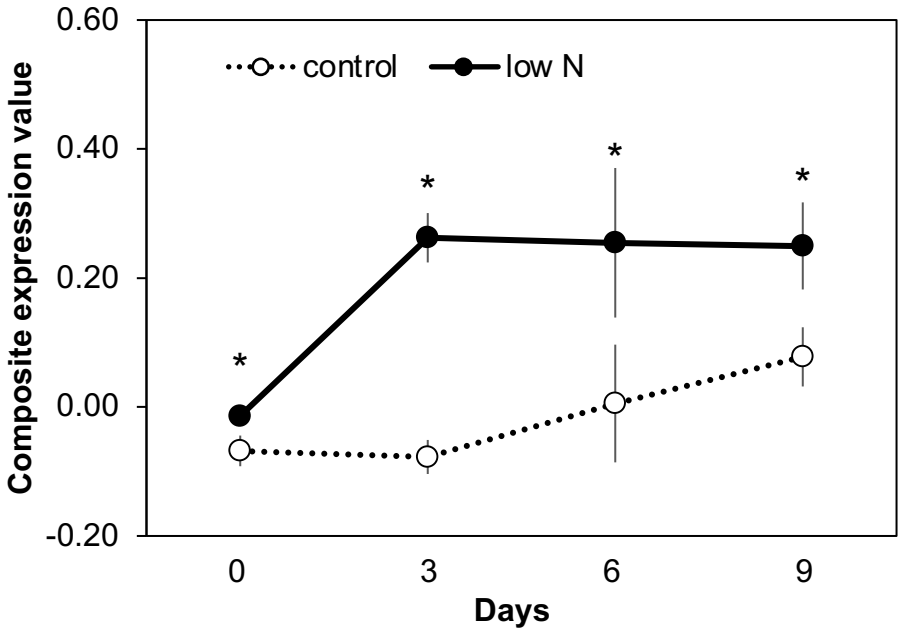

Figure 1.8. Changes in the expression of the genes selected in response to low nitrogen (N) and other nutrient stress conditions. (**A**) heatmap showing fold changes in the expression of 11 genes selected as low-N-responsive genes and (**B**) time-course change of the composite expression value calculated from the 11 genes expressed in low-N and control seedlings. Values are means ± SD (n = 3). Asterisks indicate significant differences between low-N and control seedlings (Student's *t*-test, $p < 0.05$).

1.3.2 Evaluation of leaf chlorophyll content and gene expression as nitrogen status biomarkers for soil-grown sorghum plants

In the previous section, analyses using hydroponically cultured plants demonstrated that the SPAD value as the index of leaf chlorophyll content and the expression of low N-inducible genes were promising as the N status biomarkers in sorghum seedlings. However, in plants grown in the field, those parameters may respond to low N in a different manner from that in juvenile plants grown under controlled condition. In addition, different genotypes may respond differently to the stress, possibly making the biomarker selected in one genotype not useful in other genotypes. Thus, in this part, I investigated the N response of SPAD value and gene expression in multiple sorghum genotypes grown in the fields, with the aim of examining the applicability of these parameters to the actual nutritional diagnosis.

1.3.2.1 Growth of sorghum under limited nitrogen supply

Four sorghum genotypes were grown in a 1-m^2 container under low N and control condition. Plants were fed with 200 kg N ha^{-1} or 20 kg N ha^{-1} for control and low N treatment, respectively, in the form of urea as basal application. Deficiency became visually apparent by 5 weeks after germination, as can be seen in **Figure 1.9**. These findings indicate that the low N treatment indeed affected the plant internal N status in this study. Since the color of leaves was getting pale around 9 weeks, additional urea fertilizer was applied at 100 and 10 kg ha-1 for control and low N plots, respectively.

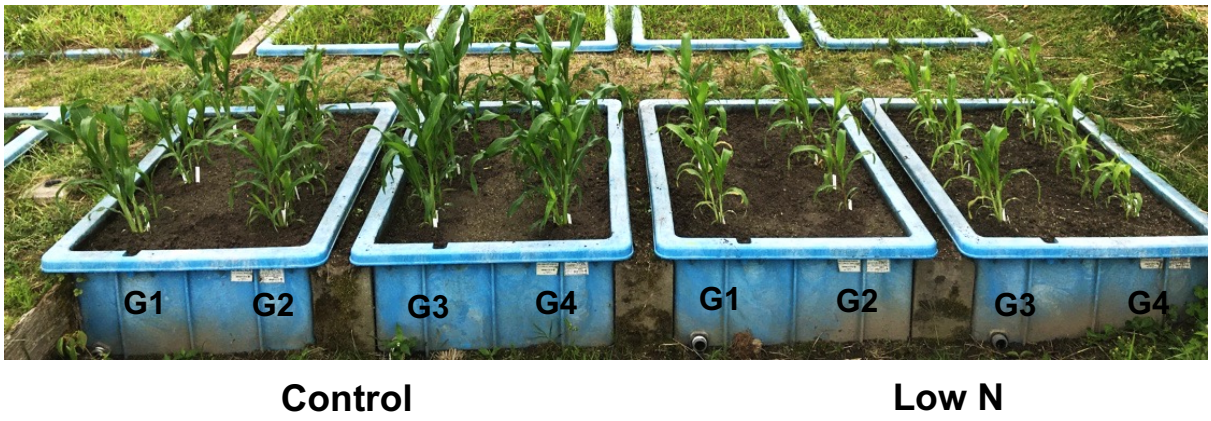

Figure 1.9. The appearance of four sorghum genotypes in five weeks after germination under control or low-N treatment, G1: BTx623, G2: G247, G3:Tanshaku, and G4: Koutoubun-DH.

1.3.2.2 SPAD chlorophyll meter analysis

Prior to the analysis of SPAD values in the field-grown plants, verification of the methods were performed. Based on the examination using hydroponically cultured seedlings, the SPAD values were measured in the third-youngest fully expanded leaves. I then examined the position within a leaf blade that could provide the most reliable results. The SPAD value was measured at 1/3, 1/2, and 2/3 positions from the base to tip of the third leaves of low-N plants and examined for their correlation with the leaf N content. **Figure 1.10** shows the relationship between the SPAD values measured at each position within the third leaves and the total N content of the leaves. The two parameters showed significant correlation ($p < 0.05$) with coefficients of 0.600, 0.618, and 0.634 for the 1/3, 1/2, and 2/3 positions from the base to tip, respectively. The correlation coefficients for the three positions were not statistically different. These results suggest that, in sorghum, the position within a leaf is not so critical in SPAD measurements for N diagnosis. Nonetheless, for consistency, it would be better to conduct the analysis at a constant position. I, therefore, measured the SPAD value at the midpoint of the blade of the third fully expanded leaves in the following analyses.

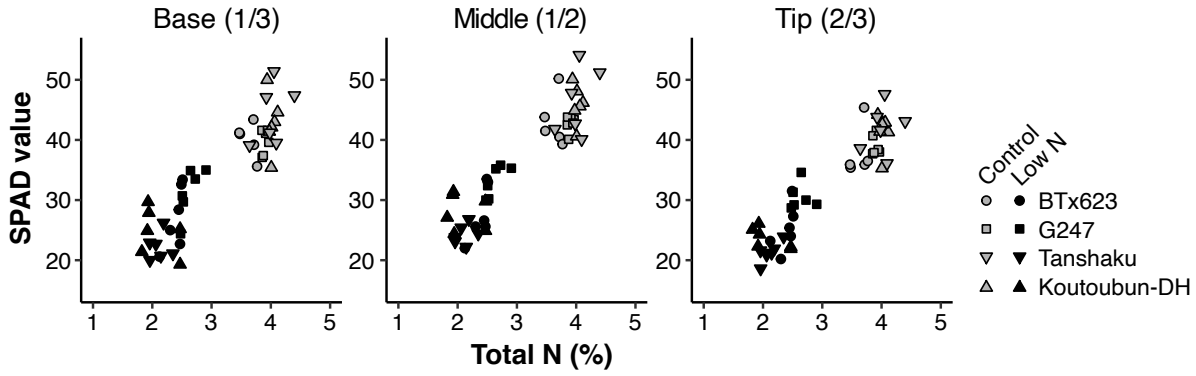

Figure 1.10. Relationship between total nitrogen (N) content in leaf and soil-plant analysis development (SPAD) values measured at various points within a single leaf blade. Four genotypes of soil-grown sorghum plants were subjected to analysis. The total N content was measured in the third-youngest fully expanded leaves of 5-week-old plants. The SPAD values were measured in the same leaves at the position corresponding to 1/3 (base), 1/2 (middle), 2/3 (tip) of the length of a leaf blade from base to tip.

After validating the method of their measurement, the SPAD values were analyzed during the growth periods of four different genotypes of soil-grown sorghum plants. In genotypes Tanshaku and Koutoubun-DH, the SPAD values were significantly lower in low-N plants than in control plants from 4 weeks after germination, whereas in BTx623 and G247, it became different after 5 weeks. The SPAD values remained higher in control plants than in low-N plants at the earlier stage, but they declined to the same level as those in low-N plants by 9 weeks (**Figure 1.11**). This decline might be caused by the depletion of N applied as the basal fertilizer. Therefore, N was supplemented by topdressing at 9 weeks, and the SPAD values became different between the treatment groups again by 11 weeks (**Figure 1.11**). These results suggest that the SPAD values indeed reflected the N status of sorghum plants, not only in young hydroponically grown seedlings of a specific genotype but also in multiple genotypes at more mature stages.

1.3.2.3 Expression of eleven candidate biomarker genes

The expression of the 11 candidate N status biomarker genes (**Figure 1.12**) was examined in soil-grown plants using a RT-qPCR analysis. In Tanshaku, the CEV of the genes in low-N plants was significantly higher than that in control plants at 3 weeks, and the difference remained significant until 5 weeks. On the other hand, the differences between the treatment groups were not clear in the other genotypes. In Koutoubun-DH, the difference could be observed only after 5 weeks. In BTx623 and G247, no significant difference was observed between the treatment groups. The time required to see the difference might reflect the severity of N deficiency in each genotype. This is suggested by the trend of SPAD values, as the decline of SPAD values in low-N plants appeared earlier and more remarkable in Tanshaku than in the other genotypes (**Figure 1.11**).

The CEV in control plants increased at later stages and was even higher than that in low-N plants at 9 weeks. This change might be due to the depletion of N applied as the basal fertilizer and hence a shift in the internal N status of control plants. However, I cannot exclude the possibility of senescence-induced expression of these genes. Taken these results together, in the soil-grown mature plants, diagnosing the N status based on the 11 genes' CEV was not as effective as in the case of hydroponically-cultured seedlings.

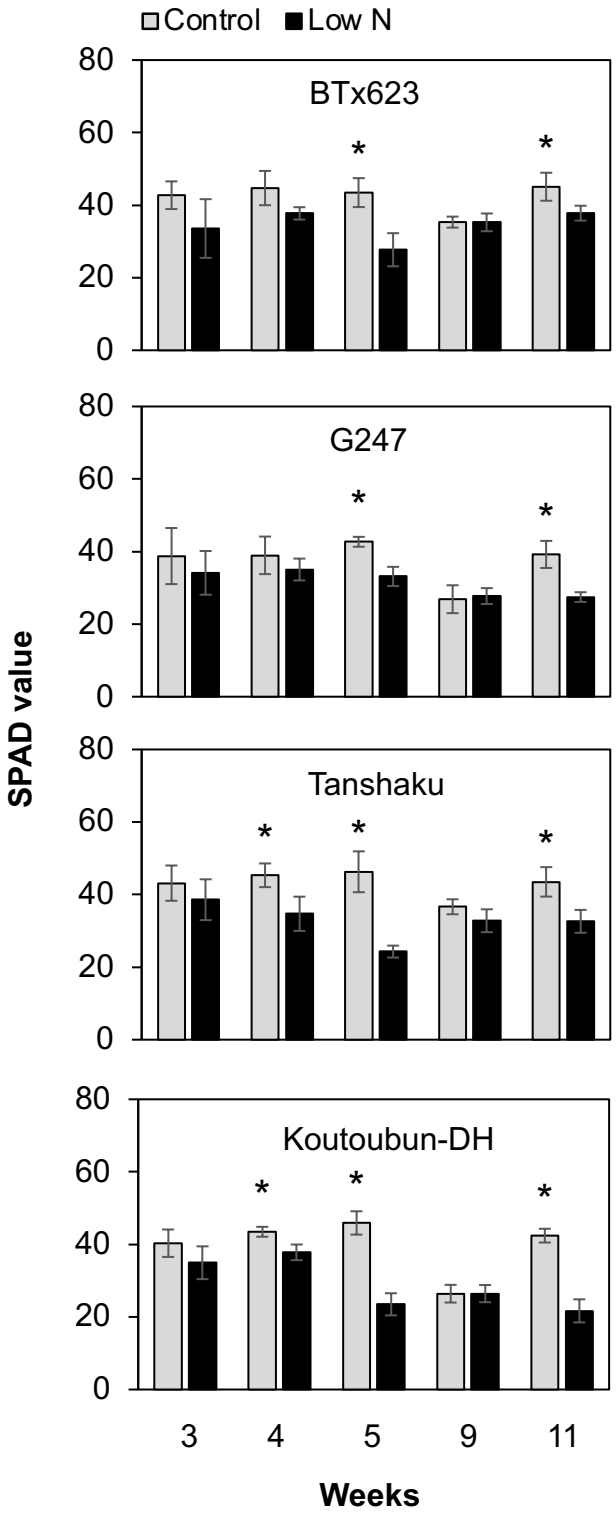

Figure 1.11. Effect of low nitrogen (N) treatment on the soil-plant analysis development (SPAD) values of four genotypes of soil-grown sorghum plants. Values are means ± SD (n = 6). Asterisks indicate significant differences (Student's *t*-test, $p < 0.05$).

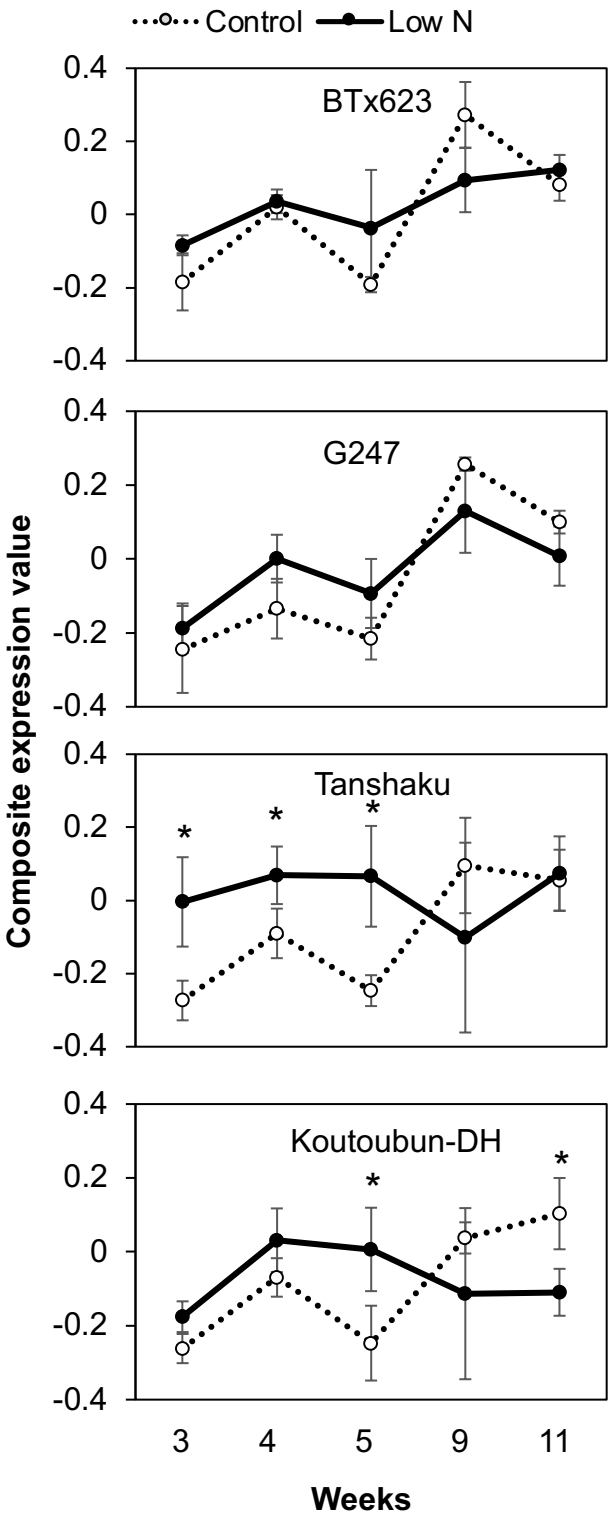

Figure 1.12. Effect of low nitrogen (N) treatment on the composite expression values of four genotypes of soil-grown sorghum plants. Values are means ± SD (n = 3). Asterisks indicate significant differences (Student's *t*-test, $p < 0.05$).

1.3.2.4 Verification experiments at additional sites

To confirm the results obtained in the previous section, additional experiments were carried out at other experimental sites and setup. Sorghum BTx623 was grown in pots with a gradient application of N at 0, 60, and 200 kg N ha^{-1} (hereafter referred to as N0, N60, and N200 treatments, respectively). The SPAD value was lower in N0 than in the other two treatments at 3, 4, and 5 weeks after gemination (**Figure 1.13A**). The CEV of 11 target genes was higher in N0 than in N60 or N200 at 3 weeks, but not at 4 and 5 weeks (**Figure 1.13B**). These results are similar to those obtained in the previous section, in that the SPAD values were different between N-sufficient and -deficient groups, whereas the difference in CEV was not obvious (**Figure 1.11-12**).

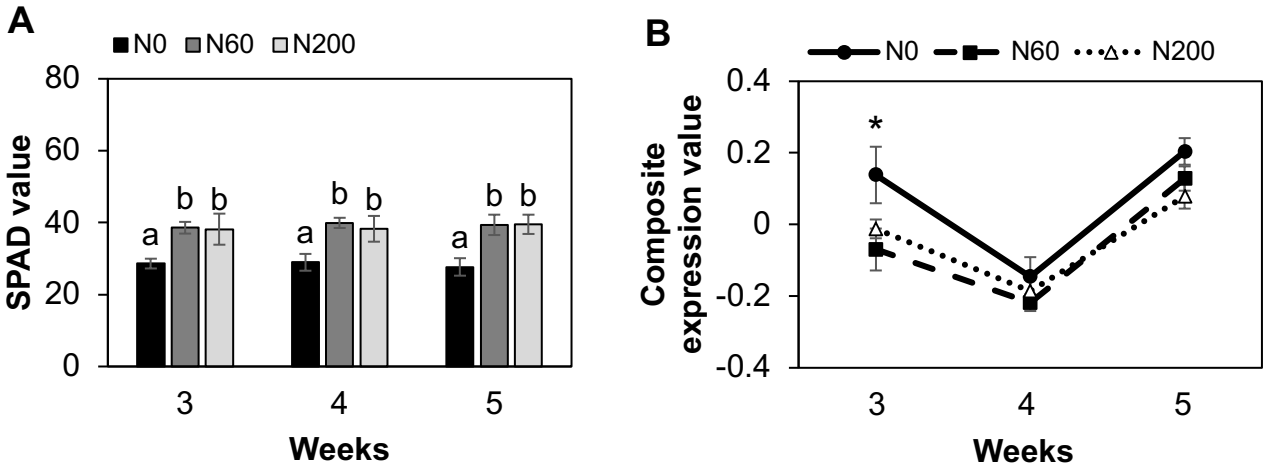

Figure 1.13. Effect of low nitrogen (N) treatment on the (**A**) soil-plant analysis development (SPAD) values and (**B**) composite expression values of pot-cultivated sorghum plants. Sorghum BTx623 plants were grown on soil treated with urea at concentrations of 0, 60, and 200 kg N ha^{-1} (referred to as N0, N60, and N200, respectively). Analyses were conducted at 3, 4, and 5 weeks after germination. Values are mean ± SD (n = 6 for SPAD and n = 3 for composite expression value). Different letters in (A) indicate significant differences by Tukey-Kramer test at $p < 0.05$. The asterisk in (B) indicates significant differences among treatment groups by one-way analysis of variance at $p < 0.05$.

Another trial was conducted under field conditions, where MFWF was applied as an N fertilizer. MFWF contains N in the form of both inorganic ammonium ions (NH_4^+) and organic matter, and the effectiveness of MFWF as a fertilizer depends on its NH_4^+ content (Matsubara et al., 2016). In this trial, MFWF was applied at the rates equivalent to 0, 90, 180, and 360 kg NH_4^+–N ha^{-1}. The SPAD value gradually increased as the MFWF dose increased (**Figure 1.14A**). These finding indicate that the SPAD value reflected the extent of N sufficiency in

plants. The CEV of the 11 selected genes tended to be higher in plants without MFWF application than in those treated with MFWF, but no statistically significant difference was observed until 5 weeks after germination (**Figure 1.4B**). These results were consistent with those obtained in the previous sections.

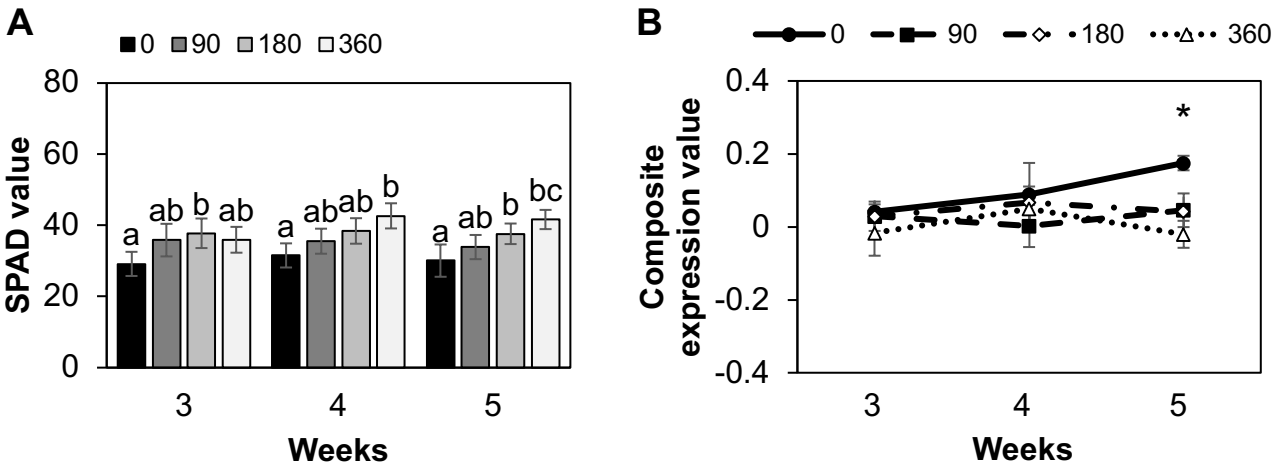

Figure 1.14. Effect of low nitrogen (N) treatment on the (**A**) soil-plant analysis development (SPAD) values and (**B**) composite expression values of field-grown sorghum plants. A commercially available genotype of sorghum was grown on plots applied with methane fermentation waste fluid as organic fertilizer at concentrations of 0, 90, 180, and 360 kg NH_4^+-N ha^{-1}. Analyses were conducted at 3, 4, and 5 weeks after germination. Values are mean ± SD (n = 6 for SPAD and n = 3 for composite expression value). Different letters in (A) indicate significant differences by Tukey-Kramer test at $p < 0.05$. The asterisk in (B) indicates significant differences among treatment groups by one-way analysis of variance at $p < 0.05$.

1.4 Discussion

In this chapter, I examined several physiological parameters in sorghum seedling treated with low N condition, with the aim of identifying biomarkers that might be useful for nutritional stress diagnosis in sorghum cultivation. I first examined morphological changes induced by N deficiency. Plants deficient with N shows characteristic appearance including leaf chlorosis or dwarfism, which may serve as the sign of nutritional disorders. Diagnosis based on visual symptoms is a low cost method requiring no special equipment, and can be conducted easily in the field (Grundon et al., 1987). The effect of N nutrition on morphological traits of sorghum plants was summarized by Szydelko-Rabska and Sowinski (2014). Plant height is one of the parameters remarkable affected by N status (Ikanovic et al., 2013). In this

study, plant height, stem diameter, leaf length, and leaf width of low N and control sorghum seedlings were compared, and all the parameters became different at 9 d after treatment. However, the differences were visually not very remarkable even at that time. In actual situation in the field, "control" plot is usually unavailable. Thus, in the field it would be difficult to identify the N deficiency solely on the morphology, at least in the early stage of deficiency.

Nitrate anion in plants is the fraction of N which has been taken up but unused for growth, thus it can be regarded as surplus and hence the index of N sufficiency of the plants. Diagnosing N status by nitrate concentration in plant sap has been proposed indeed (Wiedenfeld et al., 2009; Awada, 2016). In this study, nitrate concentration was clearly different between the treatment. However, still detectable amounts were present in low N plants even after 9 days after treatment, by the time plant growth has already been impaired (**Figure 1.3B**). This result suggest that the judgement of N sufficiency cannot be rendered solely on the absence or presence of nitrate. In addition, nitrate accumulation can be affected by the factors other than the dose of fertilizers, including light intensity (Chang et al., 2013). Another difficulty is the variety in nitrate concentration among different organs and ages. Gleadow et al. (2016) reported that nitrate content is higher in young seedlings than in older plants. Nitrate content in internal plant tends to be higher in leaf sheaths comparing to other organs in sorghum (Worland et al., 2017), making it difficult to determine at which age and part of plants the analysis should be performed. Considering these points, nitrate-based diagnosis of N sufficiency of sorghum may not be such straightforward.

The SPAD value is a convenient index of the leaf chlorophyll content, which is known to be correlated with the leaf N content. The SPAD values of seedling leaves differed between the treatment groups as early as 6 days after starting the treatment (**Figure 1.4**), which was earlier than the morphological changes became apparent. Changes in SPAD values consistent with the N application regime were also observed in the tests using multiple soil-grown genotypes at different locations (**Figure 1.11**, **Figure 1.13A**, **Figure 1.14A**). These results confirmed that the SPAD value could be a useful marker for early detection of N shortage in sorghum plants.

Eventually, I considered the conditions for the proper measurement of the SPAD value. In the examination using hydroponically cultured seedlings, the correlation between SPAD values and shoot N content was higher in the third fully expanded leaves than in the first and second leaves. Similar results have been reported in rice (Yang et al., 2014; Yuan et al., 2016), and this was probably due to the preferential distribution of N into younger leaves, which makes older leaves more sensitive to N limitations. On the other hand, the position within a single leaf

blade showed no significant effect on the measurement of SPAD values (**Figure 1.10**). This result was different from that reported for rice, which showed significant positional effect within a single leaf blade (Yuan et al., 2016). The reason for this difference is not clear at present, but it might be due to the differences in leaf anatomies of different species (Xiao et al., 2016). Taking the results together, I propose the midpoint of the third-youngest fully expanded leaves as the point of measurement in the SPAD analysis of sorghum.

Homologs of the maize N status marker genes (Yang et al. 2011) were examined for their response to low N. The CEV seemed higher in low N than in control seedlings, but the difference was not statistically significant (**Figure 1.6B**). According to the result, the homolog genes were inappropriate as the N status biomarkers in sorghum plants. Then, I looked for the low N-responsive genes in sorghum via screening with RNA sequencing followed by validation with RT-qPCR. Eleven genes responsive to low-N conditions were identified in sorghum seedlings (**Figure 1.8**). Their CEV was modulated by low-N treatment faster than any other parameter examined in this study. These results suggest that gene expression analysis can be useful as a tool for early and sensitive detection of N deficiency in sorghum plants. In the case of soil-grown sorghum plants, the CEV calculated from this specific set of genes did not respond clearly to N status, yet I observed trends generally consistent with the regime of N application (**Figures 1.12-14**). Thus, the gene expression analysis could be made applicable for practical purposes if more suitable marker genes are selected. The CEV of 11 genes selected in this study was lower in soil-grown plants than in hydroponically cultured seedlings under both N-sufficient and -deficient conditions (**Figure 1.8** and **Figures 1.12-14**). These 11 genes might be highly expressed in the young seedling stage but not in the later growth stages, and hence the extent of modulation might be modest in soil-grown plants even under N limitation. In this study, I used a strategy to screen marker genes in seedlings grown under controlled laboratory conditions to ensure reproducibility between trials. However, using plants growing under real field conditions may be more appropriate to identify practically usable marker genes, although more trials would be necessary to isolate true N-responsive genes out of the numerous genes induced by environmental fluctuations.

Chapter 2

Plant nitrogen status modulates cell wall composition in *Sorghum bicolor*

2.1 Introduction

The impact of N supply on sorghum biomass accumulation has been well documented (Adams et al., 2015; Sowiński & Głąb, 2018). However, information on the effect of N status on the quality of sorghum biomass is limited. The quality of biomass as the feedstock for energy production depends on its composition. When sorghum bagasse is considered as a lignocellulose feedstock for bioethanol production, the contents and composition of polysaccharide and lignin would be the matter. The major polysaccharides in sorghum cell wall, which is the principal components of the bagasse, include cellulose and hemicelluloses such as noncrystalline (1→4)-β-D-glucans, mixed linkage (1→3), (1→4)-β-D-glucan (MLG), arabinoxylan, glucuronoxylan, or xyloglucan (Goto et al., 1991). Both the glucans and xylans can be utilized in liquid biofuel production after decomposed to the component monosaccharides, hence the contents and composition of polysaccharides are important properties of biomass. Lignin is the polymers of phenylpropanoids that fortify the cell wall structure. As such, higher lignin content can lead to higher cell wall recalcitrance, which reduces the efficiency of ethanol production from the cell wall (Boerjan et al., 2003; Ralph et al., 2004; Umezawa, 2010). On the other hand, higher lignin content gives higher heating value, thus it can be a merit when the cell wall, or bagasse, is considered as the source of solid biofuels such as pellet, chip, or biochar. As another class of aromatic compounds, hydroxycinnamates such as ferulic acids (FA) and *p*-coumaric acid (*p*CA) also occur in sorghum cell walls, to provide ester cross-linking between polymers. The hydroxycinnamates also affect the cell wall digesbility (Sato-Izawa et al., 2020).

There have been several reports on the impact of N supply on these cell wall components in grasses. For example, lignin content was decreased by N fertilizer application in rice (*Oryza sativa*) (Zhang et al., 2017), maize (*Zea mays*) (Sun et al., 2018), and Brachypodium (*Brachypodium distachyon*) (Głazowska et al., 2019). In contrast, in giant miscanthus (*Miscanthus* × *giganteus*), N fertilizers increased cell wall lignin content (Arundale et al., 2015). While, N supply did not significantly affect lignin content in two genotypes of sugar cane (*Saccharum* spp.) (Salvato et al., 2017). These findings suggest that the N supply-induced modulation of cell wall components differs among plant species. Therefore, in this

chapter, I investigated N deficiency-induced changes in sorghum cell walls, with the aim of getting insights on the effects of N nutrition status on the quality of sorghum cell wall as the feedstock for biomass energy production. The study was conducted with hydroponically cultured seedlings as the model system, and the properties of cell walls from N-deficient plants were compared with those from the plants receiving sufficient amount of N, through a comprehensive analysis of chemical, two-dimensional short-range ^{1}H-^{13}C heteronuclear single quantum coherence (HSQC) nuclear magnetic resonance (NMR), gene expression, immunohistochemical, and enzymatic saccharification analyses.

2.2 Materials and Methods

2.2.1 Plant growth condition and treatment

2.2.1.1. Seedling stage – Hydroponic culture

As a main experimental setup of this study, the seedlings of sorghum (*S. bicolor*) cv. BTx623 were cultivated hydroponically in a culture room and subjected to low-N treatment, as previously described in Chapter 1.

Two additional experimental setups were also conducted, including:

2.2.1.2. Mature stage – Hydroponic culture

The one-week-old seedlings of sorghum (*S. bicolor*) cv. BTx623 were cultured hydroponically in the full-strength Yoshida B medium and incubated in the greenhouse for four weeks. The 5-week-old seedlings were transferred to the Yoshida B culture medium containing 0.25, 2.5, or 5 mM N as low-, medium-, or high-N treatment, respectively. The aerial parts of the 13-week-old (eight weeks after N treatments) sorghum cell walls at early heading stage were used for lignin content and composition analyses.

2.2.1.3. Mature stage – Soil culture

A field experiment using 1-m^2 containers was carried out using four sorghum genotypes; BTx623, G247, Tanshaku (commercial dwarf sorghum), and Koutoubun-DH (commercial sweet sorghum). The soil was supplemented with N fertilizer (urea) with either 200 or 400 kg N ha^{-1} as medium- or high-N treatment, respectively. Two containers were prepared for each treatment. The cell walls of sorghum plants at seed ripening stage were used for lignin content and composition analyses.

2.2.2 Chlorophyll content determination

Chlorophyll content was measured in the third youngest fully expanded leaves, as previously described in Chapter 1, using the Soil Plant Analysis Development (SPAD)-502 plus chlorophyll meter.

2.2.3 Nitrogen content analysis

For N content analysis, the aerial parts of the 6-week-old (3 weeks after low-N treatments) seedlings were dried in an oven at 70 °C and pulverized to a fine powder using a T-351 pulverizing machine (Rong Tsong Iron Co., Taichung, Taiwan). The nitrogen content was analyzed using an NC analyzer as previously described in Chapter 1.

2.2.4 Cell wall preparation

The cell wall residue (CWR) was prepared as described previously (Yamamura et al., 2012) using the same dried powder sample as for N content analysis. The powder sample was further pulverized to a finer powder (TissueLyser, Qiagen, Hilden, Germany). The powder was sequentially extracted 20 times with methanol at 60 °C, five times with hexane at room temperature, and five times with distilled water at 60 °C. The residue was freeze-dried to obtain the CWR.

2.2.5 Lignin content and composition analyses

Lignin content of CWR was determined using a thioglycolic acid lignin method (Suzuki et al., 2009). The ultraviolet absorbance of thioglycolic acid lignin was measured at 280 nm using an SH-1000 lab microplate reader (Corona Electric Co., Ltd., Ibaraki, Japan).

Determination of lignin composition was conducted by a thioacidolysis analysis. The assay was performed as previously described (Yamamura et al., 2012). The released lignin monomers were derivatized with *N*,*O*-bis(trimethylsilyl) acetamide and quantified by gas chromatography-mass spectrometry (GC-MS) (GCMS-QP 2010 Ultra, Shimadzu, Kyoto, Japan) using 4,4'-ethylenebisphenol as an internal standard (Yue et al., 2012).

2.2.6 Alkaline-releasable *p*-hydroxycinnamic acid content analysis

Cell wall-bound *p*CA and FA were released by a mild-alkaline treatment and quantified by GC-MS, as previously described (Yamamura et al., 2011). Approximately 10-mg aliquots of CWR samples were placed in tubes and mixed with 1 M NaOH (1.5 mL), then degassed with oxygen-free N_2. The suspension was incubated at 25 °C for 24 h with gentle shaking. The

suspension was centrifuged and the supernatant was transferred to a new tube, *o*-coumaric acid was added as an internal standard, then subjected to GC-MS analysis.

2.2.7 Glycosyl residue composition and crystalline cellulose analyses

Glycosyl residue composition was determined by alditol acetate methods (Hayashi, 1989). Approximately 15 mg of CWR samples were suspended in a 540 µL thermostable α-amylase (Megazyme, Bray, Ireland) solution that was diluted 30-fold with 100 mM sodium acetate buffer, then incubated at 100 °C for 12 min. The suspension was cooled to about 40 °C, added with 18 µL of amyloglucosidase (Megazyme), and incubated at 50 °C for 30 min. The residue was washed twice with distilled water and twice with methanol, then dried under vacuum for 2 h. An aliquot of the destarched CWR was subjected to a hydrolysis with 2 M TFA at 100 °C for 5 h. The released monosaccharides were reduced with sodium borohydride and converted to alditol acetates using acetic anhydride. The alditol acetates were quantified using GC-MS (GCMS-QP 2010 Plus, Shimadzu) equipped with SP-2330 column (30 m × 0.25 mm × 0.2 µm film thickness, SUPELCO, Bellefonte, PA, USA) using *myo*-inositol as an internal standard.

The residues left after hydrolysis were used to quantify the crystalline cellulose. The residues were added to the Updegraff reagent (Updegraff, 1969) and heated at 100 °C for 30 min, washed twice with distilled water and acetone, and then hydrolyzed with 72% sulfuric acid (Hattori et al., 2012) at 30 °C for 1 h. The released glucose was quantified using the Glucose CII test kit (Wako Pure Chemicals Industries, Osaka, Japan).

2.2.8 Uronic acid content analysis

Uronic acid content of CWR was measured by the *m*-hydroxydiphenyl assay (Blumenkrantz & Asboe-Hansen, 1973) using galacturonic acid as a standard. The absorbance was measured at 520 nm using an SH-1200 lab microplate reader (Corona Electric Co., Ltd.).

2.2.9 Calcium content analysis

Cell wall calcium content was determined by atomic absorption spectroscopy (AA-6200, Shimadzu) after digesting the CWR with nitric and sulfuric acids.

2.2.10 Methylation analysis

Polysaccharides in CWR were methylated using NaOH and methyl iodide (Wang et al., 1995). To the CWR (10 mg) suspended in 600 µL DMSO, 600 µL of NaOH-DMSO suspension, and 300 µL of methyl iodide were added. The suspension was sonicated for 5 min and incubated at ambient temperature for 3.5 h with stirring. After adding 900 µL of distilled water, the per-*O*-methylated CWR was rinsed with chloroform, air-dried, and then subjected to hydrolysis of matrix polysaccharides with 4 M TFA at 120 °C for 1 h. Partially methylated monosaccharides released into the supernatant were converted to alditol acetates and analyzed by GC-MS (GCMS-QP 2010 Plus) equipped with SP-2330 column (SUPELCO). The molar ratio of the peaks was calculated using the peak area and the effective carbon-response factors (Sweet et al., 1975).

2.2.11 2D HSQC NMR

Finely ball-milled CWR samples (~60 mg) were swelled in DMSO-d_6/pyridine-d_5 (4:1, v/v) for the gel-state whole cell wall NMR analysis, as described previously (Kim & Ralph, 2010; Mansfield et al., 2012). NMR spectra were acquired on a Bruker Avance III 800US system (800 MHz, Bruker Biospin, Billerica, MA, USA) fitted with a cryogenically cooled 5-mm TCI gradient probe (Bruker Biospin). Adiabatic 2D HSQC NMR experiments were conducted using the standard implementation ('hsqcetgpsp.3') with parameters described in the literature (Kim & Ralph, 2010; Mansfield et al., 2012). Data processing and analysis were performed using the Bruker TopSpin 4.1 software (Bruker Biospin) as described previously (Dumond et al., 2021; Miyamoto et al., 2019; Tarmadi et al., 2018). For volume integration analysis, the aromatic contour signals from lignin and hydroxycinnamates (C2–H2 correlations from **G** and **F**; C2–H2/C6–H6 correlations from **S** and **P**; and C2′–H2′/C6′–H6′ correlations from **T**, **S**, **P**, and **T** integrals were logically halved) and polysaccharide anomeric signals were manually integrated and each signal was normalized based on the sum of the **S** and **G** lignin aromatic signals ($\mathbf{½S_{2/6} + G_2}$) (Dumond et al., 2021).

2.2.12 Immunofluorescent histochemical analysis

The aboveground parts of 3-week-old sorghum seedlings were sampled and fixed in 4% paraformaldehyde in 50 mM phosphate buffer (pH 7.4). Samples were dehydrated in a graded ethanol series (30%, 50%, 70%, 80%, 90%, 95%, and 99.5%) and then embedded in LR White Hard Grade (London Resin Co. Ltd., Reading, UK). For immunofluorescence histochemistry, transverse sections 0.5 µm thick were cut using an Ultracut E microtome (Reichert-Jung,

Vienna, Austria). The sections were blocked with 3% (w/v) skim milk in Tris-buffered saline (TBS; 20 mM Tris-HCl, 154 mM NaCl, pH 8.2) for 30 min and incubated at 4 °C for one d with either of the following monoclonal antibodies: anti-xylan (LM10, PlantProbes), anti-arabinoxylan (LM11, PlantProbes), anti-xyloglucan (LM15, PlantProbes), anti-glucuronoxylan (LM28, PlantProbes), anti-MLG (400-3, Biosupplies, Australia), and anti-callose (400-2, Biosupplies Australia). The sections were washed three times with TBS and incubated at 35 °C for 2 h with either goat anti-rat immunoglobulin (IgG) conjugated to Alexa Fluor 488 (Molecular Probes, Oregon, USA) or with goat anti-mouse IgG conjugated to Alexa Fluor 488 (Molecular Probes) for PlantProbes antibodies or Biosupplies antibodies, respectively. The slides were washed three times with TBS and once with deionized water. After drying, the sections were mounted using ProLong Diamond (Thermo Fisher Scientific, Oregon, USA), and observed under a fluorescence microscope (BX50 with BX-FLA fluorescent light attachment; Olympus, Tokyo, Japan) using a U-MWIB3 filter set (Olympus; 460–490 nm excitation, 515 nm long-pass emission).

2.2.13 Immunogold labeling analysis

For immunogold labeling, ultrathin transverse sections were cut using an Ultracut E microtome and transferred to 300-mesh nickel grids (Nisshin EM Co. Ltd., Tokyo, Japan). The grids were blocked in 20 μL of 0.1% (w/v) sodium azide in TBS containing 1% BSA at room temperature for 30 min. They were then incubated with 20 μL of LM11 and MLG at 4 °C for one day. After washing three times with TBS, the grids were incubated at 35 °C for 2 h either with 10 nm colloidal gold conjugated secondary antibody goat anti-rat IgG or anti-mouse IgG (BBI solutions, Crumlin, UK) for LM11 or MLG, respectively. The grids were washed three times with TBS and once with deionized water, stained with 2% uranyl acetate for 10 min, and then washed again with deionized water. The grids were observed under a JEM-1400 transmission electron microscope (JEOL, Tokyo, Japan) operated at 100 kV.

2.2.14 Gene expression analyses

RNA-sequencing data of sorghum seedlings from the Chapter 1 (accession number DRA010070) were used for the analysis of the change in transcriptome induced within 3 or 6 d after low N treatment. For RT-qPCR analysis, total RNA was extracted from fully expanded uppermost leaves of 6-week-old (3 weeks after low-N treatments) seedlings using the Total RNA Extraction Kit Mini (Plant) (RBC Bioscience, New Taipei City, Taiwan) according to

the manufacturer's instructions with on-column deoxyribonuclease treatment. First-strand cDNA was synthesized as described previously in Chapter 1 using ReverTraAce DNA polymerase (Toyobo, Osaka, Japan). Quantitative PCR analyses were performed as previously described previously in Chapter 1 using KDO SYBR qPCR mix (Toyobo) on TaKaRa PCR Thermal Cycler Dice Real Time System II TP 960 (Takara Bio, Shiga, Japan). The primers used for PCR are listed in **Table 2.1**. The amounts of the targets were estimated by ΔΔCt method using the gene encoding a serine/threonine-protein phosphatase (PP2A) as an internal control (Reddy et al., 2016).

2.2.15 Enzymatic saccharification analysis

Enzymatic saccharification analysis of CWR was performed as previously described (Hattori et al., 2012). Briefly, CWR samples were destarched and suspended with an enzyme cocktail containing Celluclast 1.5 L (Novozymes, Bagsvaerd, Denmark) (1.1 filter paper units), Novozyme 188 (Novozymes) (2.5 cellobiase units), and Ultraflo L (Novozymes) (65 μg) in sodium citrate buffer (pH 4.8). The reaction mixture was incubated in a rotary heat-block at 50 °C for 24 h. Quantification of the released glucose was performed using a Glucose CII test kit.

Table 2.1. List of primers used for reverse transcription-quantitative PCR analysis.

Gene name	Gene ID	Forward primer (5′→3′)	Reverse primer (5′→3′)
CESA	Sb02g010110	TAATGTTGCCAGCCTGTGGT	GAACACAGCAAAGAGGTGCG
CSL	Sb07g004110	CTCTCCTACAACTGGCCGTG	GCCGCCTCACCATATCATCA
Endo-1,4-β glucanase	Sb01g008860	CAAGTTTGCCAGGTCACAGC	GCGCTTCGGGTACTTGTTTC
Pectate lyase	Sb08g004905	CCACCATGGCCAGAGGTATG	CTCAGGAGCTTGGATAGCGG
Glucan-1,3-β-glucosidase	Sb03g045460	GGCTCACCTACACCAACCTG	GCCCCTGGTTGTACTTCCTC
GAUT	Sb01g012060	GCCGAGAGAGAAAAGCCGAG	TCAGGCGAGGTAAATGGTGG
EXP	Sb03g038290	CAGTTCTAGCACGCCCCTC	AGGAAATGCCTAAGCGGGTG
XTH	Sb10g028570	GATAAGTACCGCTTCCCGCA	CAAGTCATCATGCACACGGC
GSL	Sb04g038510	CTTATCAAACTGCCGCCGTG	TGCGTCTCGAGAATCGACTG
LAC	Sb03g039970	CCTTCCTCAGCACAAGGAGC	CGAGGTTCCCGGTTGATCTC
RG-I lyase	Sb07g024560	AGGGAGAACGCGATAGCAAG	CAATCCCTGAAACGGGCTCT
PAL	Sb04g026520	CCAAAGTACAGCGGCTCAAG	CAAGAACATGCGCATTGCAG
4CL/ Bmr2	Sb04g005210	CATCTCCAAGCAGGTGGTGT	ATTGCACGTAACAAGGCACG
CAD/ Bmr6	Sb04g005950	TACCCTATGGTCCCTGGGC	GCCGTCAGTGTAGACATCGT
C3'H	Sb09g024210	ACCTTCTGCACCACTTCGAG	AGGCACCTCACATCTCAACG
F5H/ CAld5H	Sb01g017270	ATGGCGGAGATGATGCACAG	CGTCTCCTTGATGACGCACT
COMT/ CAldOMT/ Bmr12	Sb07g003860	TTAATGGCCTAGCCTGCCTC	CGCAGAGACAATTCGACAGC
PP2A	XM_002453490	AACCCGCAAAACCCCAGACTA	TACAGGTCGGGCTCATGGAAC

CESA: *Cellulose synthase A*, *CSL*: *cellulose synthase-like*, *GAUT: homogalacturonan α-1,4-galacturonosyltransferase, EXP*: *expansin, XTH*: *xyloglucan endotransglucosylase/hydrolase*, *GSL*: *glucan synthase-like/callose synthase*, *LAC*: *laccase*, *RG-I*: *rhamnogalacturonan I*, *PAL*: *phenylalanine ammonia-lyase*, *4CL*: *4-coumarate CoA ligase*/*Brown midrib 2* (*Bmr2*), *CAD*: *cinnamyl alcohol dehydrogenase*/*Brown midrib 6* (*Bmr6*), *C3'H*: *p-coumaroyl ester 3-hydroxylase*, *F5H*: *ferulate 5-hydroxylase* (=*coniferaldehyde 5-hydroxylase*, *CAld5H*), *COMT*: *caffeate/5-hydroxyferulate* O-*methyltransferase* (=*5- hydroxyconiferaldehyde* O-*methyltransferase*, *CAldOMT*)/*Brown midrib 12* (*Bmr12*), and *PP2A*: *serine/threonine-protein phosphatase.*

2.3 Results

2.3.1 Lignin content and composition

The hydroponically grown sorghum seedlings were cultivated using a standard culture medium and a medium containing a low level of N (1/10th), as control and low-N treatments, respectively. The low-N treatment apparantely inhibited the plant growth as shown in **Figure 2.1**. Furthermore, the treatment reduced the dry weight of seedlings by 51%, with decreased chlorophyll and N contents (**Figure 2.2**). The result confirmed that the seedlings were indeed under N deficient condition in this study.

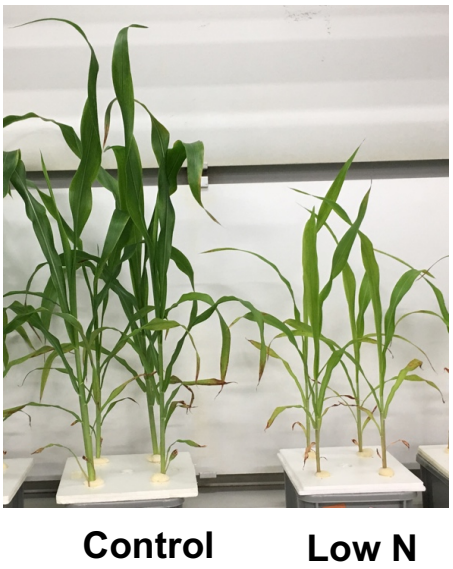

Figure 2.1. The appearance of hydroponically grown sorghum seedlings at 3 weeks after low-N treatment.

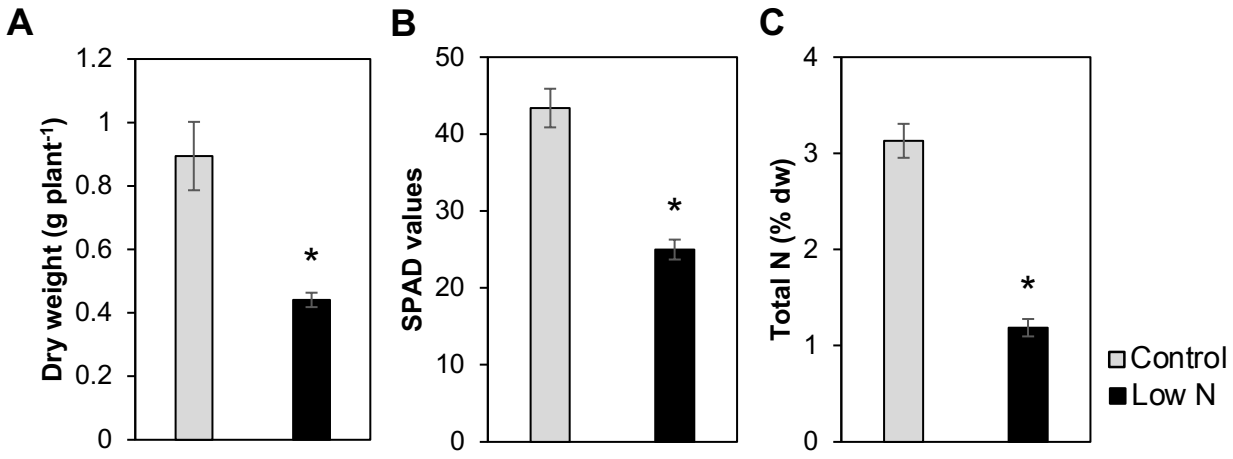

Figure 2.2. Effect of low-N treatment on hydroponically grown sorghum seedlings growth. (**A**) Dry weight, (**B**) soil-plant analysis development (SPAD) values, and (**C**) N content of hydroponically grown sorghum seedlings cultivated under control or low-N condition at 3 weeks after treatment. Values are means ± SD (n = 3). Asterisks indicate significant differences between control and low-N plants. (Student's *t* test, $p < 0.05$).

The impacts of low-N treatment on cell wall properties of hydroponically sorghum seedlings were then examined by a series of chemical analyses. First, the thioglycolic acid lignin analysis revealed that N supply did not affect lignin content significantly (**Figure 2.3**). However, the lignin-aromatic composition was modulated, as revealed by 27% decrease of thioacidolysis-derived syringyl/guaiacyl monomer (S/G) ratio in low-N plants as compared to control plants (**Figure 2.3**). The change was ascribed to a 48% increase of G-type lignin monomer yield under low-N condition (**Figure 2.3**).

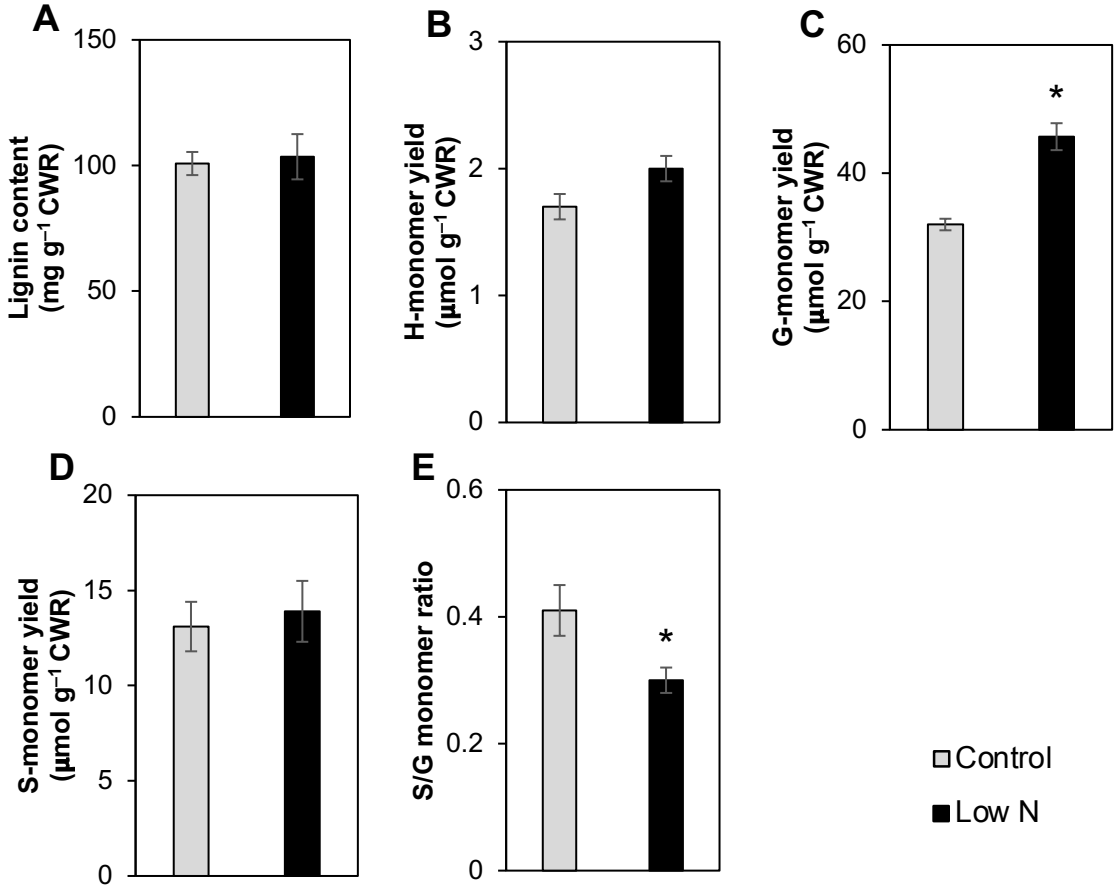

Figure 2.3. Effect of low-N treatment on lignin content and composition of hydroponically grown sorghum seedlings cultivated under control or low-N condition at 3 weeks after treatment. (**A**) Lignin content, (**B**) *p*-hydroxyphenyl (H)-monomer yield, (**C**) guaiacyl (G)-monomer yield, (**D**) syringyl (S)-monomer yield, and (**E**) S/G monomer ratio. CWR: cell wall residue. Values are given as mean ± SD (n = 3). Asterisks indicate significant differences between control and low-N plants (Student's *t* test, $p < 0.05$).

In order to confirm the unchanged lignin content and alteration of lignin composition by N level in more mature plants, two additional experiments were conducted both in hydroponic and soil cultures. I found that lignin content was not significantly affected by the level of N supply in more mature sorghum plants both in hydroponic and soil cultures (**Figure 2.4A**, **Figure 2.5A)**. The level of N supply modified the lignin composition in hydroponically grown mature sorghum plants, as shown by the lower thioacidolysis-derived S/G ratio in low-N plants compared to high-N plants (**Figure 2.4B)**. While, the lignin composition was not substantially modulated by the level of N supply in four examined sorghum genotypes cultivated in soil culture (**Figure 2.5B)**.

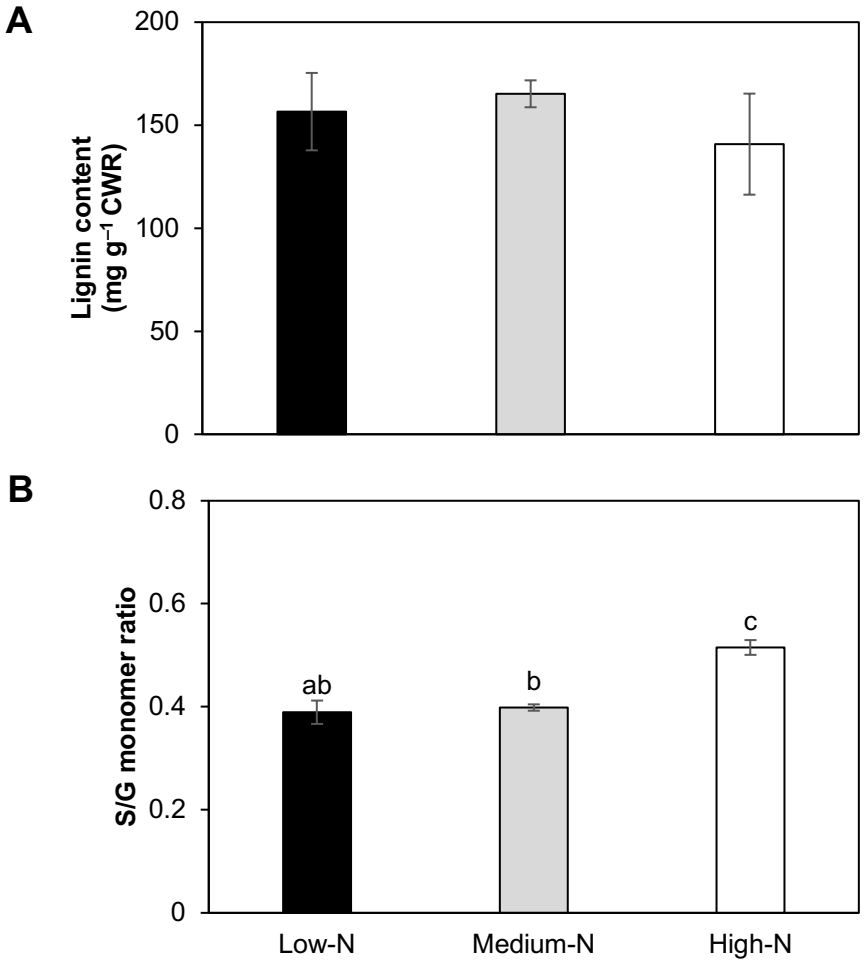

Figure 2.4. Effect of the level of N supply on lignin content and composition of hydroponically grown mature sorghum plants at the heading stage (13-week-old) cultivated under low-, medium-, or high-N treatment. **(A)** Lignin content, and **(B)** S/G monomer ratio. Bars are means ± SD (n = 3). Different letters mean a significant difference (Tukey-Kramer test, $p < 0.05$).

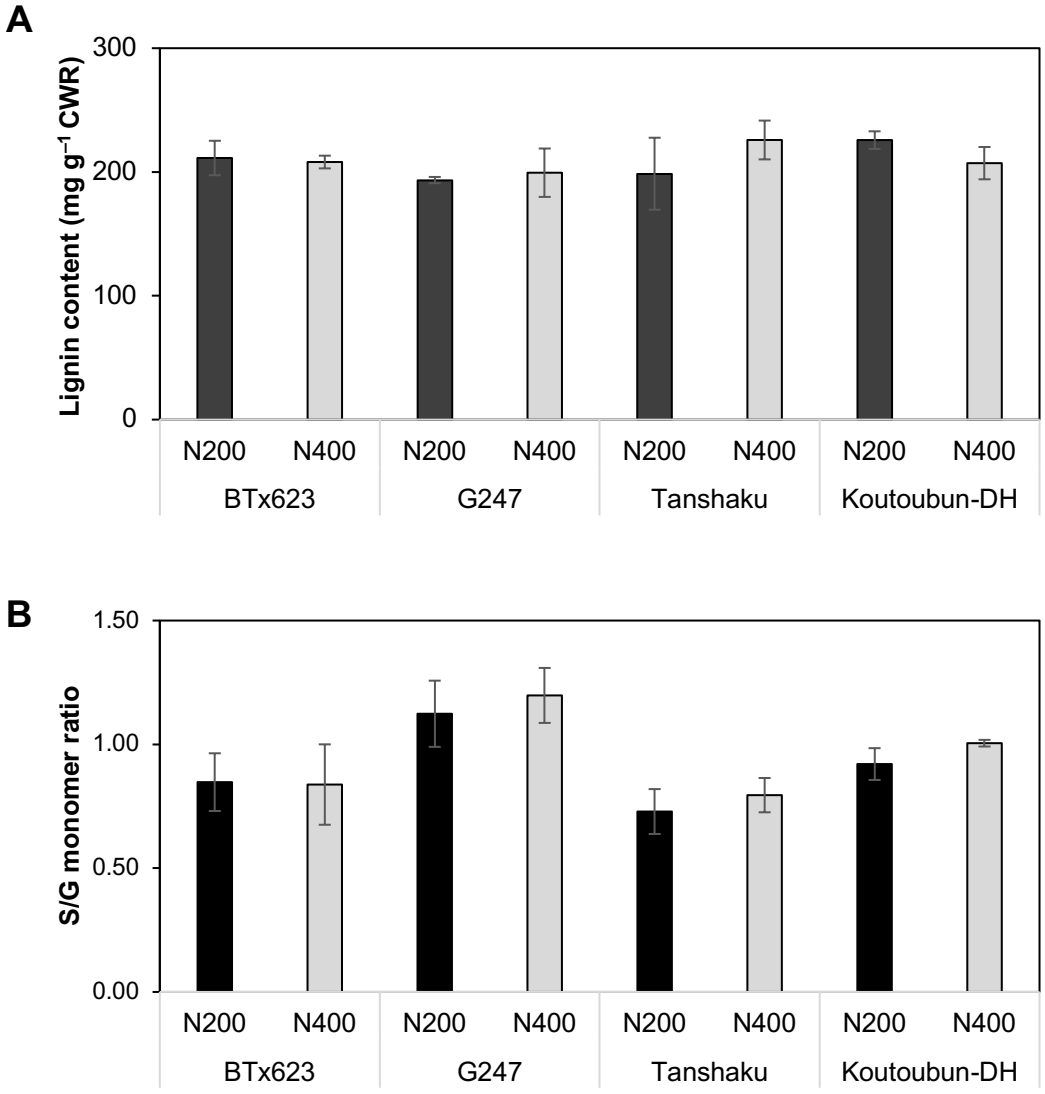

Figure 2.5. Effect of the level of N supply on lignin content and composition of four genotypes of soil grown mature sorghum plants cultivated under 200 or 400 kg N ha^{-1} treatment (N200 or N400, respectively). **(A)** Lignin content, and **(B)** S/G monomer ratio. Bars are means ± SD (n = 3).

To definitely observe the early impact of N level on sorghum cell wall properties and to minimize the intervention from other factors, the further analyses were conducted using the samples from hydroponically grown sorghum seedlings throughout this study.

2.3.2 Cell wall-bound *p*-hydroxycinnamic acid content

Content of cell wall-bound *p*CA, which possibly attached to lignin, was not different between control and low-N plants. Contents of FA, which cross-links arabinoxylans to each other and to lignin, was increased by 56% under low-N condition (**Figure 2.6**).

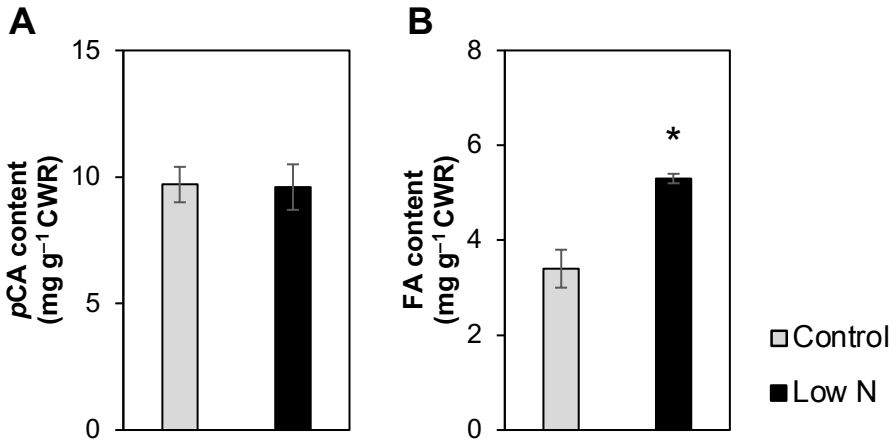

Figure 2.6. Effect of low-N treatment on cell wall-bound *p*-hydroxycinnamic acid content of hydroponically grown sorghum seedlings cultivated under control or low-N condition at 3 weeks after treatment. (**A**) *p*-Coumarate (*p*CA) content, and (**B**) ferulate (FA) content. CWR: cell wall residue. Values are given as mean ± SD (n = 3). Asterisks indicate significant differences between control and low-N plants (Student's *t* test, $p < 0.05$).

2.3.3 Polysaccharide fraction of cell wall

Concerning the polysaccharide components, the content of crystalline cellulose tended to be higher in low-N plants (**Figure 2.7**). The glycosyl residue composition analysis of the trifluoroacetic acid (TFA)-soluble fraction indicated that the low-N plants contained more arabinosyl, xylosyl, galactosyl, and glucosyl residues than control plants (**Figure 2.7**). The change in glucose content was most remarkable, as it increased more than two-fold upon low-N treatment. Meanwhile, the uronic acid and calcium (Ca) contents were decreased by 18% and 45% in low-N plants, respectively (**Figure 2.7**).

Furthermore, methylation analysis revealed the presence of at least 16 glycosyl residues with different linkages in the cell wall of sorghum seedlings (**Table 2.2**). Of the sugar residues listed in **Figure 2.7**, content of mannose, which probably derived from mannan, remained unaffected by low-N treatment. Hence, the abundance of detected residues was estimated as the relative amount to 4-linked mannosyl residue. The residues appearently increased by low-N treatment include 3- or 4-linked glucosyl and 4- or 3,4-linked xylosyl residues (**Table 2.2**). The increase in the amount of 3-linked glucosyl residue suggested an increase of callose [(1→3)-β-D-glucan] and/or MLG, whereas the increase of 4-linked glucosyl residue suggested an increase of noncrystalline (1→4)-β-D-glucan. The increased amount of 4- and 3,4-linked xylosyl residues were possibly due to an increase of xylans with or without substitution, such as xylan, arabinoxylan, or glucuronoxylan.

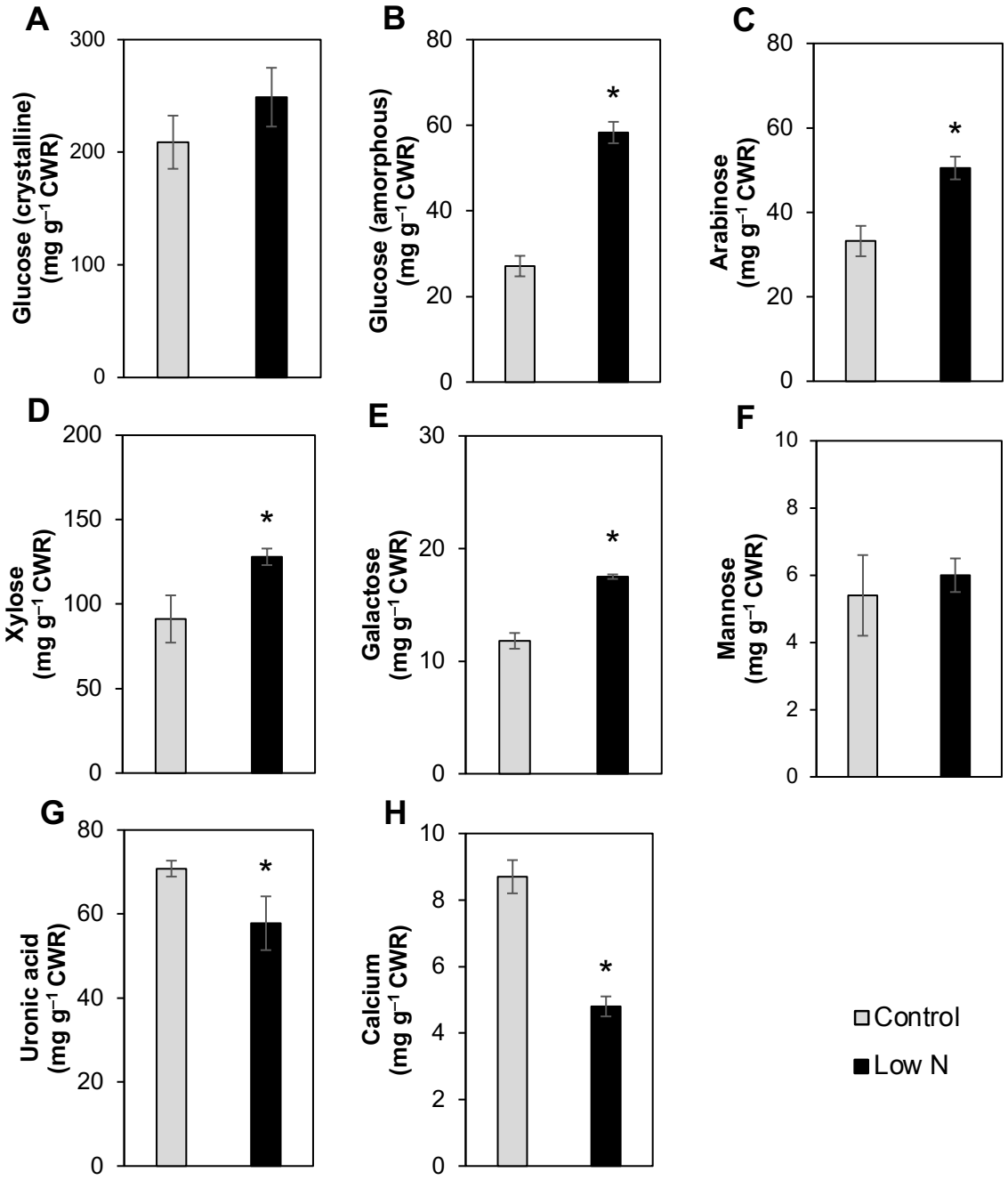

Figure 2.7. Cell wall mineral and polysaccharides contents of hydroponically grown sorghum seedlings cultivated under control or low-N condition at 3 weeks after treatment. (**A**) Glucose content from crystalline cellulose, (**B**) glucose content from matrix polysaccharides, (**C**) arabinose content, (**D**) xylose content, (**E**) galactose content, (**F**) mannose content, (**G**) uronic acid content, and (**H**) calcium content. CWR: cell wall residue. Values are given as mean ± SD (n = 3). Asterisks indicate significant differences between control and low-N plants (Student's *t* test, $p < 0.05$).

Table 2.2. Glycosyl linkage composition of the cell walls of hydroponically-grown sorghum seedlings cultivated under control and low-N conditions at 3 weeks after treatment.

Residue	Position of *O*-CH_3 group	Deduced linkage	Relative abundance	
			Control	Low N
Arabinose	3,5	2-linked furanose	0.35	0.33
	2,5	3-linked furanose	0.59	0.62
	2,3	4-linked pyranose	1.53	1.65
Xylose	2,3,4	terminal	0.77	1.08
	2,3	4-linked pyranose	5.35	8.46
	2	3,4-linked pyranose	2.53	3.67
Galactose	2,3,4,6	terminal	1.17	0.86
	3,4	2,6-linked	0.37	0.15
	2,4	3,6-linked	0.96	0.88
	2,3	4,6-linked	2.31	2.08
Glucose	2,3,4,6	terminal	2.29	4.51
	2,4,6	3-linked	0.94	1.11
	2,3,6	4-linked	13.13	21.47
Mannose	2,3,4,6	terminal	0.43	0.39
	2,3,6	4-linked	1.00	1.00
	2,6	3,4-linked	0.81	0.84

Relative abundance of the residues was calculated as molar ratio relative to 4-linked mannosyl residue. The averages of duplicate (control) or triplicate (low-N) determinations are shown. Values are the average of two (control) or three (low N) replicate samples.

2.3.4 2D HSQC NMR

In order to further investigate the low N-induced alteration of cell wall composition and structure suggested by chemical analyses, I conducted two-dimensional short-range ^{1}H-^{13}C HSQC NMR analysis. The relative intensities of G-lignin unit and FA signals with respect to total lignin aromatic signals (S + G) were increased in low-N plant cell walls compared with those in control plant cell walls (**Figure 2.8**). The result is in accordance with the data from chemical analysis (**Figure 2.3**) in that thioacidolysis monomer yield of G-lignin unit and FA content were increased by low-N treatment. The S/G ratio estimated based on the NMR signal intensities was lower in the cell wall of low-N plants than that in the cell wall of control plants (**Figure 2.8**), which was also consistent with the result of chemical analysis (**Figure 2.3**).

In terms of sugar components, the relative intensities of glucose, arabinose and galactose signals per total lignin aromatic signals (S + G) were higher in low N plants than in control plants (**Figure 2.8**), which was also in agreement with the results of chemical analysis (**Figure 2.7**). It is currently unclear why xylose signal was not modulated by low N treatment in NMR analysis (**Figure 2.8**), whereas it was found to be increased by low N treatment in the chemical analysis (**Figure 2.7**). The relative intensity of glucuronic acid signal was apparently lower in the cell wall of low N plants than in the cell wall of control plants (**Figure 2.8**), which could be consistent with the observed decrease in uronic acid content in chemical analysis (**Figure 2.7**).

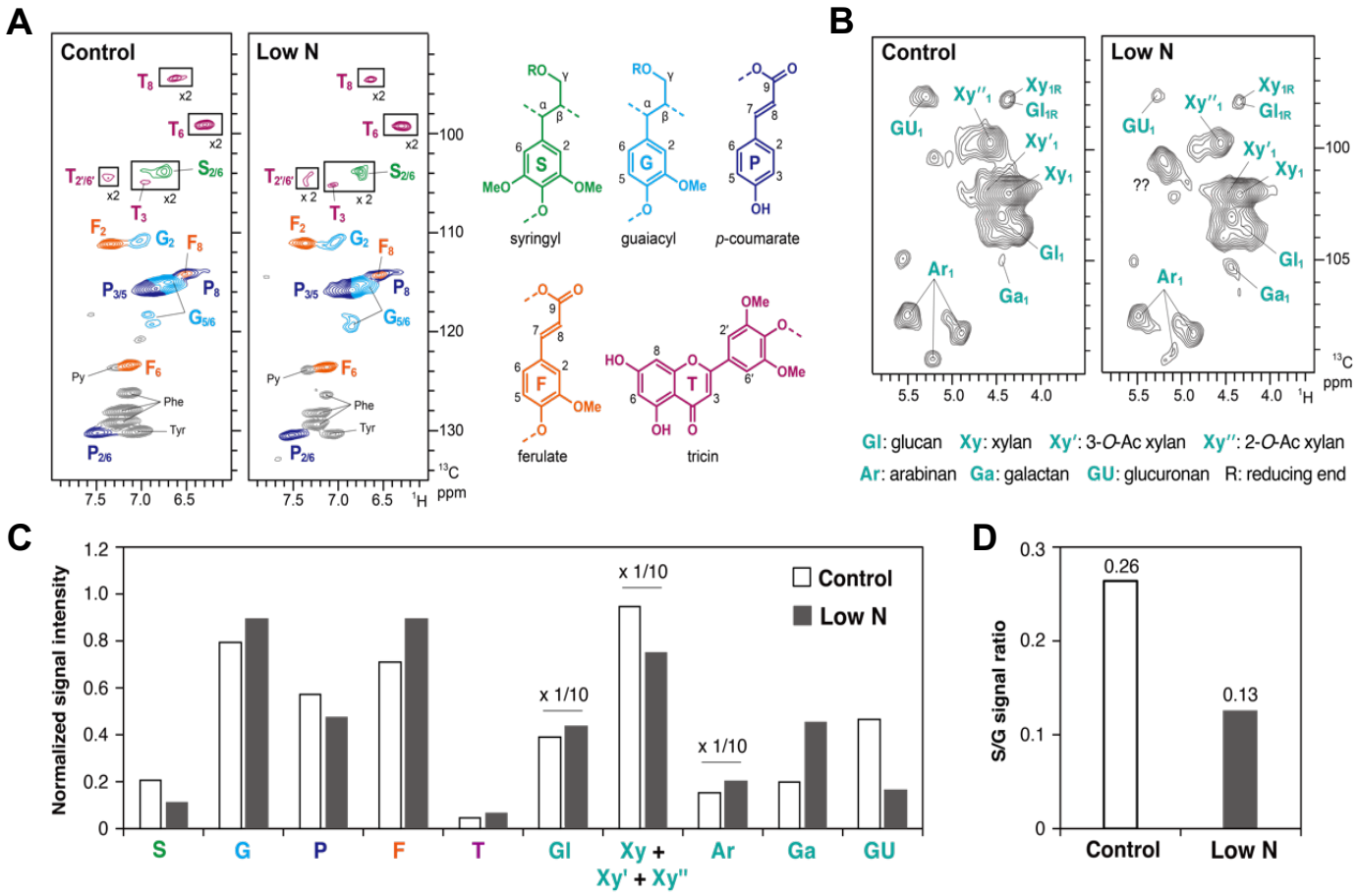

Figure 2.8. Two-dimensional short-range ^{1}H-^{13}C correlation nuclear magnetic resonance (2D HSQC NMR) spectra of the cell walls of hydroponically-grown sorghum seedlings cultivated under control and low-N conditions at 3 weeks after treatment. The NMR spectra were acquired with composite samples prepared from three replicates. (**A**) Aromatic sub-regions showing signals from major lignin hydroxycinnamate aromatic units. Contours are color-coded to match the displayed structures. Boxes labeled x 2 means regions with scale vertically enlarged 2-fold. (**B**) Anomeric sub-regions showing signals from major cell wall polysaccharide units. Py, pyridine (solvent). (**C**) Normalized intensity of major lignin, hydroxycinnamate and polysaccharide signals expressed on a S + **G** = 1 basis. Data labeled x 1/10 indicate that the reported values are divided by a factor 10 for visualization purposes. (**D**) S/G signal ratio.

2.3.5 Immunofluorescent histochemistry

The abundance and localization of several glucans and xylans were examined by immunostaining. In sections from the aboveground part of sorghum seedlings, which mainly consisted of developing leaf sheath and leaf blade tissues, fluorescence signals from anti-MLG antibody and anti-(1→3)-β-D-glucan (callose) antibody were distributed in all parts of the section, including epidermal, mesophyll, cortical, and vascular tissues (**Figure 2.9**). These signals from both anti-MLG and callose antibodies in cortical sclerenchyma were more intense in low-N plants than in control plants. Conversely, the signals in epidermal tissues were lower in low-N plants than in control plants (**Figure 2.9A**). Signals from anti-xyloglucan antibody (LM15) were present only in phloem and curved epidermal tissues and were stronger in low-N plants than in control plants (**Figure 2.9A**). The fluorescence signals from the antibodies recognizing arabinoxylan (LM11) and xylan (LM10) occurred specifically in epidermal tissues and vascular bundles, and the signals were more intense in low-N plants than in control plants (**Figure 2.9B**). These signals were also detected in epidermal cells in low-N plants, but not in the control plants (**Figure 2. 9B**). Mesophyll cells were not stained by antibodies in either low-N or control plants. The fluorescence signal from anti-glucuronoxylan antibody (LM28) was present in vascular bundles, excluding cortical sclerenchyma cells, but not in epidermal or mesophyll tissues in both low-N and control plants. Glucuronoxylan signals in vascular bundles were more intense in low-N plants than in control plants (**Figure 2. 9B**). Taken together, these results suggest that the amounts and/or distribution of several glucans and xylans were modified under low-N conditions.

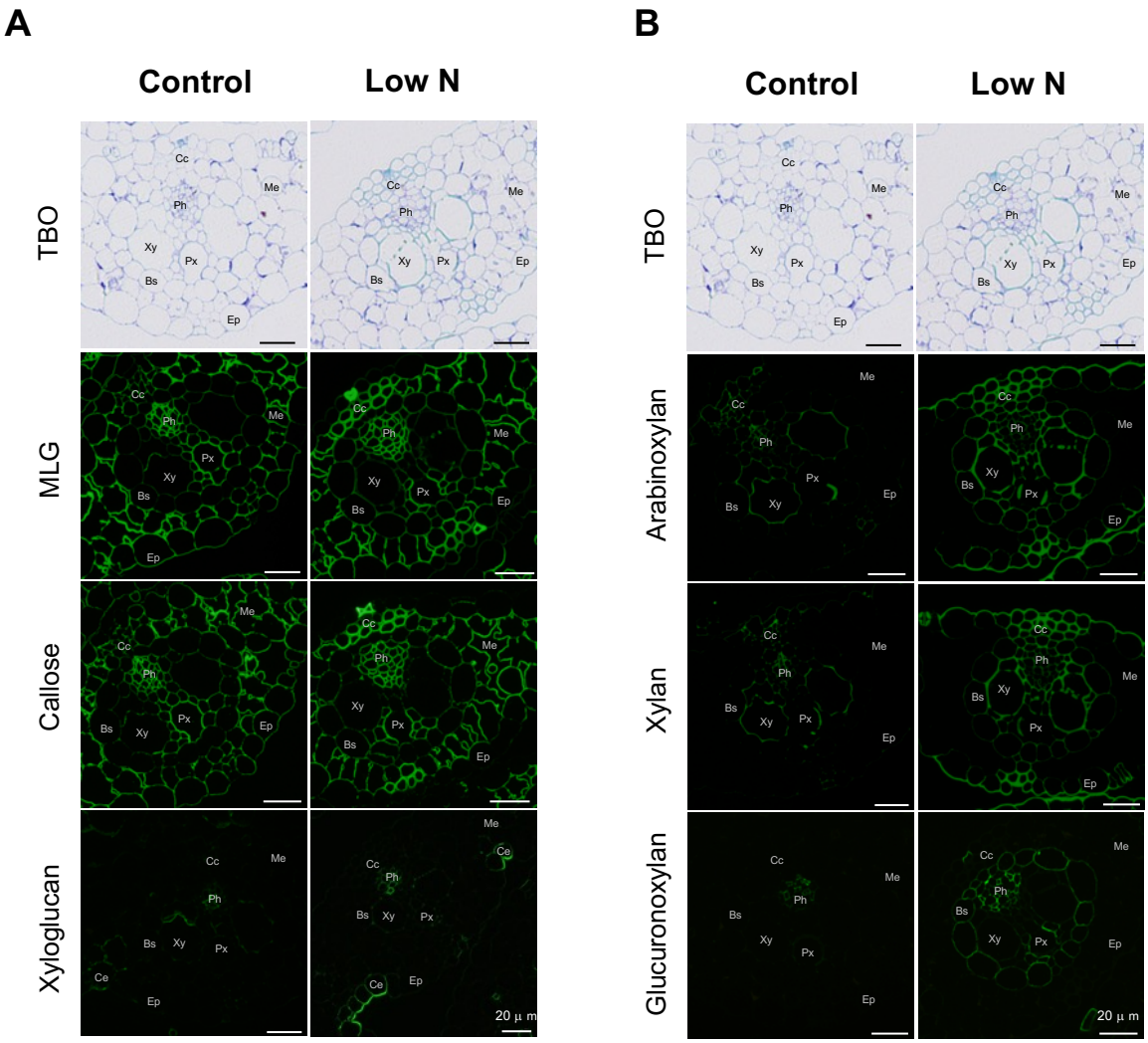

Figure 2.9. Immunofluorescent histochemical analyses of hydroponically grown sorghum seedlings cultivated under control or low-N conditions at 3 weeks after treatment. (**A**) Immunofluorescent labeling of glucose-containing polysaccharides using anti-mixed-linkage (1→3), (1→4)-β-D-glucan (MLG), (1→3)-β-D-glucan (callose), and xyloglucan antibodies, and (**B**) Immunofluorescent labeling of xylose-containing polysaccharides using anti-arabinoxylan, xylan, and glucuronoxylan antibodies, Ep: epidermal tissues, Ce: curved epidermal tissues, Cc: cortical cells, Me: mesophyll tissues, Bs: bundle sheath, Xy: xylem, Px: protoxylem, Ph: phloem.

2.3.6 Immunogold labeling analysis

As MLG and arabinoxylan are the two most abundant hemicellulosic polysaccharides in cell walls of young, elongating organs of grasses (Peng et al., 2012), I investigated their abundance and distribution in low-N and control seedlings using immunoelectron microscopy. With the anti-MLG antibody, the labeling in the cortical cell and xylem walls was more abundant in low-N plants than in control plants. In contrast, essentially no labeling was observed in the secondary cell walls of low-N plant epidermal cells, whereas abundant labeling was found in the corresponding region of control plants (**Figure 2.10A**). With the anti-arabinoxylan antibody, cortical cell and xylem walls in low-N plants were labeled more heavily than those of control plants (**Figure 2.10B**). The difference in labeling abundance was more apparent in the secondary cell walls of the epidermal tissues (**Figure 2.10B**). These results are in line with the observation in immunofluorescence microscopy analysis (**Figure 2.9**).

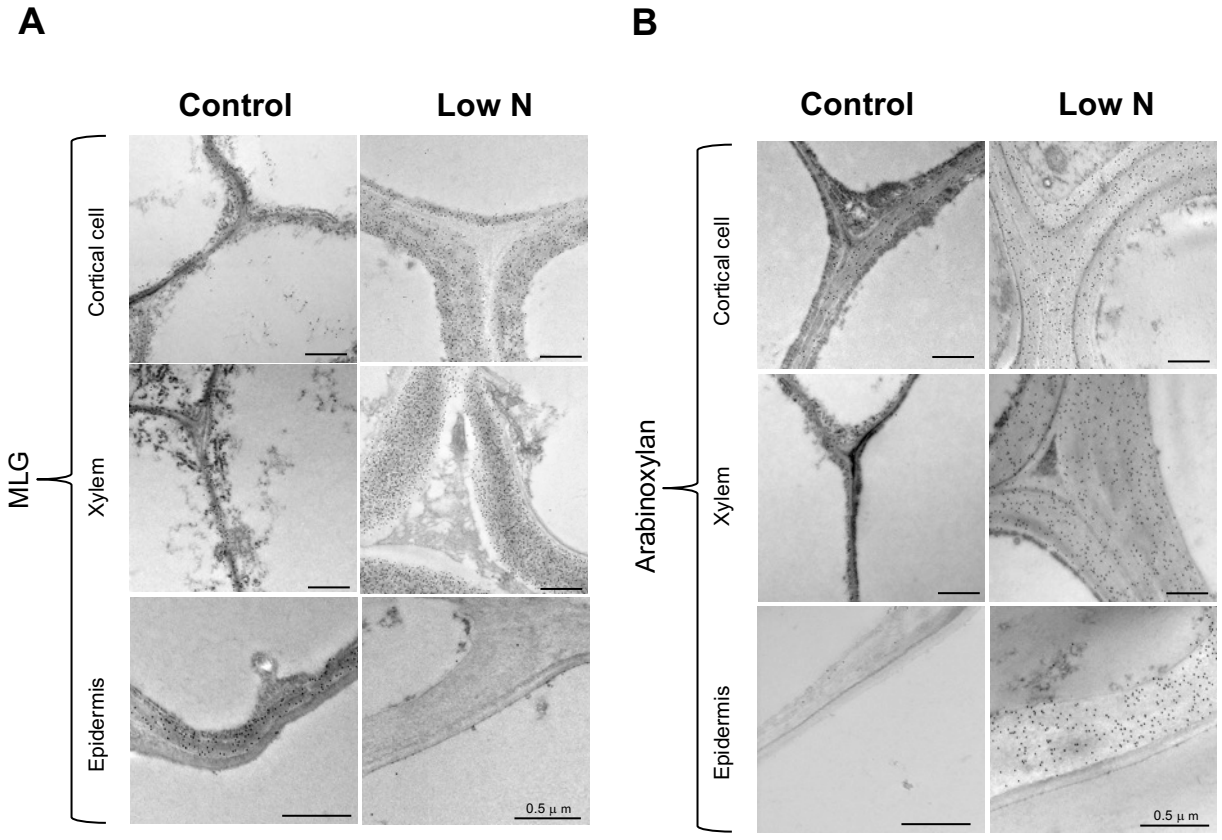

Figure 2.10. Immunogold labeling using (**A**) anti-mixed-linkage (1→3), (1→4)-β-D-glucan (MLG), and (**B**) arabinoxylan antibodies of hydroponically grown sorghum seedlings cultivated under control or low-N conditions at 3 weeks after treatment.

In addition, the secondary cell walls of cortical, xylem and epidermal tissues appeared thicker in low-N plants than in control plants (**Figure 2.10**). We then estimated their cell wall thickness by image analysis. The result confirmed that the secondary cell walls in these tissues were significantly thicker in low-N plants (**Figure 2.11**).

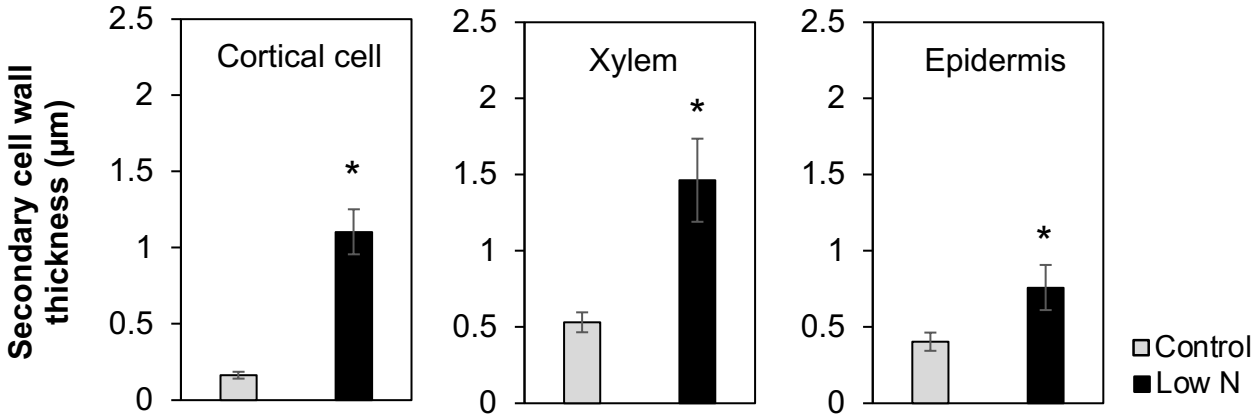

Figure 2.11. Cell wall thicknesses of cortical, xylem, and epidermal cells of hydroponically grown sorghum seedlings cultivated under control or low-N conditions at 3 weeks after treatment. Values are given as mean ± SD (18 measurements from 6 individual cells for cortical cells, 9 measurements from 3 individual cells for xylem, and 12 measurements from 4 individual cells for epidermal cells). Asterisks indicate significant differences between control and low-N plants (Student's *t* test, $p < 0.05$).

2.3.7 Gene expression

To further confirm the effects of N limitation on sorghum cell wall and to obtain insights into the mechanism underlying the changes, I conducted gene expression analyses. Sorghum genes related to cell wall biosynthesis and modification were selected according to a previous report (Rai et al., 2016), and their expression under low-N conditions was investigated by referring to data from RNA-sequencing analysis of N-deficient sorghum seedlings in Chapter 1. Of the genes examined, the *endo-1,4-β-glucanase* (Sb01g008860) encodes a homolog of Arabidopsis KORRIGAN 1 (KOR1), which plays an essential role in cellulose biosynthesis as an integral part of the cellulose synthase complex (Vain et al., 2014). Hence, although the gene has been categorized as a glycosyl hydrolase in the list (**Figure 2.12**), it is more likely to be involved in cellulose biosynthesis rather than glycan degradation. Three days after initiating the low-N treatment, expression of the genes encoding cellulose synthase (CESA) and endo-1,4-β-glucanase was upregulated in low-N plants, whereas expression of two

genes encoding glucan 1,3-β-glucosidase, an enzyme degrading callose, was downregulated (**Figure 2.7**). Expression of other glucan-related genes, including *cellulose synthase-like proteins* (*CSL*) and *glucan synthase-like proteins* (*GSL*), were not statistically different between low N and control plants (**Figure 2.12**). A similar tendency was observed with the expression of these genes at 6 d, but the statistically significant difference was not demonstrated between control and low-N plants (**Figure 2.12**).

The expression of a gene encoding xyloglucan endotransglucosylase/hydrolase (*XTH*) was downregulated in low-N plants, while the expression of *endo-xylanase* was not modulated significantly (**Figure 2.12**). As for the expression of pectin-related genes, a gene for β-galactosidases (BGAL), which possibly catalyzes the degradation of rhamnogalacturonan I (RG-I) side chains, was downregulated by low N treatment at 6 d (**Figure 2.12**). Meanwhile, no significant change was observed in other pectin-related genes, including *homogalacturonan α-1,4-galacturonosyltransferases* (*GAUT*), *polygalacturonases* (*PGases*), *pectate and pectin lyase*, *RG-I lyase*, *pectin methylesterase*, and *pectin acetylesterase* (**Figure 2.12**). Expression of *laccase* (*LAC*), which may be involved in lignin monomer polymerization, was not significantly modulated by low-N treatment (**Figure 2.12**).

The results from RNA sequencing analysis suggested altered expression of cell wall-related genes in sorghum seedlings at 3 or 6 d after low-N treatment. I then further assessed the impact of N limitation on cell wall-related gene expression at 3 weeks after treatment, using a reverse transcription-quantitative PCR (RT-qPCR) analysis. The target genes chosen were those showing the largest change (either up- or down-regulated under low N supply) in each group (**Figure 2.12**). As shown in **Figure 2.13**, the analysis confirmed the upregulated expression of *CESA* and *endo-1,4-β-glucanase* under low-N conditions. Furthermore, the analysis demonstrated upregulation of *CSL*, *pectate lyase*, *GAUT*, and *expansin* (*EXP*) and downregulation of *glucan-1,3-β-glucosidase* in low-N plants (**Figure 2.13**), although their expression was not changed significantly at 3 or 6 d as revealed by RNA sequencing analysis (**Figure 2.12**). Statistically significant changes were not observed with the other targets, including *XTH*, *GSL*, *LAC*, and *RG-I lyase* (**Figure 2.13**). These results confirmed the effect of low N condition on cell wall components in hydroponically-grown sorghum seedlings.

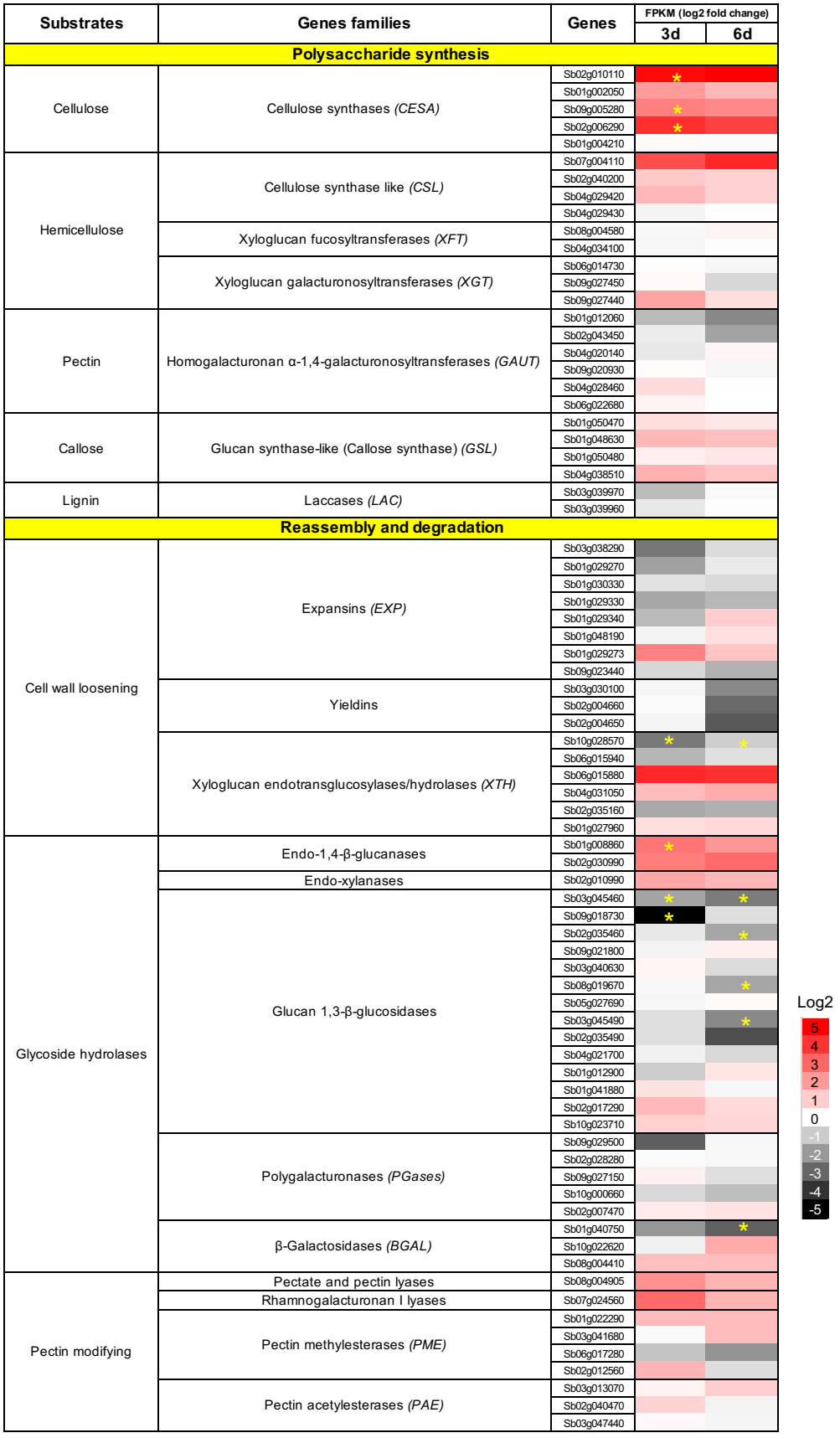

Figure 2.12. Heatmap showing the change in expression of known cell wall-related genes in hydroponically grown sorghum seedlings in response to low-N condition at 3 and 6 days after treatment. The $\log_2$ values of the fold change (low-N/control) are shown. Asterisks indicate significant difference between treatments (n = 3, q value < 0.05).

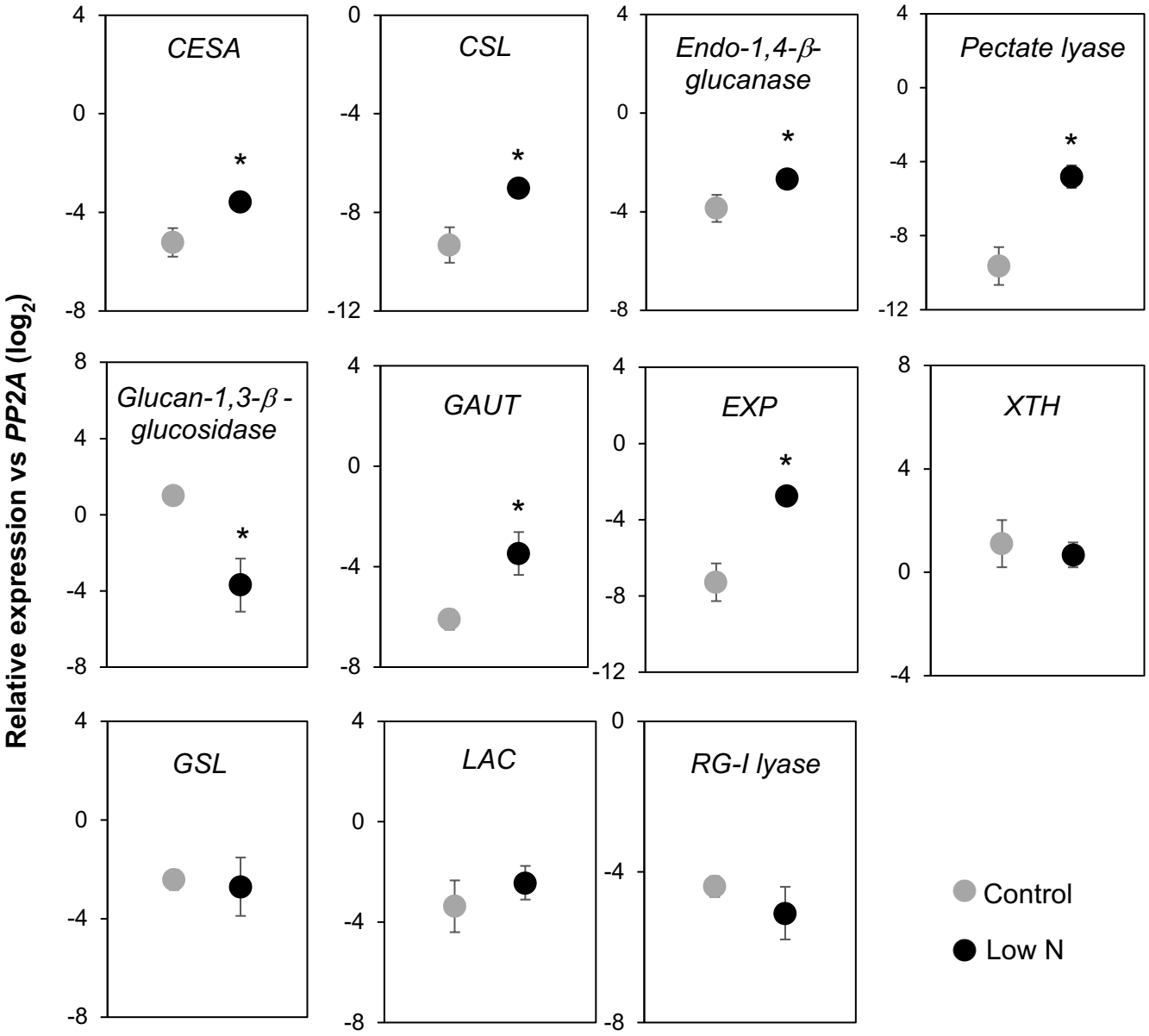

Figure 2.13. Reverse transcription-quantitative PCR analysis of the expression of selected cell wall polysaccharide metabolism-related genes in low nitrogen (N)-treated hydroponically grown sorghum seedlings. The analysis was conducted at 3 weeks after treatment. *CESA*: *Cellulose synthase A*, *CSL*: *cellulose synthase-like*, *GAUT: homogalacturonan α-1,4-galacturonosyltransferase, EXP*: *expansin, XTH*: *xyloglucan endotransglucosylase/hydrolase*, *GSL*: *glucan synthase-like/callose synthase*, *LAC*: *laccase*, and *RG-I*: *rhamnogalacturonan I*. The expression of each gene was analyzed as transcript abundance relative to *PP2A* (XM_002453490). Values are means ± SD (n = 3). Asterisks indicate significant differences between control and low-N plants. (Student's *t* test, $p < 0.05$).

Multiple known genes involved in lignin biosynthesis were also included in the analysis (**Figure 2.14**). Of these, *phenylalanine ammonia lyase* (*PAL*) (Agarwal et al., 2016), *4-coumarate CoA ligase* (*4CL*)/*Brown midrib 2* (*Bmr2*) (Saballos et al., 2012), *cinnamyl alcohol dehydrogenase* (*CAD*)/*Brown midrib 6* (*Bmr6*) (Saballos et al., 2008), and p-*coumaroyl ester 3-hydroxylase* (*C3'H*) (Saballos et al., 2012) did not show significant changes following the low-N treatment (**Figure 2.14**). On the other hand, two genes associated with S-lignin biosynthesis, that is, *ferulate 5-hydroxylase* (*F5H*) (=*coniferaldehyde 5-hydroxylase*, *CAld5H*) (Tetreault et al., 2020) and *caffeate/5-hydroxyferulate* O-*methyltransferase* (*COMT*) (=*5-hydroxyconiferaldehyde* O-*methyltransferase*, *CAldOMT*)/*Brown midrib 12* (*Bmr12*) (Bout & Vermerris, 2003; Li et al., 2000) were downregulated in low-N plants (**Figure 2.14**).

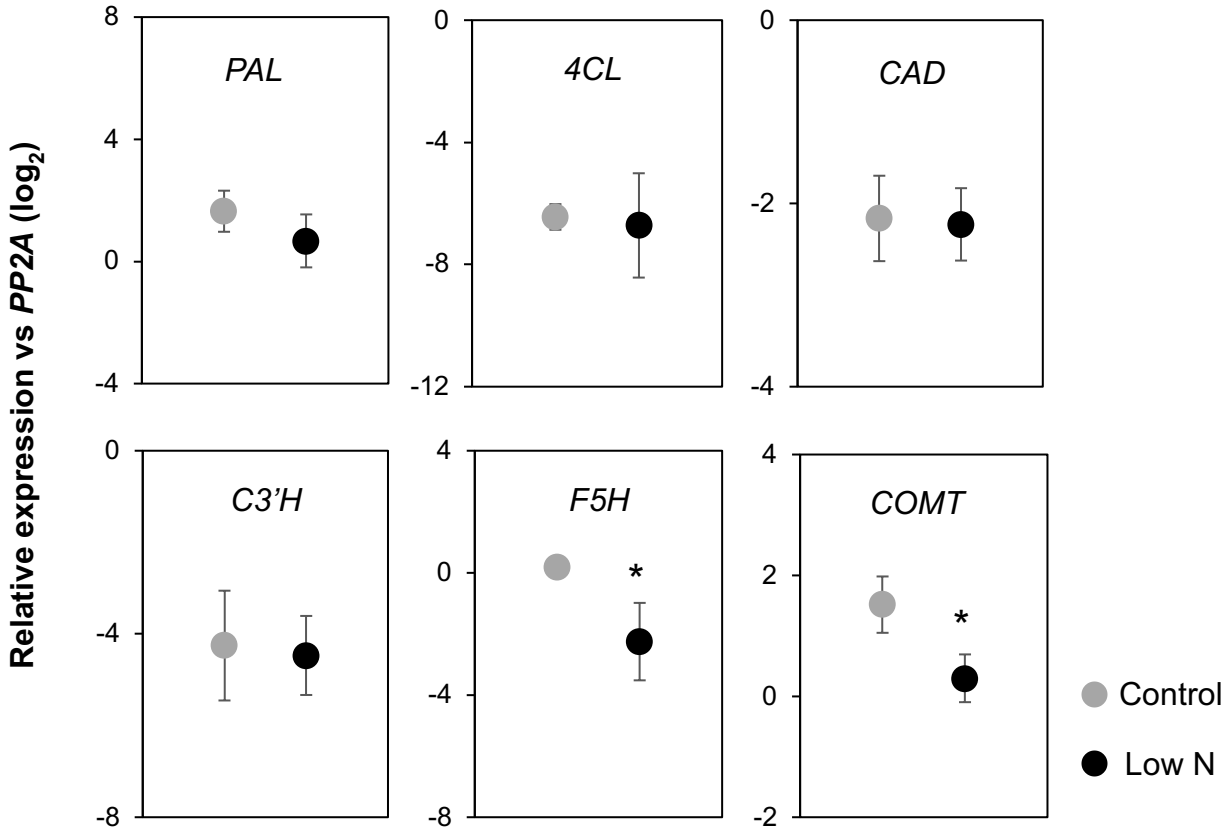

Figure 2.14. Reverse transcription-quantitative PCR analysis of the expression of selected lignin biosynthesis-related genes in low nitrogen (N)-treated hydroponically grown sorghum seedlings. The analysis was conducted at 3 weeks after treatment. *PAL*: *phenylalanine ammonia-lyase*, *4CL*: *4-coumarate CoA ligase*/*Brown midrib 2* (*Bmr2*), *CAD*: *cinnamyl alcohol dehydrogenase*/*Brown midrib 6* (*Bmr6*), *C3'H*: *p-coumaroyl ester 3-hydroxylase*, *F5H*: *ferulate 5-hydroxylase* (=*coniferaldehyde 5-hydroxylase*, *CAld5H*), and *COMT*: *caffeate/5-hydroxyferulate* O-*methyltransferase* (=*5- hydroxyconiferaldehyde* O-*methyltransferase*, *CAldOMT*)/*Brown midrib 12* (*Bmr12*). The expression of each gene was analyzed as transcript abundance relative to *PP2A* (XM_002453490). Values are means ± SD (n = 3). Asterisks indicate significant differences between control and low-N plants. (Student's *t* test, $p < 0.05$).

2.3.8 Enzymatic saccharification

To assess the possible relevance of the changes in cell wall for biomass utilization, I compared the saccharification performance of low-N and control cell walls. The cell walls were hydrolyzed using a cocktail of commercially available cellulolytic enzymes, and the released glucose was quantified after 24-h incubation. The amount of glucose released from the cell wall of low-N plants was 28% higher than that from the cell wall of control plants (**Figure 2.15**).

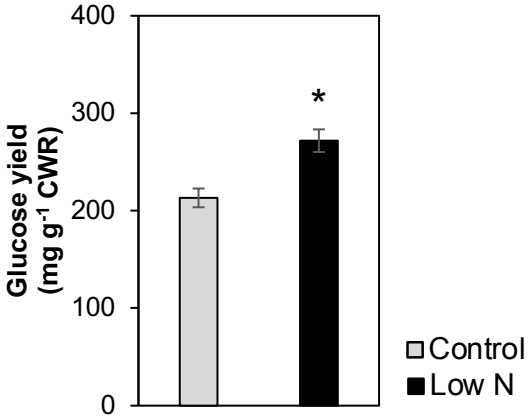

Figure 2.15. Enzymatic saccharification of cell walls after 24 h of enzymatic hydrolysis of hydroponically grown sorghum seedlings cultivated under control or low-N conditions at 3 weeks after treatment. Values are given as mean ± SD (n = 3). Asterisks indicate significant differences between control and low-N plants (Student's *t* test, $p < 0.05$).

2.4 Discussion

In this chapter, I elucidated that the level of N supply could affect the properties of sorghum cell wall through a series of analyses. Firstly, N deficiency can modulate the cell wall lignin composition and structures of hydroponically sorghum plants. Although the lignin content estimated by the thioglycolic acid analysis was not significantly different between low-N and control plants in hydroponically sorghum seedlings (**Figure 2.3A**), the sum of contents of thioacidolysis-derived lignin monomers (H + G + S) was significantly higher in low-N plant cell wall than in control plant cell wall (**Figure 2.3B-D**). A similar finding has been reported for maize under low N supply (Sun et al., 2018). Such a discrepancy about the estimated amount may arise if the same amounts of lignin monomer units are polymerized differently, as the thioacidolysis assay detects only the units linked with β-*O*-4 linkages. Hence, the result in this study in turn suggests a N deficiency-induced modulation of the polymerization pattern of

lignin monomers, leading to an increased percentage of thioacidolysis-susceptible β-*O*-4 linkages. I confirmed that the level of N supply did not substantially affect the content of lignin both in more mature stages of hydroponically and soil grown sorghum plants (**Figure 2.4A**, **Figure 2.5A**). I also demonstrated an unchanged in lignin content of mature stem from the multiple soil grown sorghum genotypes cultivated under different N supply (**Figure 2.5A**). Similarly, the content of lignin was not affected by the level of N supply in two sugar cane genotypes (Salvato et al., 2017). These results suggest that the level of N supply did not modify lignin content in sorghum plant both in seedling and mature stages, and in different sorghum genotypes.

Although the total lignin content were not different significantly between the treatment, their composition was modulated, as shown by a substantially lower S/G ratio in low-N cell walls of hydroponically grown seedlings (**Figure 2.3E**, **Figure 2.8**). Both the chemical and NMR analysis indicated an increase of G lignin monomers under low N condition. Meanwhile, the content of S lignin monomers was either not different or lower in low N plants as indicated by chemical and NMR analysis, respectively (**Figure 2.3E**, **Figure 2.8**). Thus, N limitation might cause a shift in lignin monomer synthetic pathway in favor of G rather than S monomer synthesis as simply shown in **Figure 2.16**. The responses may be explained as the result of lowered availability of *S*-adenosylmethionine, which is synthesized from methionine and used as the methyl donor in the conversion of G precursors to S precursors (Roje, 2006). In addition, I also found that the S/G monomer ratio was decline by lowering N supply in more mature hydroponically sorghum plants compared with high-N treated plants (**Figure 2.4B**), whereas the difference was not obvious in four examined soil grown sorghum plants (**Figure 2.5B**). In comparison with other studies, the direction of low N-induced change in S/G ratio varies among reports, as it was increased in poplar (Pitre et al., 2007), *Eucalyptus* (Camargo et al., 2014) or maize (Sun et al., 2018). Thus, although the N deficiency-induced modulation of lignin monomer composition is common, the specific response may vary depending on species and condition such as the severity of deficiency. Such a modulation may arise at least partly through the transcriptional change of the genes for the monomer synthetic pathway, as the expression of *F5H* (*CAld5H*) and *COMT* (*CAldOMT*)/*Bmr12*, the genes required for S-lignin synthesis, were significantly downregulated in low-N plants (**Figure 2.14**), while the genes involved in earlier steps of the pathway (*PAL, 4CL*/*Bmr2*, *CAD*/*Bmr6*, and *C3'H*) did not show significant modulation (**Figure 2.14**).

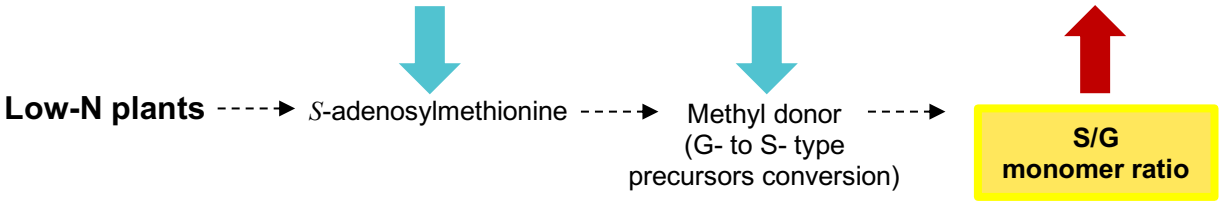

Figure 2.16. Schematic flow of the effect of low-N treatment on the modulation of lignin composition reflected by the syringyl/guaiacyl (S/G)-type monomer ratio in hydroponically sorghum seedlings.

Limitation of N also affected the polysaccharide moiety of the cell wall in sorghum. The low-N plant cell wall contained more cellulose and hemicellulose, non-cellulosic glucans and xylans, as revealed by the chemical, NMR, and immunohistochemical analyses. Possibly consistent with this notion, the content of cell wall-bound FA, which mediates inter-arabinoxylan or arabinoxylan-lignin crosslinking, substantially increased under low-N condition (**Figure 2.6**, **Figure 2.8**). The electron microscopy analysis also showed that the cell walls of low-N plants were thicker than that of control plants (**Figure 2.11**), probably due to an enhanced formation of the secondary cell walls. A previous study also reported a thickening of sorghum cell wall under N limited condition (Makino & Ueno, 2018), particularly in bundle sheath cells. The current results showed that the low N-induced thickening of cell wall occurred in tissues other than bundle sheath as well, including cortical, xylem, and epidermal cells (**Figure 2.11**). Observed increase in the amount of cellulose and hemicellulose might be due in part to this estimated enhanced formation of secondary cell walls, as cellulose and hemicellulose are the two major components of secondary cell walls. However, specific accumulation of hemicellulose should also be involved, as suggested from the denser labeling of secondary cell walls in immunoelectron microscopy (**Figure 2.10**). At least a part of the change in hemicellulose content was caused via modulated expression of genes for the synthesis and/or degradation of these polysaccharides, as revealed by the RNA-sequencing and RT-qPCR analyses (**Figure 2.12**, **Figure 2.13**). Notably, those changes of cell wall-related gene expression occurred as early as 3 d after initiating the low-N treatment, suggesting that the modulation of cell wall components could be an adaptation strategy for N starvation.

The explanation of the enhanced hemicellulose fractions caused by limiting N supply is briefly shown in **Figure 2.17**. Under the condition of insufficient N supply, plants limit the synthesis of N-containing molecules such as proteins and amino acids. The metabolic

adjustment reduces the demand for carbon skeletons for N assimilation. The surplus carbon may be accumulated as starch, or turned to synthesis of cell wall materials, as suggested in maize leaves (Schlüter et al., 2012). Hoch (2007) reported that hemicelluloses in cell wall are not only structural components but also the mobile carbon stores in plants. The increase of glucans and xylans observed in this study might also be such sink of surplus carbon. Possibly consistent with the finding in this study, application of N fertilizer slightly reduced the content of hemicellulose in giant mischanthus (Arundale et al., 2015), which is also a grass with C4 photosynthesis.

Uronic acid content was decreased under low N condition (**Figure 2.7**). As I did not analyze the molecular identity of the uronic acids in this study, it is difficult to judge if the observed decrease was of galacturonic acid residues in pectin or glucuronic acid residues in hemicelluloses. Signals from NMR analysis suggested a decrease of glucuronic acid residues in low N plant cell walls, but the analysis tells only a relative amount between the treatment, hence it remains unknown how much of the detected decrease in uronic acid could be explained by that of glucuronic acid. However, since the expression of *GAUT* tended to be downregulated (**Figure 2.13**), at least the synthesis of polygalacturonate, the major component of pectin, should have been decreased under N deficiency. Such an effect of N limitation on pectin has been reported in several previous reports. For example, amount of pectin was reduced under low-N condition in grapevine callus (Fernandes et al., 2013). The form of N supply also affected the pectin content and structure in Brachypodium cell wall (Głazowska et al., 2019). Considering these findings together, it is possible that N deficiency leads to a decrease of cell wall pectin also in sorghum. However, the practical significance of the decrease in pectin, if any, would be limited, as pectin constitutes only a minor fraction of the cell wall in grasses (O'Neill et al., 1990).

The present study was mainly conducted with hydroponically grown seedlings, which was different from the practical situation of biomass crop production. Nonetheless, the study should give us insights as to whether or not the nutrient supply could affect the properties of sorghum cell walls. There was indeed some difference between the cell walls of low-N and control plants, including lignin monomer composition and polysaccharide content. I then considered possible impacts of these changes on the usability of this material as the feedstock for biomass energy production. The cell wall of low-N and control plants were not different in the amount of lignin, but the S/G lignin monomer ratio was lower in the former than the latter. Lower S/G ratio gave higher enzymatic digestibility in maize cell wall, and its effect exceeded that of the difference in lignin content (He et al., 2018). In addition, low-N plant cell wall

contained more cellulose and non-cellulosic glucans, which can be converted into fermentable sugars. As such, the cell wall of low-N plants could be favorable as the feedstock for biomass ethanol production, and the enzymatic saccharification of low-N plant cell wall indeed produced higher amount of glucose compared to control plant cell walls. However, considering the extent of changes induced by N limitation and critical importance of N to support vigorous plant growth, it would be more reasonable to supply enough amount of N as fertilizers to get sufficient yields. In this study as an example, the 51% reduction of biomass production due to N deficiency cannot be compensated by 28% increase of enzymatic saccharification performance.

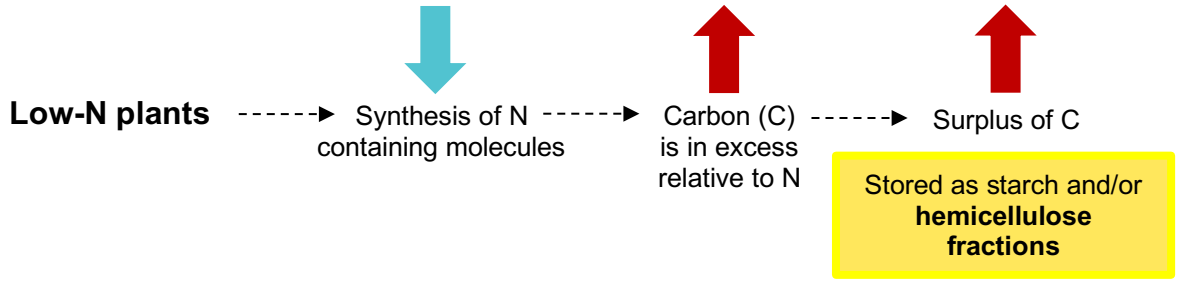

Figure 2.17. Schematic flow of the effect of low-N treatment on the increased of hemicellulose fractions in hydroponically sorghum seedlings.

Chapter 3

Alteration of cell wall lignin structures by limiting silicon supply in *Sorghum bicolor*

3.1 Introduction

The quality of plant biomass as the feedstock for bioenergy is highly dependent on the composition and structure of cell walls (lignocellulose), which are mainly composed of cellulose, hemicelluloses, and lignin (Hatfield et al., 2017). Lignin content and structure can be modulated by environmental factors, including nutritional conditions (Moura et al., 2010).

In the previous chapter, I revealed that the level of N supply significantly affected the structure of lignin in the cell walls of hydroponically grown sorghum seedlings. As a plant nutrient, silicon (Si) may influence cell wall composition, including lignin content and structure (Głazowska et al., 2018; Suzuki et al., 2012). Silicon is contained in plants at 0.1–10% of dry weight. The majority of Si in plants exists in the form of silica in the cell walls and intercellular spaces of leaf epidermal tissues (Ma & Yamaji, 2006). Similar to lignin, the silica deposited in tissues contributes to tissue mechanical strength (Ma & Yamaji, 2006, 2008). As a mechanically important component of plant tissue, the supply of Si may affect the content and/or structure of lignin in cell walls.

The mutants of brachypodium and rice defective in Si uptake accumulate more lignin than wild-type plants (Głazowska et al., 2018; Suzuki et al., 2012). In sorghum, the interaction of Si and lignin has been reported in root endodermal tissues, in which Si as silica emerged only after the initiation of lignification in the inner tangential cell walls. The silica was estimated to be deposited specifically on the newly polymerized coniferyl alcohol (G-lignin unit) (Soukup et al., 2017, 2020; Zexer & Elbaum, 2020). However, with regards to sorghum shoot cell walls, limited information is available on the effect of Si supply on lignin properties. To address this shortfall, the objective of this chapter was to analyze the changes induced by Si limitation in the cell walls of the shoots of hydroponically grown sorghum seedlings to determine the effects of Si supply on lignin and other cell wall components in this species. As a result, the limitation of the Si supply was found to lead to a change in the content and structures of lignin. The mechanical properties and calorific value was also changed, suggesting that Si uptake is a factor that affects the properties of sorghum lignocellulose biomass.

3.2 Materials and Methods

3.2.1 Plant growth condition and treatment

Cultivation was carried out in a culture room maintained at 25°C with a 16/8 h light/dark cycle. Sorghum seeds (*S. bicolor*, cv. BTx623) were germinated and grown on vermiculite for a week. The seedlings were transferred to a full-strength Yoshida B hydroponic culture medium and grown further for two weeks as described previously in Chapter 1. The 3-week-old seedlings were transferred to Yoshida B culture medium containing Si at 50 or 0 mg SiO_2 L^{-1} and cultured for three weeks. Silicon was added in the form of silicic acid. A solution of sodium silicate containing Si at approximately 35% as SiO_2 was passed through a column of Dowex 50W-X8 (H^+ form) equilibrated with distilled water. The Si concentration in the effluent was determined colorimetrically and used as the Si stock solution. The aerial parts of 6-week-old (three weeks after Si treatments) seedlings were used for subsequent analyses.

3.2.2 Silicon content analysis

The aerial parts of the seedlings were dried in an oven at 70°C and pulverized to a fine powder using a T-351 pulverizing machine (Rong Tsong Iron Co., Taichung, Taiwan). Approximately 20 mg of powder was ashed and melted with 200 mg Na_2CO_3 and then diluted to 20 ml with distilled water. The Si concentration in the solution was measured using the colorimetric molybdenum blue method at 600 nm (UV-1700; Shimadzu, Kyoto, Japan).

3.2.3 Cell wall chemical analyses

The cell wall residue (CWR) was prepared as previously described in Chapter 2. The cell wall Si content was analyzed as described above for the plant Si content. Cell wall chemical analyses including, lignin content, thioacidolysis-derived lignin composition, cell wall-bound *p*CA and FA, uronic acid content, calcium content, crystalline cellulose content and glycosyl residue composition were conducted as previously described in Chapter 2.

3.2.4 2D HSQC NMR analysis

The analysis and data processing of 2D HSQC NMR were performed as previously described in Chapter 2. For volume integration analysis, the aromatic contour signals from lignin and hydroxycinnamates (C2–H2 correlations from **G** and **FA**, C2–H2/C6–H6 correlations from **S** and ***p*CA**, and C2′–H2′/C6′–H6′ correlations from **T**, **S**, ***p*CA**, and **T** integrals were logically halved) and polysaccharide anomeric signals were manually integrated,

and each signal was normalized based on the sum of the total NMR signals (Dumond et al., 2021).

3.2.5 Scanning electron microscopy

Fresh hand-cut specimens of the aboveground parts of the seedlings were immersed in 70% ethanol for 2 weeks. The specimens were cut (±1 mm thick) and dehydrated in a graded ethanol series (30%, 50%, 70%, 80%, 90%, 95%, and 99.5%), followed by *t*-butyl alcohol. The obtained sections were freeze-dried and coated with platinum using an ion sputter (E-1045; Hitachi, Tokyo, Japan), and then observed under a field emission scanning electron microscope (S-4800; Hitachi) at an accelerating voltage of 10 kV coupled with an energy dispersive X-ray analyzer (Genesis XM2; EDAX, Tokyo, Japan).

3.2.6 Histochemical analyses

Fresh hand-cut specimens of the aboveground parts of the seedlings were immersed in 70% ethanol for a week. The specimens were cut (±30 μm thick) using a sliding microtome (REM-710; Yamato Kohki Industrial Co., Ltd., Saitama, Japan). For lignin staining with acriflavine, the sections were stained with 1% (w/v) acriflavine in water for 2 min, washed with 80% ethanol, and observed under a fluorescence microscope (BX50 with BX-FLA fluorescent light attachment; Olympus, Tokyo, Japan) with U-MWIB3 filter set (460–490 nm excitation, 515 nm long-pass emission) (Olympus). For lignin staining with the phloroglucinol-HCl method or flavonoid staining with the vanillin-HCl method, the transverse sections were incubated in 2% (w/v) phloroglucinol or 1% (w/v) vanillin in 95% ethanol, respectively. The sections were then immersed in 6 M HCl, mounted on slides, and observed under a light microscope (BX50; Olympus, Tokyo, Japan). For cellulose or (1→3)-β-D-glucan (callose) deposition analyses, fresh transverse sections were incubated in 0.01% (w/v) calcofluor white (Biotium Inc., California, USA) in deionized water or 0.01% (w/v) aniline blue in 0.08 M phosphate buffer (pH 9.0) for 10 min. The sections were then observed under a fluorescence microscope (BX50 with BX-FLA fluorescent light attachment) with a WU filter set (330-385 nm excitation, 420 nm long-pass emission) (Olympus).

3.2.7 Immunofluorescence labeling

Immunofluorescence labeling analyses of arabinoxylan, MLG, and callose were conducted as previously described in Chapter 2.

3.2.8 Gene expression analyses

3.2.8.1 RNA sequencing analysis

Total RNA was extracted from the tip of the youngest fully expanded leaves of the seedlings, as previously described in Chapter 1. Strand-specific RNA sequencing analysis was performed at GENEWIZ, Inc. (Tokyo, Japan) following the standard protocol. Sequencing was performed on the Illumina HiSeq platform (Illumina, San Diego, CA, USA) in a 2×150 bp paired-end configuration. For each sample, 22–26 million reads were obtained. The short-read data sets were deposited in the DNA Data Bank of Japan (DDBJ) Sequence Read Archive under accession number DRR324378-DRR324383. Sequence analysis was performed using the Galaxy web tool available at https://usegalaxy.org/ (Afgan et al., 2018). The reads were quality-checked using FastQC version 0.72 (https://www.bioinformatics.babraham.ac.uk/projects/fastqc/), mapped to the *S. bicolor* gene model Sbi1 (http://www.phytozome.net) using HISAT2 version 2.1.0 (Kim et al., 2015), and the transcript abundances were estimated using featureCounts version 1.6.4 (Liao et al., 2014). The count data from three biological replicates for each treatment were used to identify differentially expressed genes (DEGs) using DESeq2 version 2.11.40.6 (Love et al., 2014).

Gene ontology (GO) enrichment analysis of the DEGs was conducted by the singular enrichment method using the AgriGO webtool (http://bioinfo.cau.edu.cn/agriGO/analysis.php) (Tian et al., 2017). Overrepresentation of the annotation in DEGs was examined by Fisher and Yekutieli tests, with an adjusted p value < 0.05 as the significance threshold. The functional annotations listed in **Table 3.8-11** refer to the Morokoshi sorghum transcriptome database (http://sorghum.riken.jp/Home.html) (Makita et al., 2015).

3.2.8.2 Reverse transcription-quantitative PCR analysis

Reverse transcription-quantitative PCR analysis (RT-qPCR) was performed using RNA extracted from the tip of the youngest fully expanded leaves of the seedlings. For this experiment, I used different sets of samples from those used for RNA sequencing analysis. Total RNA extraction, first-strand cDNA synthesis, and RT-qPCR analyses were conducted as previously described in Chapter 1. The gene encoding PP2A was used as an internal control (Reddy et al., 2016). The PCR primers used are listed in **Table 3.1**.

Table 3.1. List of primers used for reverse transcription-quantitative PCR analysis.

Gene name	Gene ID	Forward primer (5′→3′)	Reverse primer (5′→3′)
HCT	Sb10g005780	GTAGTGCAGTGCAGACATGC	TATCTACGCAGTTCCGCTCG
CCoAOMT	Sb10g004540	CAAGCACCCATGGAACCTGA	TGGCCAAGATCGTGCCGTC
CCR	Sb07g021680	AGCAGCCGTACAAGTTCTCG	CCGTATCGTAGAGCGACTGG
F5H (*CAld5H*)	Sb01g017270	ATGGCGGAGATGATGCACAG	CGTCTCCTTGATGACGCACT
CAD/Bmr6	Sb04g005950	TACCCTATGGTCCCTGGGC	GCCGTCAGTGTAGACATCGT
PAL	Sb04g026520	CCAAAGTACAGCGGCTCAAG	CAAGAACATGCGCATTGCAG
COMT (*CAldOMT*)/ *Bmr12*	Sb07g003860	TTAATGGCCTAGCCTGCCTC	CGCAGAGACAATTCGACAGC
4CL/Bmr2	Sb04g005210	CATCTCCAAGCAGGTGGTGT	ATTGCACGTAACAAGGCACG
C3'H	Sb09g024210	ACCTTCTGCACCACTTCGAG	AGGCACCTCACATCTCAACG
CESA	Sb02g010110	TAATGTTGCCAGCCTGTGGT	GAACACAGCAAAGAGGTGCG
CSL	Sb07g004110	CTCTCCTACAACTGGCCGTG	GCCGCCTCACCATATCATCA
Endo-1,4-b glucanase	Sb01g008860	CAAGTTTGCCAGGTCACAGC	GCGCTTCGGGTACTTGTTTC
EXP	Sb03g038290	CAGTTCTAGCACGCCCCTC	AGGAAATGCCTAAGCGGGTG
XTH	Sb10g028570	GATAAGTACCGCTTCCCGCA	CAAGTCATCATGCACACGGC
GSL	Sb04g038510	CTTATCAAACTGCCGCCGTG	TGCGTCTCGAGAATCGACTG
Glucan-1,3-b-glucosidase	Sb03g045460	GGCTCACCTACACCAACCTG	GCCCCTGGTTGTACTTCCTC
GAUT	Sb01g012060	GCCGAGAGAGAAAAGCCGAG	TCAGGCGAGGTAAATGGTGG
Pectate lyase	Sb08g004905	CCACCATGGCCAGAGGTATG	CTCAGGAGCTTGGATAGCGG
RG-I lyase	Sb07g024560	AGGGAGAACGCGATAGCAAG	CAATCCCTGAAACGGGCTCT
PP2A	XM_002453490	AACCCGCAAAACCCCAGACTA	TACAGGTCGGGCTCATGGAAC

HCT: *hydroxycinnamoyl-CoA shikimate/quinate hydroxycinnamoyltransferase*, *CCoAOMT*: *caffeoyl-CoA* O-*methyltransferase*, *CCR*: *cinnamoyl CoA reductase*, *F5H*: *ferulate 5-hydroxylase* (=*coniferaldehyde 5-hydroxylase*, *CAld5H*), *COMT*: *caffeate/5-hydroxyferulate* O-*methyltransferase* (=*5-hydroxyconiferaldehyde* O-*methyltransferase*, *CAldOMT*)/*Brown midrib 12* (*Bmr12*), *CAD*: *cinnamyl alcohol dehydrogenase/Brown midrib 6* (*Bmr6*), *PAL*: *phenylalanine ammonia-lyase*, *4CL*: *4-coumarate CoA ligase/Brown midrib 2* (*Bmr2*), and *C3'H*: *p-coumaroyl ester 3-hydroxylase*. *CESA*: *cellulose synthase A*, *CSL*: *cellulose synthase-like*, *EXP*: *expansin, XTH*: *xyloglucan endotransglucosylase/hydrolase*, *GSL*: *glucan synthase-like/callose synthase*, *GAUT: homogalacturonan α-1,4-galacturonosyltransferase,* and *RG-I*: *rhamnogalacturonan I.*

3.2.9 Mechanical property analyses

The aboveground parts of the seedlings were cut (± 90 mm) and the fully expanded leaves were removed and immersed in 70% ethanol. The samples were dried at room temperature for 3 days, then in a chamber set at 25°C and 60% relative humidity for 4 days. The dried samples (n = 4) were subjected to a three-point bending test (Little Senstar, Tokyo, Japan) with a span length of 65 mm and a loading rate of 10 mm min^{-1}. Changes in the force and deflection values were recorded. The linear curve of these values was used to calculate the modulus of elasticity (MOE) based on the following equation:

$$\mathrm{MOE} = \frac{Fl^3}{12\pi r^4 d}$$

where F is the force (N), l is the span length (mm), r is the specimen radius (mm), and d is the deflection height (mm). The samples were then cut (± 30 mm) and used for microfibril angle (MFA) analysis. Both ends of the rolled samples were covered with a heat-shrink tube (5 mm in length and 0.5 mm in diameter). X-ray diffraction patterns were acquired using an R-axis Rapid II diffractometer (Rigaku, Tokyo, Japan). Cu Kα radiation was generated at 50 kV and 100 mA. The microfibril orientation was derived from the azimuthal distribution of the 200 reflections, as described previously (Thomas et al., 2015).

3.2.10 Determination of heating value

The higher heating value (HHV) of CWR samples was estimated based on their elemental composition (Yin, 2011). The HHV was calculated according to the equation HHV = 0.2949 C + 0.8250 H (kJ g^{-1}), where C and H are the carbon and hydrogen contents (% dry weight), respectively. The C and H contents were determined using a CHN analyzer (JM-10; J-Science Lab Co., Ltd., Kyoto, Japan).

3.3 Results

3.3.1 Plant growth and biomass accumulation

The shoot Si content in the seedlings with −Si treatment was significantly lower than that in the seedlings with +Si treatment. This confirmed that the Si treatment affected the plant Si status (**Figure 3.1B**). However, as shown in **Figure 3.1A**, Si supply did not cause any visible differences in plant growth. Furthermore, there was no difference between the treatments in terms of biomass yield and growth parameters, including shoot fresh weight, shoot dry weight, plant height, stem diameter, and leaf length (**Figure 3.1C-G**).

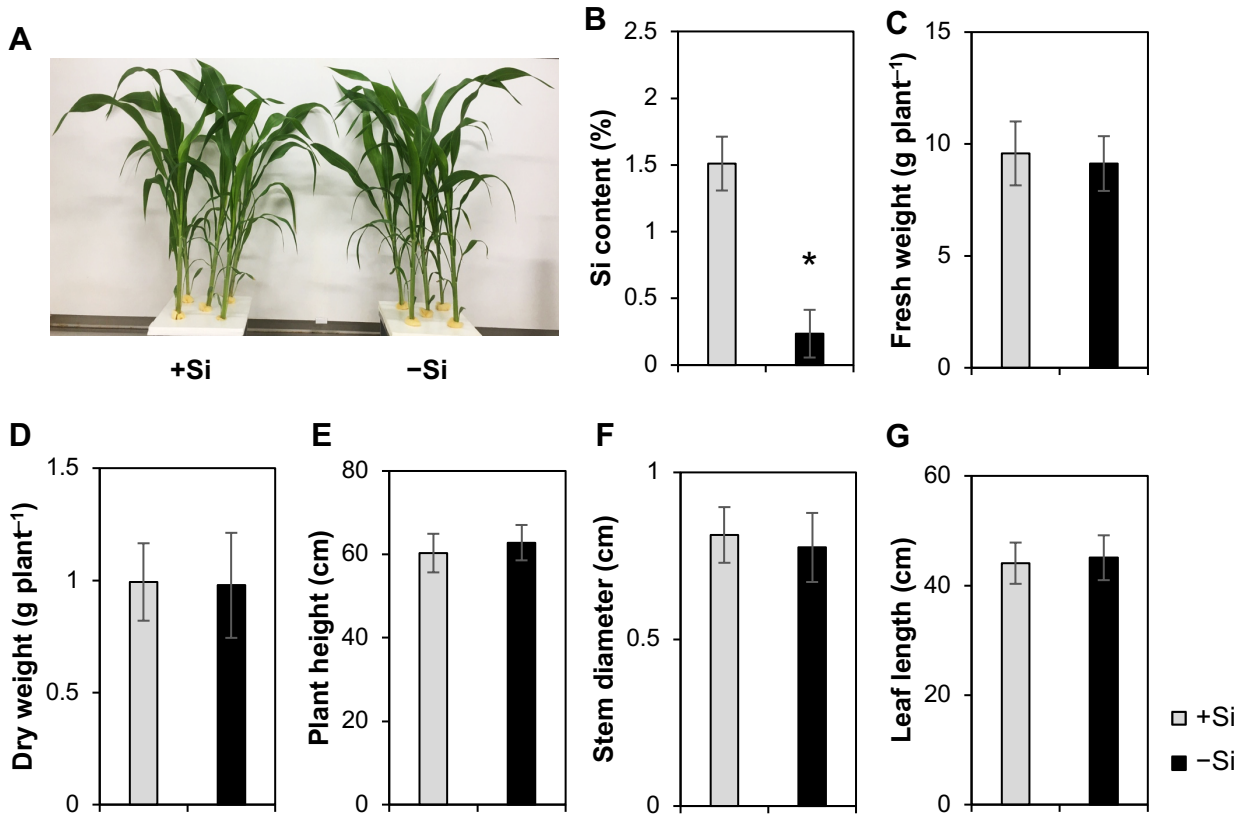

Figure 3.1. Effect of silicon (Si) treatment on growth of hydroponically grown sorghum seedlings. (**A**) Appearance, (**B**) Si content, (**C**) shoot fresh weight, (**D**) shoot dry weight, (**E**) plant height, (**F**) stem diameter, and (**G**) leaf length of sorghum seedlings grown under +Si or −Si conditions at 3 weeks after treatment. Values are given as the mean ± standard deviation (SD) (n = 8). Asterisks indicate significant differences between +Si and −Si plants (Student's *t* test, $p < 0.05$).

3.3.2 Chemical analyses of cell walls

I first examined whether Si limitation affected the composition and structures of the cell walls of hydroponically grown sorghum seedlings through a series of chemical analyses. Si limitation considerably reduced the cell wall Si content (**Figure 3.2A**). The thioglycolic acid assay indicated that −Si plants contained 31% more lignin than +Si plants (**Figure 3.2B**). The thioacidolysis assay revealed a significant increase in G and S lignin monomer yields in −Si cell walls (**Figure 3.2C-E**). The lignin aromatic composition was also altered by Si limitation, as revealed by an increase in the thioacidolysis-derived S/G lignin monomer ratio in the −Si cell walls (**Figure 3.2F**), which could be ascribed to a 32% increase in the S-type lignin monomer yield as opposed to an 18% increase in the G-type monomer yield in −Si plants (**Figure 3.2**). The content of alkali-releasable *p*CA was markedly increased by −Si treatment (**Figure 3.2G**). On the other hand, the content of alkali-releasable FA was similar between the +Si and −Si cell walls (**Figure 3.2H**).

The content of crystalline cellulose was not significantly different between treatments (**Figure 3.3A**). The amount of neutral sugars released by TFA hydrolysis tended to be higher in the −Si cell wall, but statistical significance was not detected (**Figure 3.3B-F**). The uronic acid content, which probably constituted hemicelluloses and pectin, was 29% higher in the −Si cell wall than in the +Si cell wall (**Figure 3.3G**). However, the proportion of these TFA-released neutral sugars and uronic acids remained unchanged between the +Si and −Si cell walls (**Figure 3.3I**).

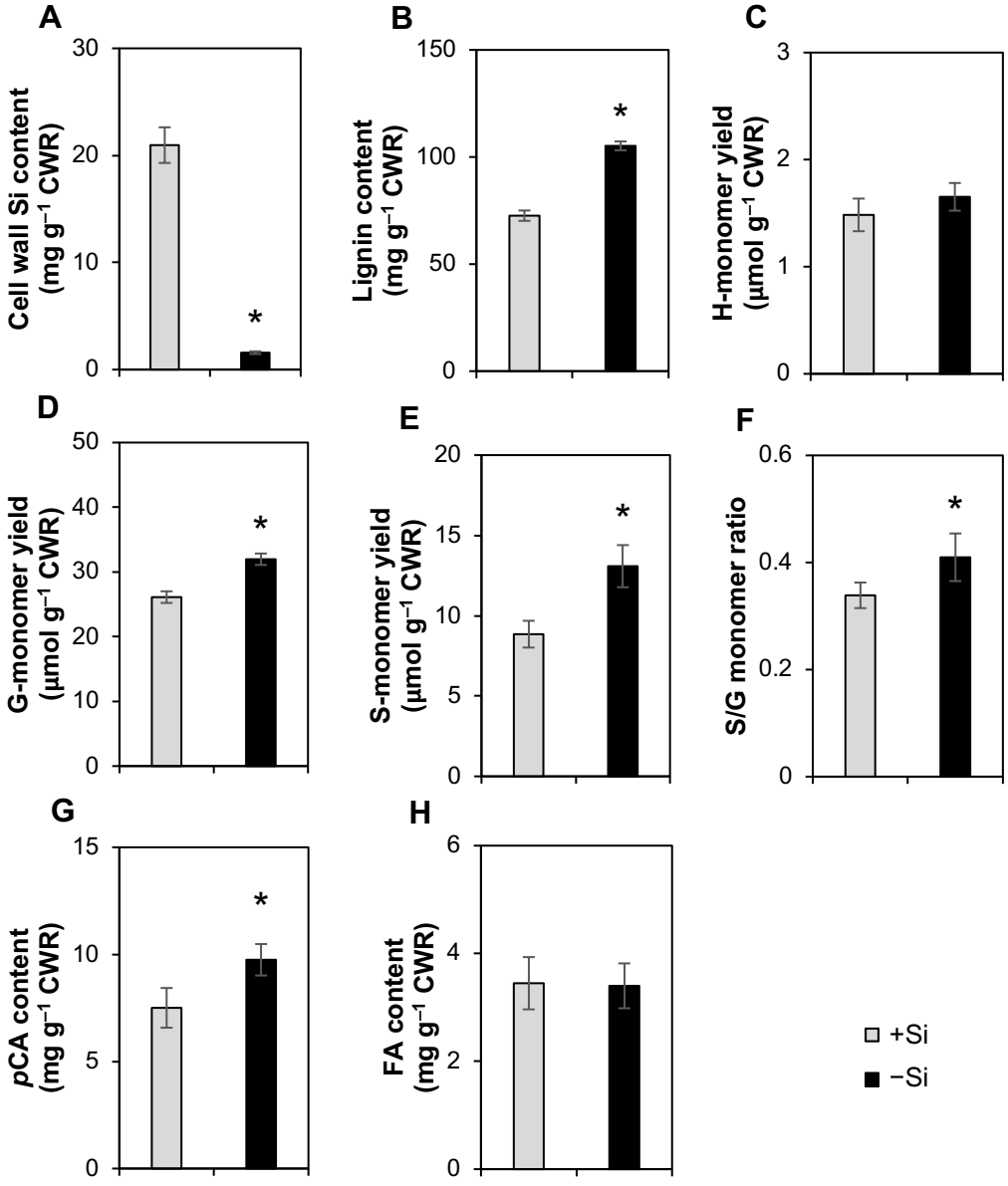

Figure 3.2. Chemical analysis data of hydroponically grown sorghum cell walls from +Si and −Si seedlings. (**A**) Cell wall Si content, (**B**) lignin content, (**C**) *p*-hydroxyphenyl (H)-monomer yield, (**D**) guaiacyl (G)-monomer yield, (**E**) syringyl (S)-monomer yield, (**F**) S/G monomer ratio, (**G**) *p*-coumarate (*p*CA) content, and (**H**) ferulate (FA) content of sorghum seedlings grown under +Si or −Si conditions at 3 weeks after treatment. CWR: cell wall residue. Values are given as mean ± SD (n = 3). Asterisks indicate significant differences between +Si and −Si plants (Student's *t* test, $p < 0.05$).

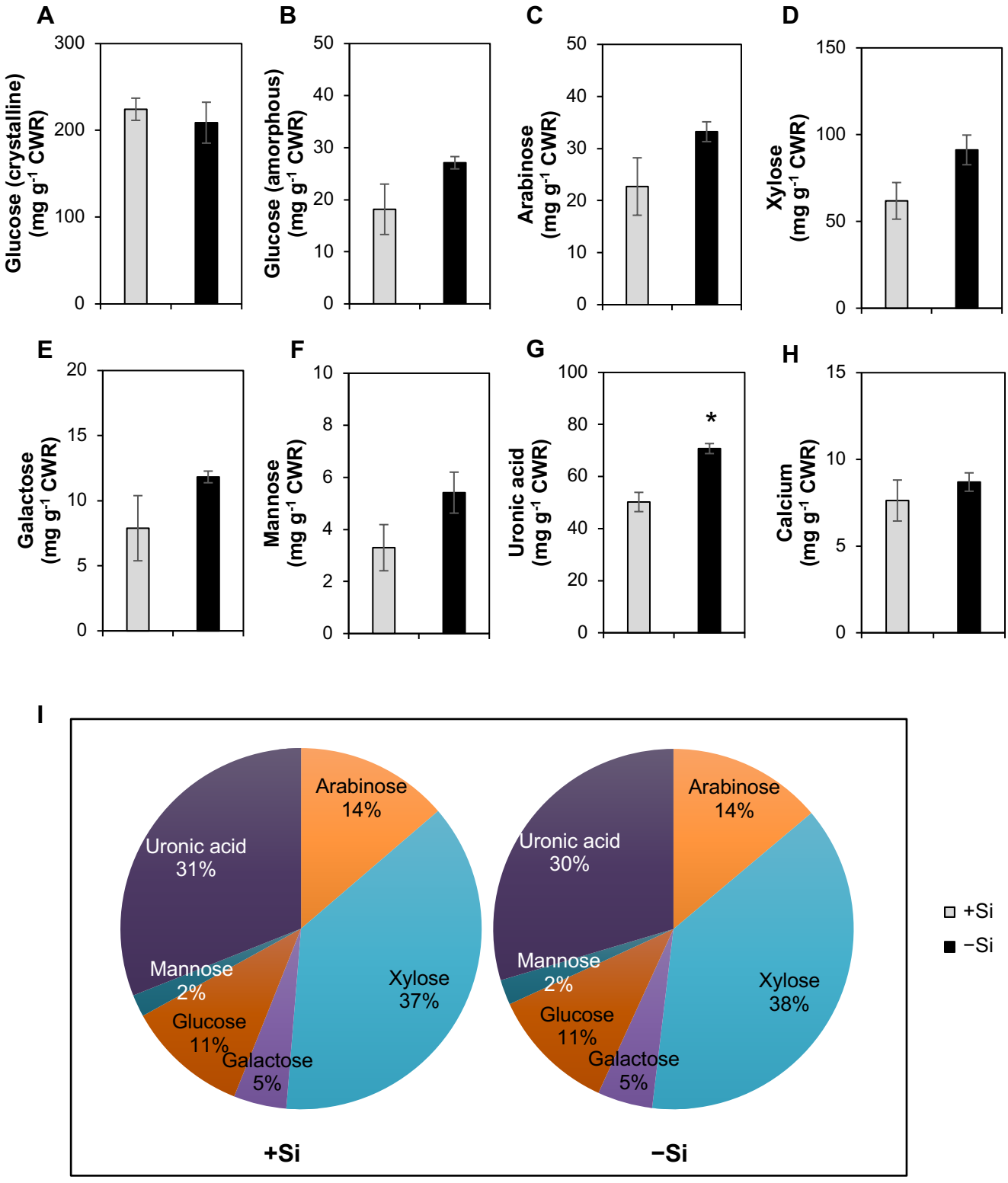

Figure 3.3. Cell wall mineral and polysaccharides contents and proportion of hydroponically grown sorghum seedlings cultivated under +Si or −Si conditions at 3 weeks after treatment. (**A**) Glucose content from crystalline cellulose, (**B**) glucose content from matrix polysaccharides, (**C**) arabinose content, (**D**) xylose content, (**E**) galactose content, (**F**) mannose content, (**G**) uronic acid content, and (**H**) monosaccharides proportion from matrix polysaccharides. CWR: cell wall residue. Values are given as mean ± SD (n = 3). Asterisks indicate significant differences between +Si and −Si plants (Student's *t* test, $p < 0.05$) for (A-G).

3.3.3 2D HSQC NMR analysis

The alteration in lignocellulose composition and structures under limited Si supply was also analyzed by 2D HSQC NMR analysis on +Si and −Si cell walls by using the gel-state whole-cell wall NMR method (H. Kim & Ralph, 2010; Mansfield et al., 2012). The aromatic sub-regions of the HSQC NMR spectra displayed well-resolved contour signals from the lignin aromatic units, such as S (**S**), G (**G**), and tricin (**T**) units, along with the signals from the hydroxycinnamate FA (**F**) and *p*CA (**P**) units (**Figure 3.4A**). In addition, the sugar anomeric sub-regions of the spectra displayed contour signals from cell wall polysaccharide components, including glucan (**Gl**), non-acetylated (**Xy**), acetylated (**Xy′** and **Xy″**) xylan, arabinan (**Ar**), galactan (**Ga**), and glucuronan (**GU**) units (**Figure 3.4B**). These contour signals were integrated and normalized based on the sum of the total NMR signals (**Figure 3.4C-D**). The relative intensities of the **S**, **G**, and **P** signals in the −Si cell walls were 37%, 11%, and 18% higher than those in the +Si cell walls (**Figure 3.4C**), corroborating the increased lignin aromatic unit and lignin-bound *p*CA levels in −Si cell walls, as revealed by the chemical analyses (**Figure 3.2**). Furthermore, in line with the thioacidolysis-derived S/G lignin monomer ratio data (**Figure 3.2F**), the **S**/**G** signal ratio was 30% higher in the −Si cell walls than in the +Si cell walls (**Figure 3.4D**). On the other hand, the lignin-bound tricin signal (**T**) was lower in the −Si cell walls than in the +Si cell walls (**Figure 3.4C**).

Regarding the polysaccharide components, the intensity of the arabinan (**Ar**) signal in the −Si cell wall was slightly higher than that in the +Si cell walls. The −Si cell wall also showed an increased glucuronan (**GU**) signal (**Figure 3.4C**). Meanwhile, the signals from glucan (**Gl**), xylan (sum of the non-acetylated and acetylated xylan signals, **Xy** + **Xy′** + **Xy″**), and galactan (**Ga**) appeared to be lower in the −Si cell walls than in the +Si cell walls (**Figure 3.4C**). Overall, the modulation of the signals by Si treatment was more remarkable in the aromatic sub-regions (**S**, **G**, and **T**) than in the sugar anomeric sub-regions (**Gl**, **Xy** + **Xy′** + **Xy″**, **Ar**, **Ga**, and **GU**). In line with the increased lignin content in the −Si cell wall, the lignin/polysaccharide signal ratio was higher in the −Si cell wall than in the +Si cell walls (**Figure 3.4D**).

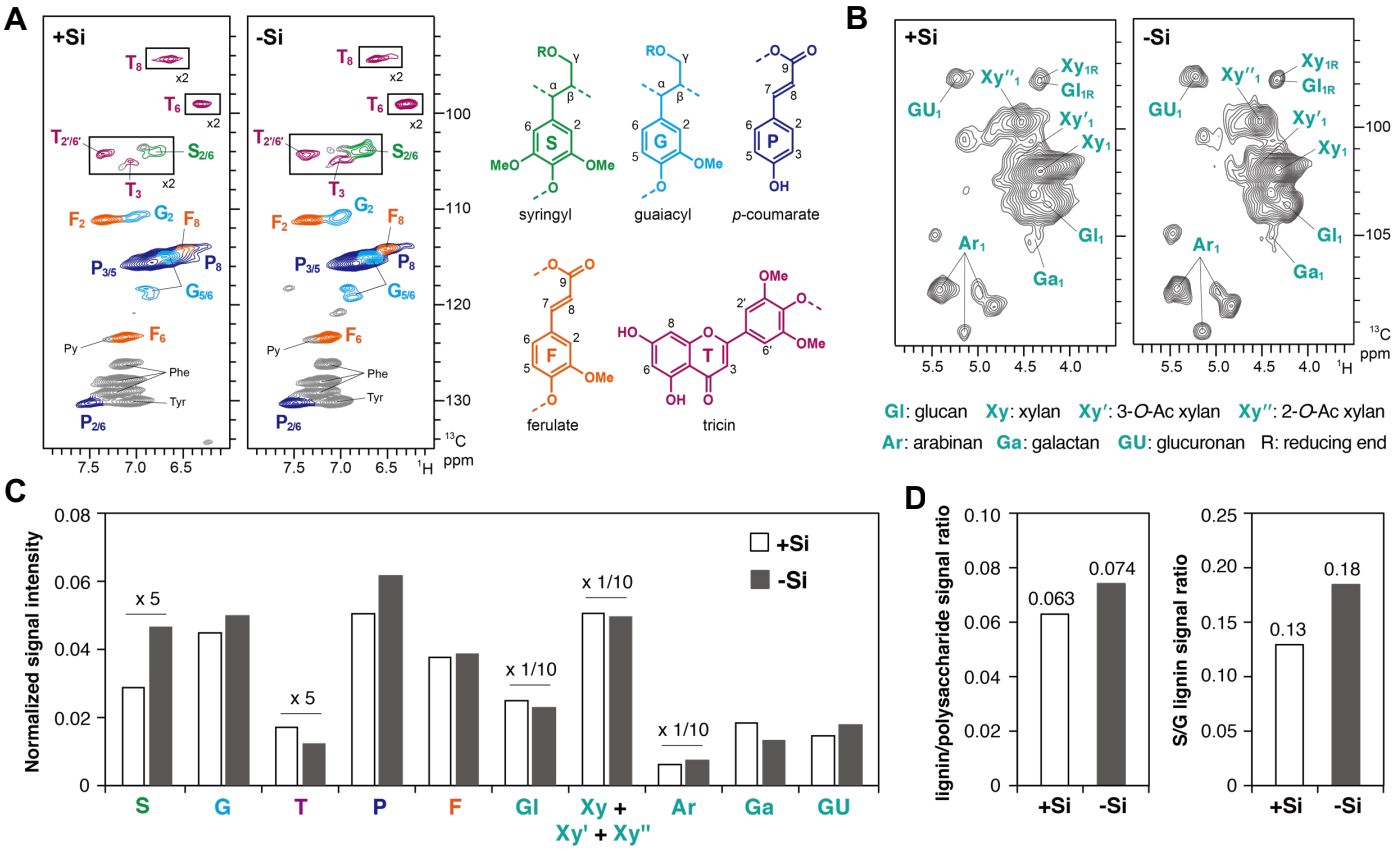

Figure 3.4. Two-dimensional short-range ^{1}H-^{13}C correlation nuclear magnetic resonance (2D HSQC NMR) spectra of the cell walls of hydroponically grown sorghum seedlings cultivated under +Si and −Si conditions at 3 weeks after treatment. (**A**) Aromatic sub-regions showing signals from major lignin hydroxycinnamate aromatic units. Contours are color-coded to match the displayed structures. Boxes labeled ×2 denote regions where the scale has been vertically enlarged two-fold. (**B**) Anomeric sub-regions showing signals from major cell wall polysaccharide units. Py, pyridine (solvent). (**C**) Normalized intensity of major lignin, hydroxycinnamate and polysaccharide signals expressed as integrals relative to the total NMR signals. Data labeled ×5 or ×1/10 denote data that has been multiplied by a factor 5 or divided by a factor 10 for visualization, respectively. (**D**) Lignin/polysaccharide and S/G lignin signal ratios. NMR spectra were collected for pooled cell wall samples prepared from three independently grown plants.

3.3.4 Histochemical analyses

The deposition and localization patterns of Si in the aboveground parts of sorghum seedlings were examined by mapping analysis using a scanning electron microscope coupled with an energy dispersive X-ray analyzer (SEM-EDX). As shown in **Figure 3.5A**, an intense Si signal was detected in the epidermis of +Si plants, whereas no signal was detected in −Si plants. The abundance and localization of lignin in the aerial parts of seedlings were examined by acriflavine (Donaldson et al., 2001) and phloroglucinol-HCl (Pomar et al., 2002) staining (**Figure 3.5B**). Compared with +Si plants, more intense staining was detected in −Si plants with both methods, suggesting that −Si plants accumulated more lignin. Enhanced staining was most remarkable in the sclerenchyma cells (**Figure 3.5B**). The transverse sections were also subjected to vanillin-HCl staining for the cell wall-bound flavonoid, which presumably represented lignin-bound tricin (Lam et al., 2017). However, no significant difference was observed between the +Si and −Si plants (**Figure 3.5B**).

Regarding the polysaccharide component in the cell walls, the deposition of cellulose was examined by staining with calcofluor white reagent. A relatively more intense fluorescence signal was detected in sclerenchyma cells, vascular bundles, and mesophyll cells (**Figure 3.6A**). The fluorescence intensity was slightly lower in −Si plants than in +Si plants, but the distribution of the signal was not clearly different between treatments (**Figure 3.6A**). For hemicelluloses, I examined the abundance and distribution of MLG and arabinoxylan in this study. The fluorescence signal from the antibody recognizing MLG occurred in all parts of the section, including the epidermis, sclerenchyma, vascular bundle, and mesophyll (**Figure 3.6B**). Meanwhile, the fluorescence signal from anti-arabinoxylan antibody (LM11) was distributed particularly in the epidermis, sclerenchyma, and vascular bundle. No difference was observed in the intensities of these signals between +Si and −Si plants (**Figure 3.6B**), suggesting that the amount of these polysaccharides was not modulated by −Si treatment. The abundance and localization of callose were examined by aniline blue staining and anti-callose antibody immunostaining (**Figure 3.6C**). Aniline blue stained epidermis, sclerenchyma, and vascular bundle but not mesophyll in both +Si and −Si plants. Epidermis and sclerenchyma were stained more intensely than the vascular bundle, and selective staining was more remarkable in −Si plants. The fluorescence signal from the anti-callose antibody was distributed in all parts of the section, including the epidermis, sclerenchyma, vascular bundle, and mesophyll. These signals were more intense in the −Si plants than in the +Si plants (**Figure 3.6C**).

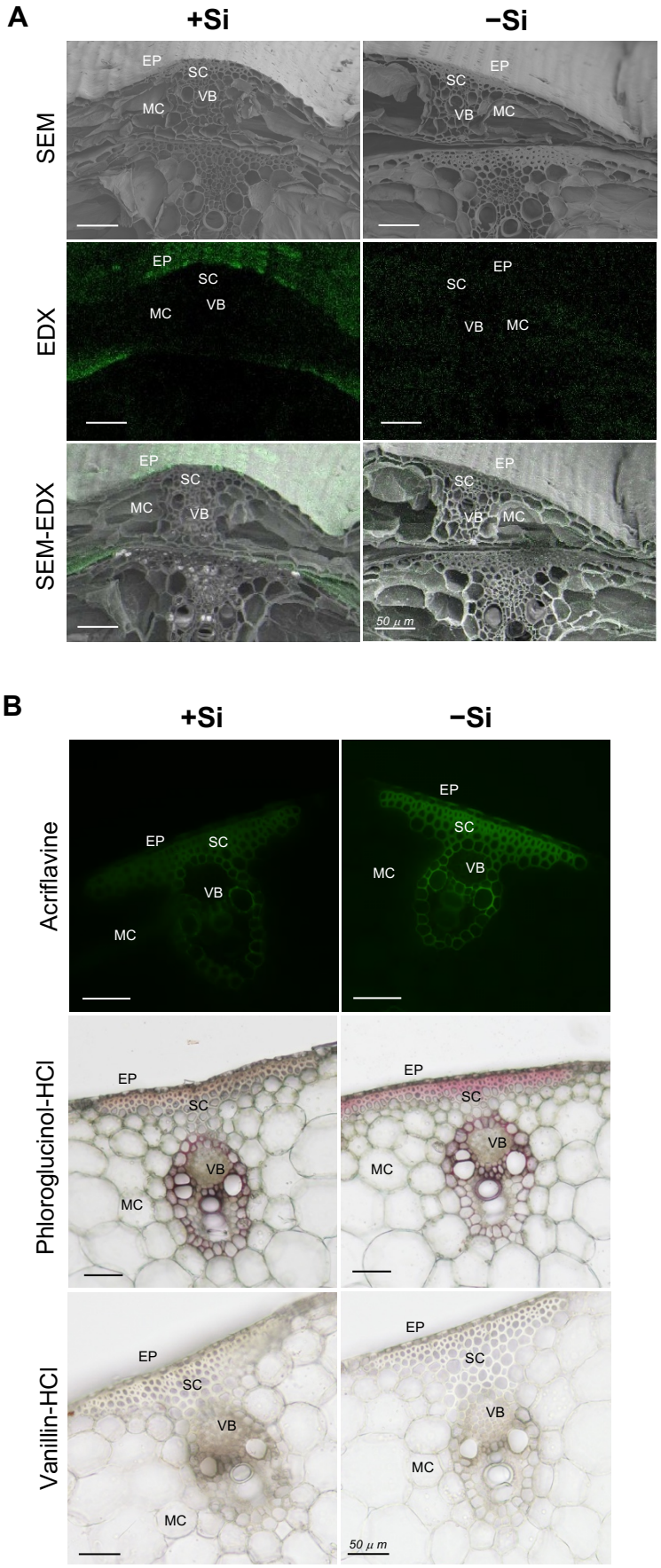

Figure 3.5. Localization of Si, lignin, and flavonoids in hydroponically grown sorghum seedlings cultivated under +Si or −Si conditions at 3 weeks after treatment. (**A**) Si mapping images obtained by SEM-EDX, and (**B**) lignin distribution using acriflavine, phloroglucinol-HCl staining, and flavonoid distribution using vanillin-HCl staining. EP: epidermis, MC: mesophyll cell, SC: sclerenchyma cell, and VB: vascular bundle.

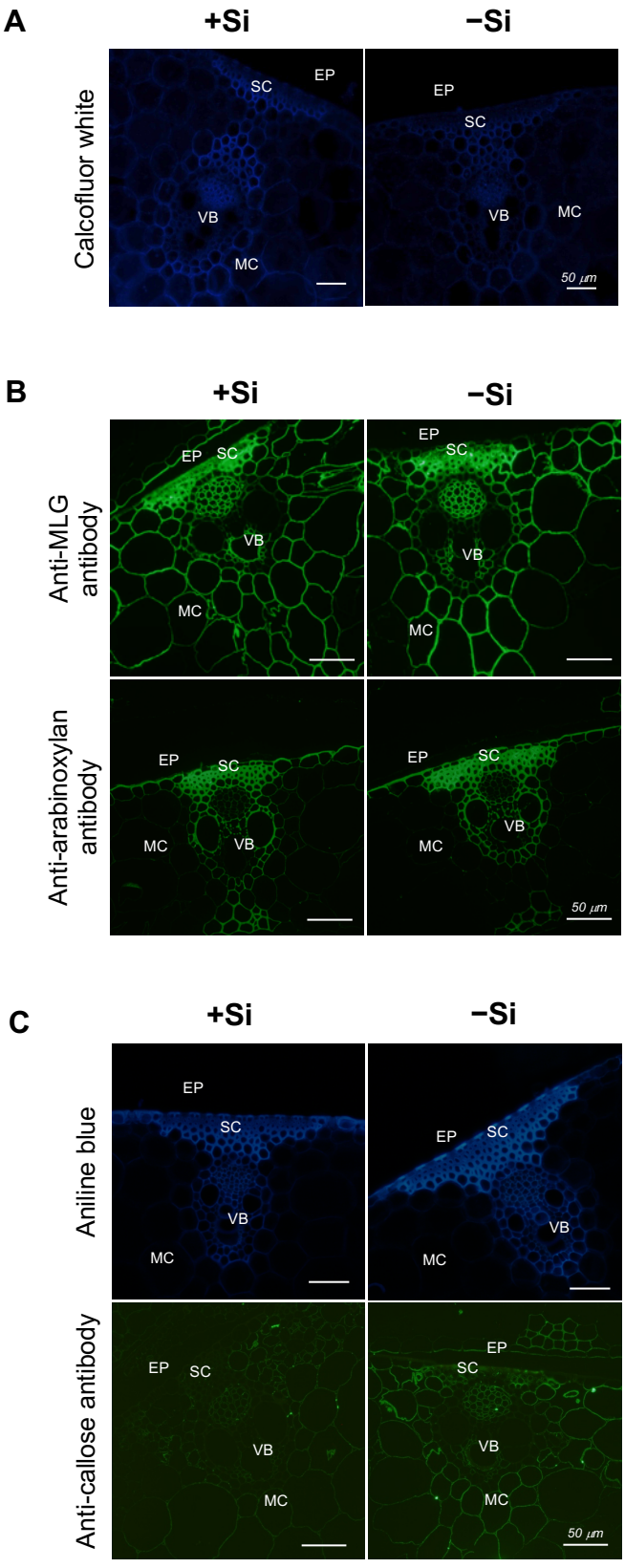

Figure 3.6. Histochemical analyses of hydroponically grown sorghum seedlings cultivated under +Si or −Si conditions at 3 weeks after treatment. (**A**) Cellulose deposition using calcofluor white staining, (**B**) hemicelluloses deposition using anti-mixed-linkage (1→3), (1→4)-β-D-glucan (MLG), and arabinoxylan antibodies, and (**C**) callose deposition using aniline blue staining and (1→3)-β-D-glucan (callose) antibody. EP: epidermis, MC: mesophyll cell, SC: sclerenchyma cell, and VB: vascular bundle.

3.3.5 RNA sequencing analysis

To obtain insights into the physiological changes underlying the alteration of sorghum cell wall properties under Si limitation, transcriptomes of +Si and −Si plants were compared by RNA sequencing. Of the 34567 expressed genes identified, 3572 were differentially expressed (adjusted p value < 0.05) between +Si and −Si seedlings at 3 weeks after starting the treatment (data not shown). Of these, the expression of 1653 and 1919 genes were up- and downregulated by −Si treatment, respectively.

Gene ontology (GO) enrichment analysis of the DEGs showed that GO terms for 50 or 69 biological processes were significantly overrepresented (adjusted p value < 0.05) among genes up- or downregulated by −Si treatment, respectively (**Table 3.2** or **Table 3.3**). Genes upregulated by −Si treatment were mainly related to localization, reproductive cellular process, response to biotic stimulus, and secondary metabolic processes, including phenylpropanoid, flavonoid, and cellular aromatic compound biosynthesis (**Table 3.2**). Terms associated with cellular carbohydrate metabolic processes and anatomical structural homeostasis were also enriched (**Table 3.2**). In addition, enrichment was also observed with terms related to mineral nutrition, including cellular nitrogen compounds and phosphorus metabolic processes (**Table 3.2**). Genes downregulated under the −Si condition included those associated with the response to abiotic and chemical stimuli, including light, radiation, abscisic acid, jasmonic acid, osmotic, salt, and water deprivation stresses (**Table 3.3**). Enrichment was also observed with GO term photosynthesis, such as light reaction and regulation of stomatal movement (**Table 3.3**).

Table 3.2. Gene ontology (GO) term enrichment in the biological process category of the differentially expressed genes (DEGs) induced by −Si or repressed by +Si treatment of sorghum seedlings at 3 weeks after treatment.

GO term	Description	Number of genes	*p* value	*q* value
GO:0051179	Localization	248	1.E-04	2.E-02
GO:0051234	Establishment of localization	234	2.E-04	3.E-02
GO:0006810	Transport	231	2.E-04	3.E-02
GO:0043412	Macromolecule modification	198	2.E-05	5.E-03
GO:0006464	Protein modification process	188	2.E-05	5.E-03
GO:0043687	Post-translational protein modification	171	2.E-05	4.E-03
GO:0006793	Phosphorus metabolic process	157	8.E-06	2.E-03
GO:0006796	Phosphate metabolic process	157	7.E-06	2.E-03
GO:0016310	Phosphorylation	150	1.E-06	5.E-04
GO:0006468	Protein amino acid phosphorylation	135	7.E-07	3.E-04
GO:0005975	Carbohydrate metabolic process	119	7.E-06	2.E-03
GO:0006519	Cellular amino acid and derivative metabolic process	111	4.E-08	4.E-05
GO:0009607	Response to biotic stimulus	107	8.E-05	1.E-02
GO:0019748	Secondary metabolic process	88	6.E-09	9.E-06
GO:0034641	Cellular nitrogen compound metabolic process	85	1.E-10	4.E-07
GO:0044262	Cellular carbohydrate metabolic process	79	9.E-07	4.E-04
GO:0006725	Cellular aromatic compound metabolic process	79	2.E-07	1.E-04
GO:0006575	Cellular amino acid derivative metabolic process	68	4.E-07	2.E-04
GO:0009698	Phenylpropanoid metabolic process	56	5.E-08	4.E-05
GO:0042398	Cellular amino acid derivative biosynthetic process	54	4.E-07	2.E-04
GO:0019438	Aromatic compound biosynthetic process	53	5.E-07	2.E-04
GO:0051186	Cofactor metabolic process	50	4.E-06	2.E-03
GO:0009699	Phenylpropanoid biosynthetic process	50	1.E-08	1.E-05
GO:0044271	Cellular nitrogen compound biosynthetic process	49	2.E-04	2.E-02
GO:0005996	Monosaccharide metabolic process	41	1.E-04	2.E-02
GO:0006732	Coenzyme metabolic process	40	2.E-06	8.E-04
GO:0019318	Hexose metabolic process	37	2.E-05	4.E-03
GO:0009812	Flavonoid metabolic process	35	2.E-07	1.E-04

GO:0009813	Flavonoid biosynthetic process	35	1.E-08	1.E-05
GO:0044275	Cellular carbohydrate catabolic process	30	3.E-04	4.E-02
GO:0008652	Cellular amino acid biosynthetic process	29	2.E-04	2.E-02
GO:0006006	Glucose metabolic process	28	4.E-05	8.E-03
GO:0019320	Hexose catabolic process	25	2.E-04	2.E-02
GO:0006007	Glucose catabolic process	25	2.E-04	2.E-02
GO:0032504	Multicellular organism reproduction	25	6.E-06	2.E-03
GO:0048609	Reproductive process in a multicellular organism	24	7.E-06	2.E-03
GO:0048610	Reproductive cellular process	23	4.E-17	3.E-13
GO:0043603	Cellular amide metabolic process	19	3.E-05	6.E-03
GO:0006084	Acetyl-coa metabolic process	17	3.E-05	6.E-03
GO:0051187	Cofactor catabolic process	16	3.E-05	6.E-03
GO:0019362	Pyridine nucleotide metabolic process	15	2.E-04	2.E-02
GO:0010876	Lipid localization	13	4.E-10	9.E-07
GO:0031400	Negative regulation of protein modification process	10	8.E-06	2.E-03
GO:0051554	Flavonol metabolic process	9	7.E-05	1.E-02
GO:0051555	Flavonol biosynthetic process	9	7.E-05	1.E-02
GO:0051552	Flavone metabolic process	9	7.E-05	1.E-02
GO:0051553	Flavone biosynthetic process	9	7.E-05	1.E-02
GO:0031396	Regulation of protein ubiquitination	8	5.E-05	1.E-02
GO:0031401	Positive regulation of protein modification process	7	1.E-04	2.E-02
GO:0060249	Anatomical structure homeostasis	7	1.E-05	3.E-03

The overrepresentation was tested by web-tool (http://bioinfo.cau.edu.cn/agriGO/analysis.php) (Fisher and Yekutieli tests, q value < 0.05).

Table 3.3. Gene ontology (GO) term enrichment in the biological process category of the differentially expressed genes (DEGs) repressed by −Si or induced by +Si treatment of sorghum seedlings at 3 weeks after treatment.

GO term	Description	Number of genes	*p* value	*q* value
GO:0050896	Response to stimulus	441	3E-04	4E-02
GO:0042221	Response to chemical stimulus	260	6E-06	2E-03
GO:0009628	Response to abiotic stimulus	226	6E-10	9E-07
GO:0010033	Response to organic substance	177	3E-05	5E-03
GO:0009719	Response to endogenous stimulus	163	3E-07	2E-04
GO:0009791	Post-embryonic development	143	3E-05	6E-03
GO:0009725	Response to hormone stimulus	142	1E-05	3E-03
GO:0009416	Response to light stimulus	111	2E-09	2E-06
GO:0009314	Response to radiation	111	5E-09	4E-06
GO:0006091	Generation of precursor metabolites and energy	89	4E-13	7E-10
GO:0044262	Cellular carbohydrate metabolic process	85	4E-06	1E-03
GO:0015979	Photosynthesis	81	2E-29	1E-25
GO:0034641	Cellular nitrogen compound metabolic process	80	1E-06	4E-04
GO:0006811	Ion transport	76	4E-04	4E-02
GO:0009737	Response to abscisic acid stimulus	68	7E-05	1E-02
GO:0006970	Response to osmotic stress	65	9E-05	1E-02
GO:0042592	Homeostatic process	59	3E-04	4E-02
GO:0009651	Response to salt stress	55	3E-04	4E-02
GO:0009733	Response to auxin stimulus	53	3E-04	4E-02
GO:0019684	Photosynthesis, light reaction	49	5E-19	2E-15
GO:0055114	Oxidation reduction	49	6E-07	3E-04
GO:0016051	Carbohydrate biosynthetic process	49	5E-04	5E-02
GO:0010035	Response to inorganic substance	46	2E-06	8E-04
GO:0009753	Response to jasmonic acid stimulus	45	2E-05	4E-03
GO:0009415	Response to water	44	2E-04	3E-02
GO:0009639	Response to red or far red light	41	1E-04	2E-02
GO:0009414	Response to water deprivation	41	5E-04	5E-02
GO:0019318	Hexose metabolic process	37	2E-04	3E-02

GO:0006073	Cellular glucan metabolic process	32	2E-04	3E-02
GO:0044042	Glucan metabolic process	32	5E-04	4E-02
GO:0042440	Pigment metabolic process	30	2E-04	3E-02
GO:0009657	Plastid organization	29	2E-06	7E-04
GO:0009642	Response to light intensity	29	2E-06	8E-04
GO:0010118	Stomatal movement	27	1E-04	2E-02
GO:0022900	Electron transport chain	26	6E-07	3E-04
GO:0048609	Reproductive process in a multicellular organism	26	7E-06	2E-03
GO:0032504	Multicellular organism reproduction	26	2E-05	4E-03
GO:0006820	Anion transport	25	4E-04	4E-02
GO:0045454	Cell redox homeostasis	24	1E-04	2E-02
GO:0006721	Terpenoid metabolic process	23	2E-04	3E-02
GO:0009767	Photosynthetic electron transport chain	22	2E-09	2E-06
GO:0009644	Response to high light intensity	22	2E-05	5E-03
GO:0016311	Dephosphorylation	22	4E-04	4E-02
GO:0010119	Regulation of stomatal movement	21	2E-04	3E-02
GO:0009886	Post-embryonic morphogenesis	20	2E-04	3E-02
GO:0010114	Response to red light	19	2E-05	4E-03
GO:0010017	Red or far-red light signaling pathway	19	2E-04	3E-02
GO:0005984	Disaccharide metabolic process	18	9E-07	4E-04
GO:0009311	Oligosaccharide metabolic process	18	6E-05	1E-02
GO:0033013	Tetrapyrrole metabolic process	17	4E-04	4E-02
GO:0048610	Reproductive cellular process	16	8E-10	1E-06
GO:0046351	Disaccharide biosynthetic process	16	1E-06	6E-04
GO:0009312	Oligosaccharide biosynthetic process	16	8E-06	2E-03
GO:0043467	Regulation of generation of precursor metabolites & energy	15	7E-06	2E-03
GO:0009765	Photosynthesis, light harvesting	14	5E-06	1E-03
GO:0005982	Starch metabolic process	13	3E-04	4E-02
GO:0042548	Regulation of photosynthesis, light reaction	12	5E-06	1E-03
GO:0010109	Regulation of photosynthesis	12	6E-06	2E-03
GO:0015977	Carbon fixation	12	3E-04	3E-02
GO:0019253	Reductive pentose-phosphate cycle	10	6E-04	5E-02

GO:0009768	Photosynthesis, light harvesting in photosystem I	9	6E-06	2E-03
GO:0005992	Trehalose biosynthetic process	9	4E-04	4E-02
GO:0005991	Trehalose metabolic process	9	4E-04	4E-02
GO:0010876	Lipid localization	8	4E-05	7E-03
GO:0009773	Photosynthetic electron transport in photosystem I	8	1E-04	2E-02
GO:0060249	Anatomical structure homeostasis	7	2E-05	5E-03
GO:0010207	Photosystem II assembly	7	1E-04	2E-02
GO:0043155	Negative regulation of photosynthesis, light reaction	7	4E-04	4E-02
GO:0010205	Photoinhibition	7	4E-04	4E-02

The overrepresentation was tested by web-tool (http://bioinfo.cau.edu.cn/agriGO/analysis.php) (Fisher and Yekutieli tests, q value < 0.05).

In addition to the biological process category, the GO analysis displayed 40 or 5 molecular functions overrepresentated among the genes up- or down-regulated by −Si treatment, respectively (**Table 3.4** or **Table 3.5**). In detail, the genes up-regulated by −Si condition mainly associated with the following GO terms: transporter activities, catalytic activities (oxidoreductase, isomerase, lyase, and transferase activities), and several bindings including nucleoside, cofactor, vitamin, nucleotide, and carbohydrate bindings (**Table 3.4**). While, the GO terms denoting chlorophyll binding, carbon-carbon lyase, and phosphoric ester hydrolase activities were enriched among the DEGs down-regulated by −Si treatment (**Table 3.5**). Lastly, the GO enrichment analysis also determined 23 or 50 cellular components overrepresentated among the genes up- or down-regulated by −Si treatment, respectively (**Table 3.6** or **Table 3.7**). The genes up-regulated by −Si condition mainly included those related to membrane and mitochondrial parts (**Table 3.6**). Whereas, the GO terms associated with chloroplast, plastid, and thylakoid parts were enriched among the DEGs down-regulated by −Si condition (**Table 3.7**).

Table 3.4. Gene ontology (GO) term enrichment in the molecular function category of the differentially expressed genes (DEGs) induced by −Si or repressed by +Si treatment of sorghum seedlings at 3 weeks after treatment.

GO term	Description	Number of genes	*p* value	*q* value
GO:0003824	Catalytic activity	840	2E-09	3E-06
GO:0016740	Transferase activity	344	3E-06	5E-04
GO:0000166	Nucleotide binding	301	2E-04	1E-02
GO:0017076	Purine nucleotide binding	259	8E-06	8E-04
GO:0032555	Purine ribonucleotide binding	244	1E-05	1E-03
GO:0032553	Ribonucleotide binding	244	1E-05	1E-03
GO:0001882	Nucleoside binding	241	2E-05	2E-03
GO:0030554	Adenyl nucleotide binding	240	2E-05	1E-03
GO:0001883	Purine nucleoside binding	240	2E-05	1E-03
GO:0032559	Adenyl ribonucleotide binding	225	3E-05	2E-03
GO:0005524	ATP binding	223	3E-05	2E-03
GO:0016491	Oxidoreductase activity	189	3E-08	2E-05
GO:0016301	Kinase activity	168	1E-06	3E-04
GO:0016773	Phosphotransferase activity, alcohol group as acceptor	155	9E-07	2E-04
GO:0005215	Transporter activity	152	4E-06	5E-04
GO:0004672	Protein kinase activity	136	1E-05	1E-03
GO:0004674	Protein serine/threonine kinase activity	127	2E-07	6E-05
GO:0004713	Protein tyrosine kinase activity	121	2E-08	1E-05
GO:0022857	Transmembrane transporter activity	118	4E-06	5E-04
GO:0022892	Substrate-specific transporter activity	116	7E-06	8E-04
GO:0022891	Substrate-specific transmembrane transporter activity	99	7E-06	8E-04
GO:0022804	Active transmembrane transporter activity	80	5E-05	3E-03
GO:0048037	Cofactor binding	71	4E-05	3E-03
GO:0015075	Ion transmembrane transporter activity	68	1E-03	4E-02
GO:0008324	Cation transmembrane transporter activity	57	8E-04	4E-02
GO:0016829	Lyase activity	50	9E-04	4E-02
GO:0030246	Carbohydrate binding	49	1E-07	5E-05

GO:0016614	Oxidoreductase activity, acting on CH-OH group of donors	38	1E-05	1E-03
GO:0005529	Sugar binding	37	1E-06	3E-04
GO:0016853	Isomerase activity	37	4E-04	2E-02
GO:0016616	Oxidoreductase activity, acting on the CH-OH group of donors, NAD or NADP as acceptor	36	3E-06	5E-04
GO:0008194	UDP-glycosyltransferase activity	34	8E-04	4E-02
GO:0004872	Receptor activity	33	2E-04	1E-02
GO:0019842	Vitamin binding	28	4E-04	2E-02
GO:0035251	UDP-glucosyltransferase activity	20	7E-04	3E-02
GO:0016811	Hydrolase activity, acting on carbon-nitrogen (but not peptide) bonds, in linear amides	14	3E-04	2E-02
GO:0015326	Cationic amino acid transmembrane transporter activity	7	6E-04	3E-02
GO:0010290	Chlorophyll catabolite transmembrane transporter activity	6	8E-04	4E-02
GO:0015431	Glutathione S-conjugate-exporting atpase activity	6	8E-04	4E-02
GO:0008281	Sulfonylurea receptor activity	6	1E-03	4E-02

The overrepresentation was tested by web-tool (http://bioinfo.cau.edu.cn/agriGO/analysis.php) (Fisher and Yekutieli tests, q value < 0.05).

Table 3.5. Gene ontology (GO) term enrichment in the molecular function category of the differentially expressed genes (DEGs) repressed by −Si or induced by +Si treatment of sorghum seedlings at 3 weeks after treatment.

GO term	Description	Number of genes	*p* value	*q* value
GO:0042578	Phosphoric ester hydrolase activity	64	3E-07	2E-04
GO:0016791	Phosphatase activity	57	2E-07	2E-04
GO:0004721	Phosphoprotein phosphatase activity	33	1E-04	5E-02
GO:0016830	Carbon-carbon lyase activity	29	9E-06	5E-03
GO:0016168	Chlorophyll binding	13	1E-05	5E-03

The overrepresentation was tested by web-tool (http://bioinfo.cau.edu.cn/agriGO/analysis.php) (Fisher and Yekutieli tests, q value < 0.05).

Table 3.6. Gene ontology (GO) term enrichment in the cellular component category of the differentially expressed genes (DEGs) induced by −Si or repressed by +Si treatment of sorghum seedlings at 3 weeks after treatment.

GO term	Description	Number of genes	*p* value	*q* value
GO:0005737	Cytoplasm	569	2E-06	3E-04
GO:0044444	Cytoplasmic part	496	5E-07	2E-04
GO:0016020	Membrane	371	3E-05	3E-03
GO:0044425	Membrane part	225	3E-06	5E-04
GO:0031224	Intrinsic to membrane	169	6E-06	8E-04
GO:0005739	Mitochondrion	151	5E-07	2E-04
GO:0016021	Integral to membrane	148	1E-05	1E-03
GO:0005829	Cytosol	128	3E-04	2E-02
GO:0012505	Endomembrane system	113	2E-04	1E-02
GO:0005783	Endoplasmic reticulum	87	2E-04	1E-02
GO:0044429	Mitochondrial part	68	1E-09	1E-06
GO:0031975	Envelope	65	6E-04	3E-02
GO:0031967	Organelle envelope	63	8E-04	4E-02
GO:0005740	Mitochondrial envelope	50	6E-07	2E-04
GO:0031966	Mitochondrial membrane	44	6E-06	8E-04
GO:0044432	Endoplasmic reticulum part	34	6E-04	3E-02
GO:0005626	Insoluble fraction	28	9E-04	4E-02
GO:0005624	Membrane fraction	27	7E-04	3E-02
GO:0031980	Mitochondrial lumen	22	2E-04	1E-02
GO:0005759	Mitochondrial matrix	22	2E-04	1E-02
GO:0070469	Respiratory chain	15	2E-04	1E-02
GO:0045271	Respiratory chain complex I	10	4E-05	4E-03
GO:0030964	NADH dehydrogenase complex	10	4E-05	4E-03

The overrepresentation was tested by web-tool (http://bioinfo.cau.edu.cn/agriGO/analysis.php) (Fisher and Yekutieli tests, q value < 0.05).

Table 3.7. Gene ontology (GO) term enrichment in the cellular component category of the differentially expressed genes (DEGs) repressed by −Si or induced by +Si treatment of sorghum seedlings at 3 weeks after treatment.

GO term	Description	Number of genes	*p* value	*q* value
GO:0044464	Cell part	1116	2E-05	5E-04
GO:0005623	Cell	1116	2E-05	5E-04
GO:0005622	Intracellular	888	3E-05	8E-04
GO:0044424	Intracellular part	858	5E-05	1E-03
GO:0043229	Intracellular organelle	779	2E-06	6E-05
GO:0043226	Organelle	779	2E-06	7E-05
GO:0043227	Membrane-bounded organelle	750	8E-09	3E-07
GO:0043231	Intracellular membrane-bounded organelle	748	9E-09	3E-07
GO:0005737	Cytoplasm	674	5E-10	2E-08
GO:0044444	Cytoplasmic part	587	2E-10	8E-09
GO:0016020	Membrane	463	8E-11	3E-09
GO:0009536	Plastid	356	1E-63	6E-61
GO:0044422	Organelle part	344	1E-03	2E-02
GO:0044446	Intracellular organelle part	341	2E-03	3E-02
GO:0009507	Chloroplast	334	2E-66	2E-63
GO:0031090	Organelle membrane	205	2E-17	1E-15
GO:0044435	Plastid part	195	4E-54	6E-52
GO:0044434	Chloroplast part	189	2E-55	6E-53
GO:0009579	Thylakoid	163	8E-55	2E-52
GO:0044436	Thylakoid part	150	1E-52	1E-50
GO:0034357	Photosynthetic membrane	149	6E-52	6E-50
GO:0009534	Chloroplast thylakoid	148	4E-52	4E-50
GO:0031976	Plastid thylakoid	148	1E-51	1E-49
GO:0031984	Organelle subcompartment	148	1E-50	9E-49
GO:0042651	Thylakoid membrane	138	1E-49	1E-47
GO:0009535	Chloroplast thylakoid membrane	135	2E-48	1E-46
GO:0055035	Plastid thylakoid membrane	135	2E-48	1E-46
GO:0009521	Photosystem	46	1E-20	9E-19

GO:0010287	Plastoglobule	39	2E-18	8E-17
GO:0009532	Plastid stroma	32	2E-06	5E-05
GO:0009523	Photosystem II	30	4E-13	2E-11
GO:0009526	Plastid envelope	30	1E-05	3E-04
GO:0031977	Thylakoid lumen	29	4E-12	2E-10
GO:0031978	Plastid thylakoid lumen	29	4E-12	2E-10
GO:0009543	Chloroplast thylakoid lumen	29	4E-12	2E-10
GO:0009941	Chloroplast envelope	27	2E-05	5E-04
GO:0009522	Photosystem I	22	4E-11	1E-09
GO:0009570	Chloroplast stroma	22	2E-04	4E-03
GO:0042170	Plastid membrane	20	6E-04	1E-02
GO:0031969	Chloroplast membrane	18	7E-04	1E-02
GO:0008287	Protein serine/threonine phosphatase complex	16	3E-03	4E-02
GO:0009528	Plastid inner membrane	14	2E-03	4E-02
GO:0030095	Chloroplast photosystem II	10	1E-06	4E-05
GO:0009654	Oxygen evolving complex	10	8E-06	2E-04
GO:0030076	Light-harvesting complex	10	3E-04	6E-03
GO:0009842	Cyanelle	8	1E-04	2E-03
GO:0030075	Plasma membrane-derived thylakoid	7	2E-04	5E-03
GO:0030093	Chloroplast photosystem I	6	4E-04	7E-03
GO:0009782	Photosystem I antenna complex	6	5E-04	1E-02
GO:0009538	Photosystem I reaction center	5	4E-04	7E-03

The overrepresentation was tested by web-tool (http://bioinfo.cau.edu.cn/agriGO/analysis.php) (Fisher and Yekutieli tests, q value < 0.05).

Differentially expressed genes associated with the GO term phenylpropanoid biosynthetic process (GO: 0009699) are listed in **Table 3.8**. These include monolignol biosynthesis-related genes, such as *hydroxycinnamoyl-CoA shikimate/quinate hydroxycinnamoyltransferase* (*HCT*), *caffeoyl-CoA* O-*methyltransferase* (*CCoAOMT*), *cinnamoyl-CoA reductase* (*CCR*), *ferulate 5-hydroxylase* (*F5H*) (*=coniferaldehyde 5-hydroxylase*, *CAld5H*), *caffeate/5-hydroxyferulate* O-*methyltransferase* (*COMT*) (*=5-hydroxyconiferaldehyde* O-*methyltransferase*, *CAldOMT*)/*Brown midrib 12* (*Bmr12*), and *cinnamyl alcohol dehydrogenase* (*CAD*)/*Brown midrib 6* (*Bmr6*) (**Table 3.8**). All these genes showed upregulated expression under the −Si condition (**Table 3.8**). Genes associated with the GO term flavonoid metabolic process (GO: 0009812) were also upregulated (**Table 3.9**), as shown in flavonoid biosynthesis genes, including *chalcone synthase* (*CHS*), *chalcone isomerase* (*CHI*), *flavanone 3-hydroxylase* (*F3H*), *dihydroflavonol 4-reductase* (*DFR*), *flavonol synthase* (*FLS*), *anthocyanidin 3*-O-*glucosyltransferase* (*UAGT*), *leucoanthocyanidin reductase* (*LAR*), and *apigenin 3'-hydroxylase/chrysoeriol 5'-hydroxylase* (*A3'H/C5'H*) (Nelson, 2009)(Lam, Lui, et al., 2019).

Table 3.8. Change in expression of phenylpropanoid biosynthetic process related genes (GO: 0009699) in hydroponically grown sorghum seedlings in response to silicon (Si) limitation at 3 weeks after treatment. The $\log_2$ values of the fold change (−Si/+Si) are shown (n = 3).

Gene ID	Functional annotation[a]	*p* value	*q* value	$\log_2$ (fold change)
Sb10g005780	Hydroxycinnamoyl-CoA shikimate/quinate hydroxycinnamoyltransferase (HCT)	8E–09	0E+00	3.4
Sb10g007920	Cytokinin-*O*-glucosyltransferase 3	4E–15	0E+00	2.7
Sb09g022480	Cytochrome P450/CYP75B97/apigenin 3′-hydroxylase/chrysoeriol 5′-hydroxylase (A3′H/C5′H)	3E–09	0E+00	2.4
Sb06g026340	Unknown	2E–06	0E+00	2.3
Sb05g008770	Disease resistance-responsive (dirigent-like protein)	4E–05	0E+00	2.3
Sb05g008780	Disease resistance-responsive (dirigent-like protein)	4E–04	1E–02	2.1
Sb06g026330	Unknown	7E–09	0E+00	2.0

Sb08g004670	Disease resistance-responsive (dirigent-like protein)	8E–04	1E–02	2.0
Sb05g008800	Disease resistance-responsive (dirigent-like protein)	1E–03	1E–02	2.0
Sb01g014540	Gibberellin 20 oxidase 2	7E–10	0E+00	2.0
Sb04g004290	Dihydroflavonol 4-reductase (DFR)	6E–05	0E+00	1.9
Sb07g021680	Cinnamoyl-CoA reductase 1 (CCR1)	3E–09	0E+00	1.8
Sb01g003330	Chalcone isomerase (CHI)	2E–07	0E+00	1.8
Sb04g024710	Cytochrome P450	1E–04	0E+00	1.8
Sb03g029070	Anthocyanidin 3-*O*-glucosyltransferase (UAGT)	8E–05	0E+00	1.7
Sb10g005170	Hydroxylase	6E–09	0E+00	1.7
Sb01g014550	2-Oxoglutarate and Fe(II)-dependent oxygenase	1E–05	0E+00	1.6
Sb01g000280	COP1-interacting protein	4E–06	0E+00	1.6
Sb03g029060	UDP-glucosyl transferase 73B5, anthocyanidin 3-*O*-glucosyltransferase	3E–05	0E+00	1.6
Sb02g038860	UDP-glucosyl transferase 78D2, anthocyanidin 3-*O*-glucosyltransferase	6E–03	4E–02	1.5
Sb10g005700	Cinnamoyl-CoA reductase 1 (CCR1)	1E–03	1E–02	1.5
Sb09g005360	Cytokinin-*O*-glucosyltransferase 1	2E–05	0E+00	1.5
Sb08g002620	Chalcone isomerase (CHI)	8E–04	1E–02	1.5
Sb05g024890	UDP-glucosyl transferase 73C7, cytokinin-*O*-glucosyltransferase 3	3E–04	0E+00	1.5
Sb03g004150	Cytokinin-*O*-glucosyltransferase 3, don-glucosyltransferase 1	1E–09	0E+00	1.5
Sb07g003860	Caffeate/5-hydroxyferulate *O*-methyltransferase (COMT) (=5-hydroxyconiferaldehyde *O*-methyltransferase, CAldOMT)/Brown midrib 12 (Bmr12)	3E–10	0E+00	1.4
Sb03g026550	Aldehyde dehydrogenase	3E–06	0E+00	1.4
Sb05g020160	Chalcone synthase (CHS)	9E–03	5E–02	1.4

Sb01g003470	Cinnamoyl CoA reductase (CCR)	1E–06	0E+00	1.4
Sb10g024350	Flavanone 3-hydroxylase (F3H)	2E–04	0E+00	1.3
Sb01g017270	Ferulate-5-hydroxylase (F5H) (=coniferaldehyde 5-hydroxylase, CAld5H)	3E–06	0E+00	1.3
Sb01g030560	Flavonol synthase (FLS)	8E–03	5E–02	1.3
Sb03g029080	Anthocyanidin 3-*O*-beta-glucosyltransferase	1E–03	1E–02	1.2
Sb06g029520	Unknown	4E–03	3E–02	1.2
Sb01g016100	MATE efflux family protein	8E–03	5E–02	1.2
Sb04g005950	Cinnamyl alcohol dehydrogenase (CAD)/Brown midrib 6, (Bmr6)	1E–05	0E+00	1.2
Sb06g029540	Leucoanthocyanidin reductase (LAR)	2E–04	0E+00	1.2
Sb03g031400	HXXXD-type acyltransferase	3E–03	2E–02	1.2
Sb10g004540	Caffeoyl-CoA *O*-methyltransferase (CCoAOMT)	2E–05	0E+00	1.2
Sb02g012620	HXXXD-type acyltransferase	7E–05	0E+00	1.1
Sb07g005070	Flavonol reductase/cinnamoyl-CoA reductase	7E–09	0E+00	1.1
Sb02g007240	1-Aminocyclopropane-1-carboxylate oxidase 2	4E–04	0E+00	1.0
Sb10g005210	Unknown	4E–04	1E–02	1.0
Sb01g050490	Naringenin, 2-oxoglutarate 3-dioxygenase	5E–03	4E–02	0.9
Sb01g003480	Cinnamoyl CoA reductase (CCR)	1E–03	1E–02	0.7
Sb03g004160	Cytokinin-*O*-glucosyltransferase 3	6E–04	1E–02	0.7
Sb08g016400	Oxidoreductase, 2-oxoglutarate-Fe oxygenase	4E–04	1E–02	0.7
Sb10g006280	Cinnamyl alcohol dehydrogenase (CAD)	4E–03	3E–02	0.7
Sb10g004340	Flavanone 3-hydroxylase (F3H)	1E–03	1E–02	0.6
Sb07g006120	26S Proteasome non-ATPase regulatory subunit 8	3E–03	2E–02	0.5

[a]According to the MOROKOSHI sorghum database.

Table 3.9. Change in expression of flavonoid metabolic process related genes (GO: 0009812) in hydroponically grown sorghum seedlings in response to silicon (Si) limitation at 3 weeks after treatment. The log2 values of the fold change (-Si/+Si) are shown.

Gene ID	Functional annotation[a]	*p* value	*q* value	log_2 (fold change)
Sb10g005780	Hydroxycinnamoyl-CoA shikimate / quinate hydroxycinnamoyl transferase (HCT)	8E-09	0E+00	3.4
Sb10g007920	Cytokinin-*O*-glucosyltransferase 3	4E-15	0E+00	2.7
Sb09g022480	Cytochrome P450/ CYP75B97/ Apigenin 3′-hydroxylase/ chrysoeriol 3′-hydroxylase (A3′H/C5′H)	3E-09	0E+00	2.4
Sb06g026340	Unknown	2E-06	0E+00	2.3
Sb01g014540	Gibberellin 20 oxidase 2	7E-10	0E+00	2.0
Sb06g026330	Unknown	7E-09	0E+00	2.0
Sb04g004290	Dihydroflavonol 4-reductase (DFR)	6E-05	0E+00	1.9
Sb01g003330	Chalcone isomerase (CHI)	2E-07	0E+00	1.8
Sb04g024710	Cytochrome P450	1E-04	0E+00	1.8
Sb03g029070	Anthocyanidin 3-*O*-beta-glucosyltransferase	8E-05	0E+00	1.7
Sb10g005170	Hydroxylase	6E-09	0E+00	1.7
Sb01g014550	2-Oxoglutarate (2OG) and Fe(II)-dependent oxygenase	1E-05	0E+00	1.6
Sb01g000280	COP1-interacting protein	4E-06	0E+00	1.6
Sb03g029060	UDP-glucosyl transferase 73B5, anthocyanidin 3-*O*-glucosyltransferase	3E-05	0E+00	1.6
Sb05g024890	UDP-glucosyl transferase 73C7, cytokinin-*O*-glucosyltransferase 3	3E-04	0E+00	1.5
Sb02g038860	UDP-glucosyl transferase 78D2, anthocyanidin 3-*O*-glucosyltransferase	6E-03	4E-02	1.5
Sb09g005360	Cytokinin-*O*-glucosyltransferase 1	2E-05	0E+00	1.5
Sb08g002620	Chalcone isomerase (CHI)	8E-04	1E-02	1.5
Sb03g004150	Cytokinin-*O*-glucosyltransferase 3, don-glucosyltransferase 1	1E-09	0E+00	1.5
Sb05g020160	Chalcone synthase (CHS)	9E-03	5E-02	1.4

Sb10g024350	Flavanone 3-hydroxylase (F3H)	2E-04	0E+00	1.3
Sb01g030560	Flavonol synthase (FLS)	8E-03	5E-02	1.3
Sb03g029080	Anthocyanidin 3-*O*-glucosyltransferase (UAGT)	1E-03	1E-02	1.2
Sb06g029520	Unknown	4E-03	3E-02	1.2
Sb01g016100	MATE efflux family protein	8E-03	5E-02	1.2
Sb03g031400	HXXXD-type acyl-transferase	3E-03	2E-02	1.2
Sb06g029540	Leucoanthocyanidin reductase (LAR)	2E-04	0E+00	1.2
Sb02g012620	HXXXD-type acyl-transferase	7E-05	0E+00	1.1
Sb10g005210	Unknown	4E-04	1E-02	1.0
Sb02g007240	1-Aminocyclopropane-1-carboxylate oxidase 2	4E-04	0E+00	1.0
Sb01g050490	Naringenin, 2-oxoglutarate 3-dioxygenase	5E-03	4E-02	0.9
Sb03g004160	Cytokinin-*O*-glucosyltransferase 3	6E-04	1E-02	0.7
Sb08g016400	Oxidoreductase, 2OG-Fe oxygenase	4E-04	1E-02	0.7
Sb10g004340	Flavanone 3-hydroxylase (F3H)	1E-03	1E-02	0.6
Sb07g006120	26S Proteasome non-ATPase regulatory subunit 8	3E-03	2E-02	0.5

[a]According to the MOROKOSHI sorghum database.

I also examined the expression of other known lignin-related genes that were not assigned to these GO terms. p-*Coumaroyl-CoA:monolignol transferase* (*PMT*) (Petrik et al., 2014; Withers et al., 2012), *coumarate 3-hydroxylase* (*C3H*) (Barros et al., 2019), *phenylalanine/tyrosine ammonia-lyase* (*PTAL*) (Barros et al., 2016; Jun et al., 2018; Y. Li et al., 2019), and *flavone synthase II* (*FNSII*) (Du et al., 2010; Lam et al., 2017) were upregulated (**Table 3.10**). The expression of *SbMYB60* (Agarwal et al., 2016; Miyamoto et al., 2020; Scully, Gries, Sarath, et al., 2016) and *SbMYB22* (Agarwal et al., 2016), the transcriptional activators of the genes involved in lignin biosynthesis, were upregulated in −Si seedlings (**Table 3.11**). On the other hand, the expression of *SbMYB42* (Agarwal et al., 2016), the transcriptional repressor of phenylpropanoid biosynthesis, was downregulated in −Si seedlings (**Table 3.11**).

Table 3.10. Change in expression of known lignin-related genes in hydroponically grown sorghum seedlings in response to silicon (Si) limitation at 3 weeks after treatment. The log2 values of the fold change (-Si/+Si) are shown.

Gene ID	Functional annotation[a]	*p* value	*q* value	log_2 (fold change)
Sb09g002910	*p*-Coumaroyl-CoA:monolignol transferase (PMT)	3E-04	0E+00	1.6
Sb01g038760	Coumarate 3-hydroxylase (C3H)	1E-04	0E+00	1.1
Sb04g026510	Phenylalanine/tyrosine amonia-lyase (PTAL)	2E-03	2E-02	1.1
Sb02g000220	Flavone synthase II (FNSII)/flavanone 2-hydroxylase (F2H, for soluble flavonoids)/CYP93G3	3E-03	2E-02	1.5
Sb06g000260	Flavone synthase II (FNSII, for tricin bound lignin)	not found in DEG list		

[a]According to the MOROKOSHI sorghum database.

Table 3.11. Change in expression of some MYB transcription factors in hydroponically grown sorghum seedlings in response to silicon (Si) limitation at 3 weeks after treatment. The log2 values of the fold change (-Si/+Si) are shown.

Gene ID	Functional annotation[a]	*p* value	*q* value	log_2 (fold change)
Sb04g031110	SbMYB60	5E-07	0E+00	2.6
Sb02g030900	SbMYB22	6E-03	4E-02	0.9
Sb07g024890	SbMYB42	3E-03	2E-02	-1.0

[a]According to the MOROKOSHI sorghum database.

3.3.6 Reverse transcription-quantitative PCR analysis

To further examine the effect of Si limitation on lignin-related gene expression, I analyzed the gene expression in +Si and −Si seedlings using reverse transcription-quantitative PCR (RT-qPCR). The upregulated expression of monolignol biosynthetic genes was also observed in this analysis, as shown by *HCT, CCoAOMT, CCR, F5H* (*CAld5H*), *COMT* (*CAldOMT*)*/Bmr12*, and *CAD/Bmr6* (**Figure 3.7**). I also examined the expression of several other genes involved in lignin biosynthesis. The expression of *phenylalanine ammonia-lyase* (*PAL*) (Agarwal et al., 2016; Jun et al., 2018) was also upregulated under −Si conditions (**Figure 3.7**). Meanwhile, the expression of *4-coumarate CoA ligase* (*4CL*)/*Brown midrib 2* (*Bmr2*) (Saballos et al., 2008, 2012) and p-*coumaroyl ester 3-hydroxylase* (*C3'H*) (Fornalé et al., 2015; Saballos et al., 2012; Takeda et al., 2018) were not significantly modulated under −Si conditions (**Figure 3.7**).

The expression of the genes potentially related to the synthesis or metabolism of cell wall polysaccharides (Rai et al., 2016) was also examined. Two genes related to callose metabolism, including *glucan synthase-like* (*GSL*) and *glucan 1,3-β-glucosidase*, were upregulated under −Si conditions (**Figure 3.8**). On the other hand, genes involved in the other cell wall polysaccharide components did not show significant modulation under −Si conditions, as shown by the expression of *cellulose synthase A* (*CESA*), *cellulose synthase-like* (*CSL*), *endo-1,4-β-glucanase*, *expansin* (*EXP*), *xyloglucan endotransglucosylase/hydrolase* (*XTH*), *homogalacturonan α-1,4-galacturonosyltransferase* (*GAUT*), *pectate lyase*, and *rhamnogalacturonan I* (*RG-I*) *lyase* (**Figure 3.8**).

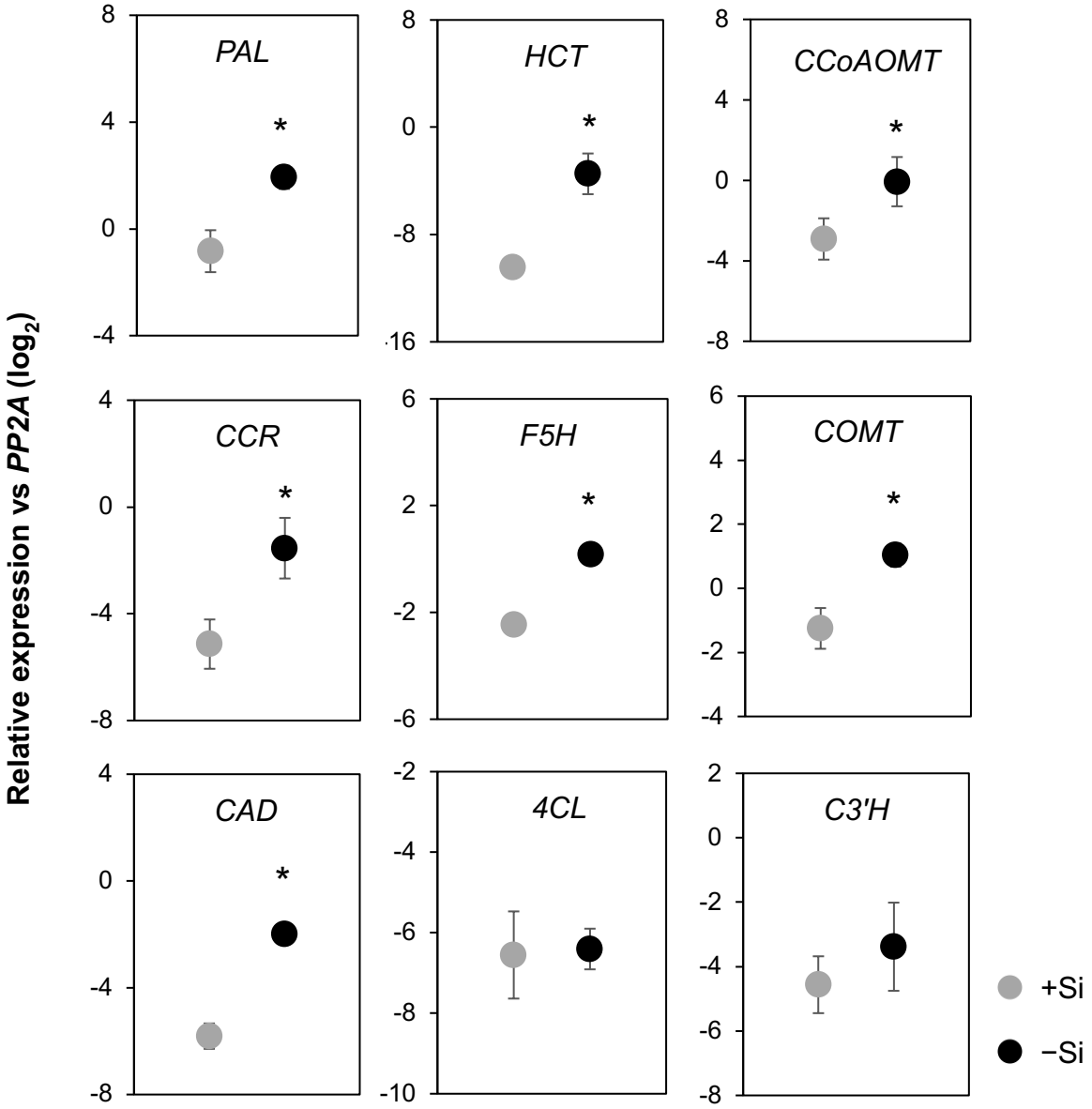

Figure 3.7. Reverse transcription-quantitative PCR analysis of the expression of lignin biosynthesis-related genes in hydroponically grown sorghum seedlings cultivated under +Si or −Si conditions at 3 weeks after treatment. *PAL*: *phenylalanine ammonia-lyase*, *HCT*: *hydroxycinnamoyl-CoA shikimate/quinate hydroxycinnamoyltransferase*, *CCoAOMT*: *caffeoyl-CoA* O-*methyltransferase*, *CCR*: *cinnamoyl CoA reductase*, *F5H*: *ferulate 5-hydroxylase* (=*coniferaldehyde 5-hydroxylase*, *CAld5H*), *COMT*: *caffeate/5-hydroxyferulate* O-*methyltransferase* (=*5-hydroxyconiferaldehyde* O-*methyltransferase*, *CAldOMT*)/*Brown midrib 12* (*Bmr12*), *CAD*: *cinnamyl alcohol dehydrogenase/Brown midrib 6* (*Bmr6*), *4CL*: *4-coumarate CoA ligase/Brown midrib 2* (*Bmr2*), and *C3'H*: *p-coumaroyl ester 3-hydroxylase*. The expression of each gene was analyzed as transcript abundance relative to *PP2A* (XM_002453490). Values are given as mean ± SD (n = 3). Asterisks indicate significant differences between +Si and −Si plants (Student's *t* test, $p < 0.05$).

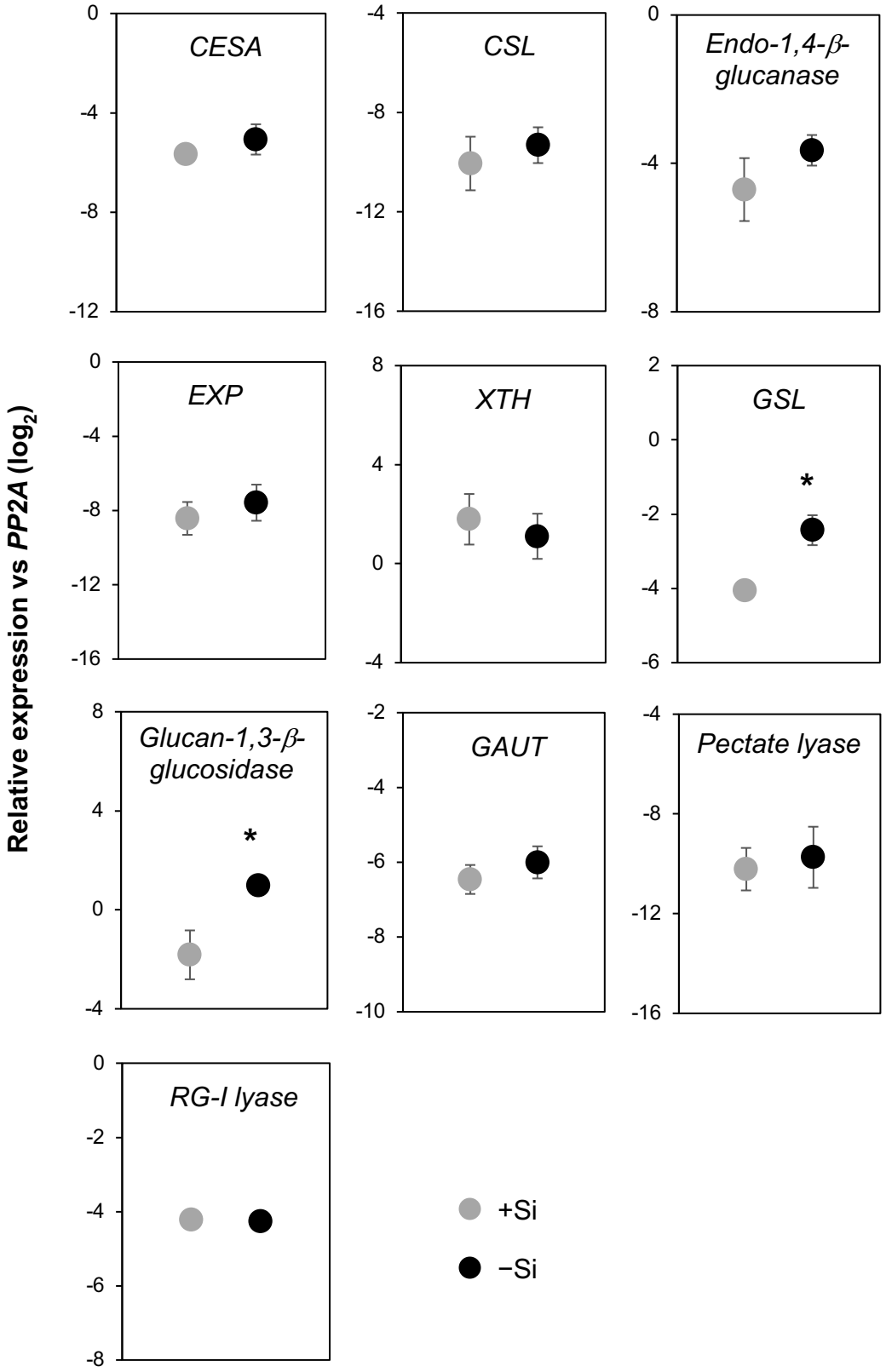

Figure 3.8. Reverse transcription-quantitative PCR analysis of the expression of the selected cell wall polysaccharide metabolism-related genes in hydroponically grown sorghum seedlings cultivated under +Si or −Si conditions at 3 weeks after treatment. *CESA*: *cellulose synthase A*, *CSL*: *cellulose synthase-like*, *EXP*: *expansin, XTH*: *xyloglucan endotransglucosylase/hydrolase*, *GSL*: *glucan synthase-like/callose synthase*, *GAUT: homogalacturonan α-1,4-galacturonosyltransferase,* and *RG-I*: *rhamnogalacturonan I*. The expression of each gene was analyzed as transcript abundance relative to *PP2A* (XM_002453490). Values are given as mean ± SD (n = 3). Asterisks indicate significant differences between +Si and −Si plants (Student's *t* test, $p < 0.05$).

3.3.7 Mechanical property analyses

The effect of Si limitation on the mechanical properties of sorghum seedlings was investigated. The modulus of elasticity (MOE) of −Si plants was significantly higher than that of +Si plants (**Figure 3.9A**), indicating that the shoots of −Si plants had stiffer tissues than +Si plants. The orientation of cellulose microfibrils in the cell wall is another factor affecting the mechanical properties of the tissue. The MFA, which denotes the angle of crystalline cellulose fibers to the longitudinal growth axis, has been found to be negatively correlated with mechanical strength in wood tissues (H. Yamamoto & Kojima, 2002). In the present study, the MFA of −Si plants measured by X-ray diffractometer was significantly lower than that of +Si plants (**Figure 3.9B**).

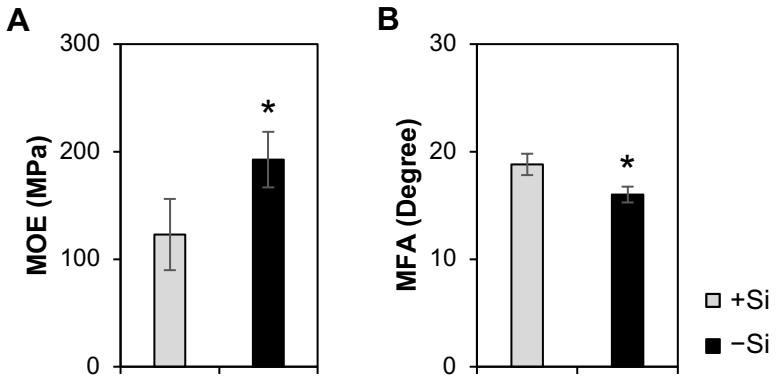

Figure 3.9. Mechanical properties of hydroponically grown sorghum seedlings cultivated under +Si or −Si conditions at 3 weeks after treatment. (**A**) Modulus of elasticity (MOE) and (**B**) microfiber angle (MFA). Values are given as mean ± SD (n = 4). Asterisks indicate significant differences between +Si and −Si plants (Student's *t* test, $p < 0.05$).

3.3.8 Estimated higher heating values

The calorific values of the cell walls from +Si and −Si seedlings were estimated as the higher heating value (HHV) calculated based on their elemental composition (Yin, 2011). The calculated HHV of the −Si cell wall was significantly higher than that of the +Si cell wall (**Table 3.12**).

Table 3.12. Effect of silicon limitation on the calorific value of hydroponically grown sorghum seedlings at 3 weeks after treatment.

	Silicon supply	
	+Si	−Si
C (% dry weight)	41.32 ± 0.47	43.67 ± 0.45 *
H (% dry weight)	5.75 ± 0.07	6.23 ± 0.15 *
Higher heating value (kJ g^{-1})	16.9 ± 0.19	18.0 ± 0.22 *

Values are means ± SD (n = 3). Asterisks indicate significant differences between +Si and −Si plants (Student's *t* test, $p < 0.05$).

3.4 Discussion

In this chapter, I investigated the Si supply dependent alteration of the cell wall properties of sorghum seedlings, as an initial step to understand the possible effect of the altered tissue content of Si on the sorghum lignocellulose. Silicon supply reportedly affects the growth of grasses, including rice (Ma et al., 1989), wheat (Neu et al., 2017), and tef (Ligaba-Osena et al., 2020). In this current study, under controlled conditions, Si supply did not cause any significant difference in the growth of sorghum seedlings (**Figure 3.1**). However, the properties of the cell wall were affected by the Si supply, as shown by the series of cell wall structural, mechanical, and heating value analyses.

Chemical analysis of the cell walls revealed that Si limitation led to an increase in the lignin content in the aboveground parts of the seedlings (**Figure 3.2A**). This change was associated with an increase in thioacidolysis-derived S and G phenylpropanoid monomer yields in the −Si cell walls. The increase was higher in the S-type than in the G-type monomers, leading to an increased S/G monomer ratio in the −Si cell wall. The content of *p*CA, which preferentially acylates the S-type monomer units in grasses (Karlen et al., 2018; Ralph, 2010), also increased in the −Si cell wall (**Figure 3.2**). These results were consistent with the lignocellulose compositional data obtained by 2D HSQC NMR analysis (**Figure 3.4**). Thus, the current data collectively indicate that Si limitation leads to an increase in the amount of lignin with increased relative abundances of S and *p*CA units in the cell walls of sorghum seedlings. At least some of these modifications were induced by transcriptional changes, as suggested by the upregulation of phenylpropanoid biosynthesis-related genes under −Si conditions (**Table 3.2**), including *PAL, PTAL*, and monolignol biosynthetic genes, such as *HCT*, *CCoAOMT*, *CCR*, *F5H* (*CAld5H*), *COMT* (*CAldOMT*)/*Bmr12*, *CAD*/*Bmr6*, and *C3H*

(**Table 3.8**, **Figure 3.7**, **Table 3.10**). In addition, the altered expression of several transcription factors was consistent with the increase in lignin content and S/G monomer ratio in the −Si cell walls. In this study, the expression of the MYB transcription factors *SbMYB60* and *SbMYB22* was upregulated in −Si seedlings, whereas the expression of *SbMYB42* was downregulated in −Si seedlings (**Table 3.11**). The overexpression of *SbMYB60* in sorghum has been shown to enhance the accumulation of lignin, particularly of the S unit, and the expression of several monolignol biosynthetic genes (Scully, Gries, Sarath, et al., 2016). The binding of MYB42 to the genes involved in monolignol biosynthesis has been shown in rice, maize, and sorghum (Agarwal et al., 2016), and the overexpression of *MYB42* suppressed lignin accumulation in sugarcane (Poovaiah et al., 2016). The observed modulated expression of these transcriptional factors further supports the notion that the increased accumulation of lignin in −Si seedlings was induced, at least partly, by transcriptional changes. In addition, the formation of *p*-coumaroylated lignin may also have been promoted, as suggested by the upregulated expression of *PMT*, a gene for the enzyme acylating monolignols with *p*-coumarate in grasses (**Table 3.10**) (Petrik et al., 2014; Withers et al., 2012). Regarding the accumulation of tricin, another grass-specific lignin monomer (Del Río et al., 2020; Lam et al., 2021; Lan et al., 2015), the effect of Si supply was not clear in this study. NMR analysis showed that the intensity of the tricin signal was lower in the −Si cell wall than in the +Si cell wall (**Figure 3.4**), whereas the histochemical analysis using vanillin-HCl staining detected no discernible difference between treatments (**Figure 3.5**). These data suggest that the amount of tricin lignin was either decreased or unchanged in the −Si cell walls. On the other hand, the expression of *A3'H/C5'H* and *COMT* (*CAldOMT*)/*Bmr12*, the genes encoding the enzymes required for tricin biosynthesis (Lam, Lui, et al., 2019; Lam, Tobimatsu, et al., 2019; Nelson, 2009), was upregulated in −Si seedlings (**Table 3.8-9**). Nevertheless, *FNSII* (Sb06g000260), which has been shown to function in the synthesis of both soluble flavone and tricin lignin units (Lam et al., 2017), was not found in the list of DEGs (**Table 3.10**). Collectively, the expression of genes involved in tricin-lignin biosynthesis was either upregulated or unchanged. Further investigation is necessary to clarify the effect of Si limitation on tricin-lignin synthesis.

Using hydroponically grown sorghum seedlings, the effect of Si supply in the cell wall polysaccharide fraction was not as notable as that in lignin in this study. Cell wall chemical analysis showed that the amounts of neutral sugars released by TFA hydrolysis and uronic acids, which together are considered to constitute cell wall matrix polysaccharides, tended to be higher in −Si plants than in +Si plants (**Figure 3.3B-G**). However, the relative amounts of these monosaccharides remained unchanged between the +Si and −Si cell walls (**Figure 3.3I**).

Hence, the composition of matrix polysaccharides was likely unchanged by the −Si treatment. Moreover, histochemical analysis suggested that the amount of MLG and arabinoxylan, the two major hemicelluloses in younger tissues of grasses, remained unaffected by Si treatment (**Figure 3.6B**). Based on these observations, it is possible that the amount of matrix polysaccharides was not affected significantly by Si supply; however, Si limitation may make the cell walls more susceptible to acid hydrolysis, by changing their structural organization, thereby releasing more monosaccharides than +Si cell walls. The 2D HSQC NMR also suggested that neutral sugars did not increase in the −Si plant cell walls (**Figure 3.4**). In addition, the content of cell wall-bound FA, which is mainly associated with arabinoxylan, was not significantly altered by −Si treatment (**Figure 3.2H**, **Figure 3.4**). In line with these observations, the expression of genes related to hemicellulose and pectin biosynthesis and metabolism, including *EXP*, *XTH*, *GAUT*, *pectate lyase*, and *rhamnogalacturonan I lyase*, was not significantly different between −Si and +Si seedlings (**Figure 3.8**). As for cellulose, calcofluor white staining of −Si seedlings yielded a slightly weaker signal than that from +Si seedlings (**Figure 3.6A**). However, the expression of *CESA* and *endo-1,4-β-glucanase* as cellulose-related genes and the content of glucose derived from crystalline cellulose were not significantly affected by −Si treatment (**Figure 3.3** and **Figure 3.8**). The reduced calcofluor fluorescence from −Si cell walls may be due to the decreased accessibility of calcofluor white to cellulose caused by enhanced lignification.

Callose was found to be increased in −Si plants, as revealed by histochemical analyses (**Figure 3.6C**). The RT-qPCR analysis showed that genes involved in both biosynthesis (*GSL*) and degradation (*glucan 1,3-β-glucosidase*) of callose were upregulated under −Si conditions (**Figure 3.8**), suggesting an enhanced turnover of this polysaccharide. However, the increment of callose may be quantitatively small, as the relative amount of glucose in TFA-released sugars remained unchanged by −Si limitation (**Figure 3.3I**). These results suggest that Si limitation does not significantly affect the polysaccharide moiety of lignocellulose in sorghum seedlings.

Based on the above considerations, in this chapter, I conclude that the nutritional status of Si significantly affected the amount and structure of lignin, but not polysaccharides, in hydroponically cultured sorghum seedlings. This assumption is consistent with the change in lignin/polysaccharide signal ratio in the 2D NMR analysis (**Figure 3.4D**), which was increased under the −Si condition. In contrast, from the Chapter 2, I have demonstrated that N supply significantly affects the polysaccharide content and composition, but not the content of lignin in the cell walls of hydroponically grown sorghum seedlings. Although both the N and Si nutritional status significantly affected the S/G lignin unit ratio, the direction of modification

was the opposite. The S/G lignin unit ratio was decreased by limiting the N supply (Chapter 2), whereas it was increased by limiting the Si supply. The different effects may reflect the difference in the synthesis of monolignols, as the expression of *F5H* (*CAld5H*), a gene involved in the biosynthesis of S lignin units in sorghum (Tetreault et al., 2020), was downregulated by limiting N supply (Chapter 2), whereas it was upregulated by limiting the Si supply in this chapter. A similar inverse relationship between lignin and Si has been reported for the shoots of hydroponically grown rice (Suzuki et al., 2012) and soil-grown brachypodium (Głazowska et al., 2018), in which mutant plants defective in Si uptake accumulated more lignin than wild-type plants. The brachypodium mutant also exhibited an altered S/G monomer ratio; however, contrary to the results from this chapter, the ratio was lower than that of the wild type (Głazowska et al., 2018). Meanwhile, several previous studies have also reported changes in polysaccharide fractions. In hydroponically grown mature rice (J. Zhang et al., 2015) and soil-grown mature brachypodium (Głazowska et al., 2018), the hemicellulose content was decreased by Si limitation. The cellulose content was increased by Si limitation in hydroponically grown oat (Hossain et al., 2007), rice (T. Yamamoto et al., 2012), and soil-grown brachypodium (Głazowska et al., 2018). In the present experimental conditions, the effects of Si limitation may be relatively limited compared with those in previous studies with other grasses, resulting in a limited effect on cell wall polysaccharides. This may also be due to differences in species, organ examined, and/or developmental stage. Indeed, the changes in hemicellulose or cellulose in rice, oat, and brachypodium have been found to be highly dependent on these factors (Głazowska et al., 2018; Hossain et al., 2007; T. Yamamoto et al., 2012).

As both Si as silica and lignin contribute to plant mechanical strength, I viewed the increased accumulation of lignin in −Si plants as an adaptive response to compensate for the loss of silica as a mechanical support (**Figure 3.10**). Consistent with this assumption, −Si plants were not mechanically weaker but rather stiffer than +Si plants (**Figure 3.9A**). A similar tendency was previously reported in rice, in which the mechanical strength of rice leaves was increased in the absence of Si (T. Yamamoto et al., 2012). Notably, the enhanced deposition of lignin in sorghum seedlings was not particularly remarkable in the epidermis, where Si was accumulated in +Si plants, but it occurred mainly in the same tissues as in +Si plants, that is, sclerenchyma and vascular bundles. Hence, the enhanced mechanical strength might be due to the enhanced deposition of lignin in its original place, but not to an ectopic accumulation. I also observed a smaller MFA in −Si plants than in +Si plants (**Figure 3.9B**). MFA represents the orientation of crystalline cellulose, wherein a smaller MFA is generally related to stiffer

tissues (H. Yamamoto & Kojima, 2002). Therefore, in addition to the increased lignin deposition, the changed orientation of cellulose fibers may also have contributed to the increased mechanical tissue strength of −Si seedlings. Currently, I have not determined the contribution of each factor to the increased mechanical strength, and this will require further investigation. In wood species, higher amounts of lignin have been found to be associated with higher MFA (Timell, 1982). The results of this study contradict these findings. The reason for this difference is unclear at present. The enhanced lignin accumulation between cellulose microfibrils may have led to an altered fiber orientation.

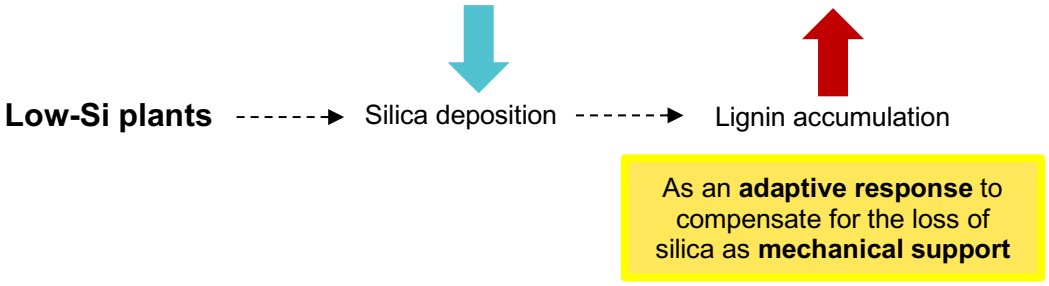

Figure 3.10. Schematic flow of the effect of –Si treatment on the increased of lignin accumulation in hydroponically sorghum seedlings.

The calorific value is the main feature of biomass that determines its performance in solid fuel applications, and it is positively correlated with lignin content (Demirbaş, 2001; Koshiba et al., 2017; Scully, Gries, Funnell-Harris, et al., 2016; Takeda et al., 2019; Umezawa, 2018). In this chapter, the estimated HHV of the cell walls of the –Si seedlings was higher than that of the +Si seedlings (**Table 3.12**). The cultivar, age, and growth conditions differed between this study and practical sorghum cultivation. Nonetheless, I believe that the findings of this study can provide information on the physiological responses of sorghum plants to Si limitation. The current results suggest that lowering the Si content in plants could promote an increased HHV in sorghum lignocellulose. A lower Si content could also lead to a reduction in the amount of ash produced upon combustion, which provides advantages in furnace maintenance (Lacey et al., 2018). Hence, limiting the Si content in the plant body can be a viable way to enhance the usability of sorghum as a biomass energy feedstock. In practice, limiting the supply of Si to crops is difficult because the soil is rich in Si and the natural supply is usually sufficient for most plant species to accumulate silica in their bodies. Engineering mutant lines with defective Si uptake may circumvent this problem. A Si uptake transporter has already been identified in sorghum (Markovich et al., 2019), and it can be a logical target for obtaining Si-depleted mutant lines for bioenergy applications.

Chapter 4

The beneficial effect of silicon to reduce nitrate content in *Sorghum bicolor*

4.1 Introduction

Sorghum biomass is also important as fodder. The fodder quality of sorghum is comparable with corn forage (Getachew et al., 2016). Feed value of sorghum can be affected by various environmental factors, including growth conditions such as nutrients and water availability (Somegowda et al., 2021).

Nitrogen (N) is required in the highest amount among the plant nutrients taken up from the soil and the N supply frequently becomes a growth limiting factor. Hence, exogenous supply of N fertilizer is common and important in crop production. Application of N fertilizer improves both yield and quality of sorghum as a fodder crop (Sher et al., 2017). However, overdose N application should be avoided, as an environmental eutrophication can be caused by the nitrate ions flowing into the water system. In addition, the nitrate accumulation in plants can be a serious problem in fodder crops (Sidhu et al., 2011). Fodder containing high amount of nitrate can cause anemia in ruminant animals (Radostits et al., 2000). Nitrate may also impair thyroid function and vitamin A- and E metabolism as the chronic effects (Bruning-Fann & Kaneene, 1993).

Grasses including sorghum are known to accumulate relatively high Si as silica in their cell walls and intercellular space of leaf epidermal tissues (Ma & Yamaji, 2006). Although the presence of Si in grasses has been considered as the defense system against attack by herbivores (Vicari & Bazely, 1993), application of Si in a cultivation of grass species did not cause significant changes in feeding preference of sheep as previously reported by (Massey et al., 2009). In addition, Si has been recognized as an essential element for normal growth and development of livestock, particularly it is involved in animal bone formation (Carlisle, 1972). Another beneficial effect of Si is to promote tolerance against unfavorable conditions, including nutritional deficiencies (Ali et al., 2020; Majumdar & Prakash, 2020). In fact, Si has been reported to mitigate nutritional stresses such as potassium (Chen et al., 2016) and iron deficiency (Teixeira et al., 2020). Wu et al. (2017) reported that Si application increased N use efficiency of rice. Gou et al. (2020) reported that Si application reduced nitrate accumulation in cucumber. Hence, Si application may exert beneficial effects in the production of sorghum as fodder, through improving plant N use efficiency and reducing leaf nitrate content. However,

information about the interaction between Si and N is still limited in sorghum. Therefore, in this chapter, I investigated the effect of Si application on nitrate accumulation in hydroponically grown sorghum plants, then considered possible mechanisms of the Si-N interaction.

4.2 Materials and Methods

4.2.1 Plant growth condition and treatment

4.2.1.1 Seedling stage

The one-week-old seedlings of sorghum (*Sorghum bicolor*, cv. BTx623) were cultivated hydroponically in the full-strength Yoshida B culture solution and incubated in the culture room maintained at 25°C with a 16/8 h light/dark cycle for two weeks as previously described in Chapter 1. The 3-week-old seedlings were transferred to the either sufficient- or low-N treatment solution. The medium for the sufficient-N treatment was Yoshida B culture solution containing 0.25 mM $(NH_4)_2$ HPO_4 and 1 mM Ca $(NO_3)_2$. The medium for the low-N treatment contained N at a concentration 1/10th that of sufficient-N treatment (0.05 mM NH_4^+ and 0.2 NO_3^-). The concentrations of calcium and potassium were maintained at the same level as that of the control using $CaCl_2$ and KH_2PO_4, respectively. Silicon was also added either 0 or 50 mg SiO_2 L^{-1} as −Si or +Si treatment, respectively, to the both N treatment culture medium. The SiO_2 solution was prepared as previously described in Chapter 3. The aerial parts of the 6-week-old (three weeks after Si treatments) seedlings were used for the analyses throughout this set of study.

4.2.1.2 Mature stage

The one-week-old seedlings of sorghum were cultured hydroponically in the full-strength Yoshida B medium and incubated in the greenhouse for four weeks. The 5-week-old seedlings were transferred to the Yoshida B culture medium containing 1 mM $(NH_4)_2$ HPO_4 and 4 mM Ca $(NO_3)_2$ as high-N treatment solutions. Silicon was also added either 0, 25, 50, 75 or 100 mg SiO_2 L^{-1} as Si0, Si25, Si50, Si75, or Si100 treatment, respectively. The aerial parts of the 13-week-old (eight weeks after Si treatments) sorghum plants at early heading stage were used for the analyses throughout this set of study.

4.2.2 Silicon content analysis

The silicon content analysis was conducted as previously described in Chapter 3.

4.2.3 Chlorophyll, total nitrogen, and nitrate content analyses

Chlorophyll, total nitrogen, and nitrate content of seedling or mature plant were analyzed as previously described in Chapter 1. Assimilated N content was calculated as the difference between total N and nitrate contents.

4.2.4 Phosphorous, potassium, calcium, and magnesium content analyses

The dried powder of aerial parts of sorghum plant at heading stage was digested with nitric and sulfuric acids for phosphorus content determination by colorimetric molybdenum blue method at 880 nm (UV-1280, Shimadzu, Kyoto, Japan). The digested sample solution was also used for potassium (K), calcium (Ca), and magnesium (Mg) contents determination by atomic absorption spectrophotometer (AA-6200, Shimadzu).

4.2.5 Gene expression analyses

RNA-sequencing data of cellular nitrogen compound metabolic process related genes (GO: 0034641) of sorghum seedlings under Si treatment condition was derived from the results in Chapter 3 (accession number DRR324378-DRR324383). For RT-qPCR analysis, total RNA was extracted from fully expanded uppermost leaves of 6-week-old (3 weeks after treatment) seedlings. Total RNA extraction, first-strand complementary DNA synthesis, and quantitative PCR analysis were conducted as previously described in Chapter 1. The functional annotation listed in **Table 4.2** and **Table 4.3** referred from the MOROKOSHI sorghum database (Makita et al., 2015). The gene encoding PP2A was used as the internal control (Reddy et al., 2016). The primers used for PCR are listed in **Table 4.1**.

Table 4.1. List of primers used for reverse transcription-quantitative PCR analysis.

Gene name	Gene ID	Forward primer (5′→3′)	Reverse primer (5′→3′)
NRT1.1	Sb01g050410	GCTAGCTAGGTGTGTCCTCG	GACTGGTGAGTGACTGCGG
NRT1.5	Sb02g007605	CTACTCGCAGATGACGTCGG	GGGATGGTGAGCTTCCACAG
NRT2.2	Sb06g020180	GTGACACGTCGAGTAGCGAG	GATTACTTGTCCCTGCGGCG
NRT2.5	Sb03g032310	CGGCGGAGGACTACTACAAC	GTGTGTGTTTCACACGTCGG
AMT1.1	Sb04g026290	CGACGAGGACATGAGCTTGA	TGGCACTATGCCCCACTAGA
AMT2	Sb03g038840	GCCCAAATTCGCCATCTCAG	GTGAACAACGGTGCGCTAAG
NR	Sb04g034470	CGGGATTCCTCAAGGACCAC	CGACGCGGTACAAATCAAGG
NiR	Sb04g034160	CTGTTCATGGAGGACGGCAT	CGCCCGTACTGGTGCTTG
GS2	Sb06g031460	ACATTGTGACGGGGCTACTG	GTGGGCCTGTTTATTCGTGC
Fd-GOGAT	Sb02g041740	CTGGAATGACTGGTGGCCTT	TCCCTCAAAATCGTGGCTCC
NADH-GOGAT	Sb03g031310	TGCTATGGCCGACTGCTATG	GCTGGGAAAGGTGTTTGTGG
CLCa	Sb10g026090	GTCGTCGGGAATGGATCTCG	GTTGTTGAAGTAGCGCAGCC
PS1G	Sb02g027900	CCTCCAGCAACGGATACGAC	CACGCGCAGTTACACTACTTG
Chlorophyllase2	Sb02g012300	GATCCCCATCCTGATCGCTG	GCTCGTAGTAGCGGTTCTGG
RCCR	Sb01g029900	GTGTCCGATAGGGTAGTGGC	GAGATTGTGGCTCGCTGGG
NYC1-like	XM_021450624	TCTGCTCGAGATCAGCTCAAA	TGCAAACTCCACAAGTGCCT
PP2A	XM_002453490	AACCCGCAAAACCCCAGACTA	TACAGGTCGGGCTCATGGAAC

NRT: *nitrate transporter*, *AMT*: *ammonium transporter*, *NR*: *nitrate reductase*, *NiR*: *nitrite reductase*, *GS*: *glutamine synthase*, *Fd-* and *NADH-GOGAT*: *ferredoxin-* and *NADH-dependent glutamate synthases*, *CLCa*: *chloride channel A*, *PS1G*: *photosystem 1 subunit* G, *RCCR*: *red chlorophyll catabolite reductase*, *NYC1-like*: *non yellow coloring1-like*, and *PP2A*: *serine/threonine-protein phosphatase.*

4.2.6 Crude protein content and *in vitro* digestibility

Crude protein content of the aerial part of the plants was estimated as 6.25 × assimilated N content (Jones 1941). The *in vitro* digestibility of cell wall residue (CWR) of sorghum seedling was determined by enzymatic saccharification analysis as previously described in Chapter 2. Percentage of released glucose to the total glucan (crystalline+amorphous) was expressed as enzymatic saccharification efficiency. Total glucan content was estimated as described previously (Lam et al., 2017).

4.3 Results

4.3.1 Plant growth and N status of sorghum seedling under Si application

Application of Si significantly increased the shoot Si content in sorghum seedlings both under sufficient and low-N conditions in this study (**Figure 4.1B**). Within +Si treatment, shoot Si content was remarkably higher under low-N than sufficient-N condition (**Figure 4.1B**). Application of Si did not significantly affect the growth and biomass accumulation of sorghum seedling in sufficient-N condition as reported in my previous study in Chapter 3. Silicon application also did not affect plant growth under low-N condition (**Figure 4.1A**, **C**).

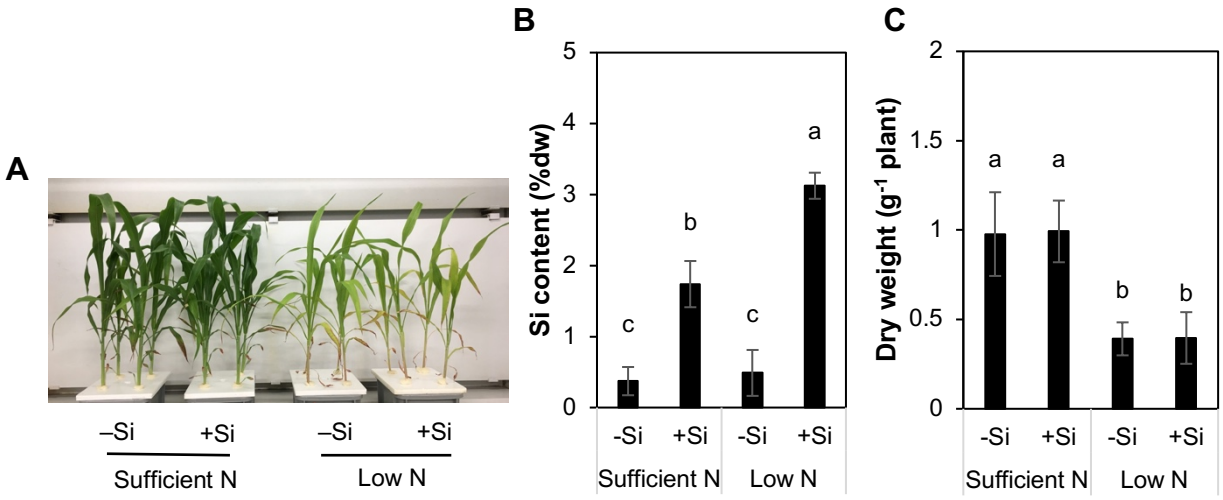

Figure 4.1. Effect of silicon (Si) application on growth of hydroponically grown sorghum seedlings in sufficient or low N supply. **(A)** Plant appearance, **(B)** Si content, and **(C)** dry weight of sorghum seedlings grown under -Si and +Si condition at 3 weeks after treatment. Bars are means ± SD (n = 6 for B; n = 8 for C). Different letters mean a significant difference (Tukey-Kramer test, $p < 0.05$).

Nitrogen supply significantly affected SPAD values, total N, assimilated N, and nitrate contents of sorghum seedling (**Figure 4.2**). The application of Si did not significantly affect the SPAD values, total N, and assimilated N contents of sorghum seedling both under sufficient and low-N supply (**Figure 4.2A-C**). Silicon application reduced nitrate content in sorghum seedling when they received the sufficient N supply (**Figure 4.2D**).

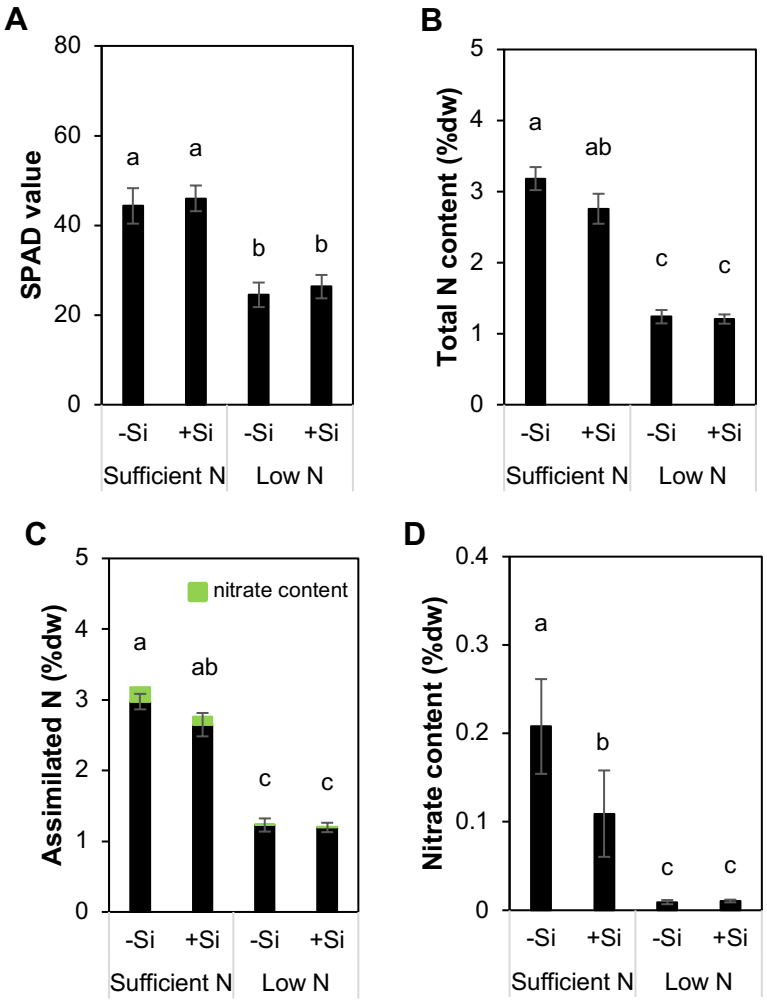

Figure 4.2. Effect of silicon (Si) application on nitrogen (N) status in sufficient or low N supply. **(A)** Soil-plant analysis development (SPAD) value, **(B)** total N content, **(C)** assimilated N, and **(D)** nitrate content of hydroponically grown sorghum seedlings cultivated under -Si and +Si condition at 3 weeks after treatment. Bars are means ± SD (n = 6). Different letters mean a significant difference (Tukey-Kramer test, $p < 0.05$).

4.3.2 Evaluation of the effect of Si application on plant growth and N status of sorghum plant at mature stage

The findings in the seedling stage were examined in mature plants grown hydroponically with five levels of Si applications (0, 25, 50, 75, and 100 mg SiO_2 L^{-1}) under high-N supply. The shoot Si content in mature sorghum plants was gradually increased by increasing Si supply from 0 until 75 mg SiO_2 L^{-1}, and it became constant between 75 and 100 mg SiO_2 L^{-1} supply (**Figure 4.3A**). The difference confirmed that the treatment indeed modulated Si status of sorghum in mature stage. The findings in which the level of Si slightly affected plant growth and biomass accumulation from seedling stage were similarly found in mature plants of sorghum, however, the dry weight of Si75-plants was higher than that of Si0 plants (**Figure 4.3B-F**).

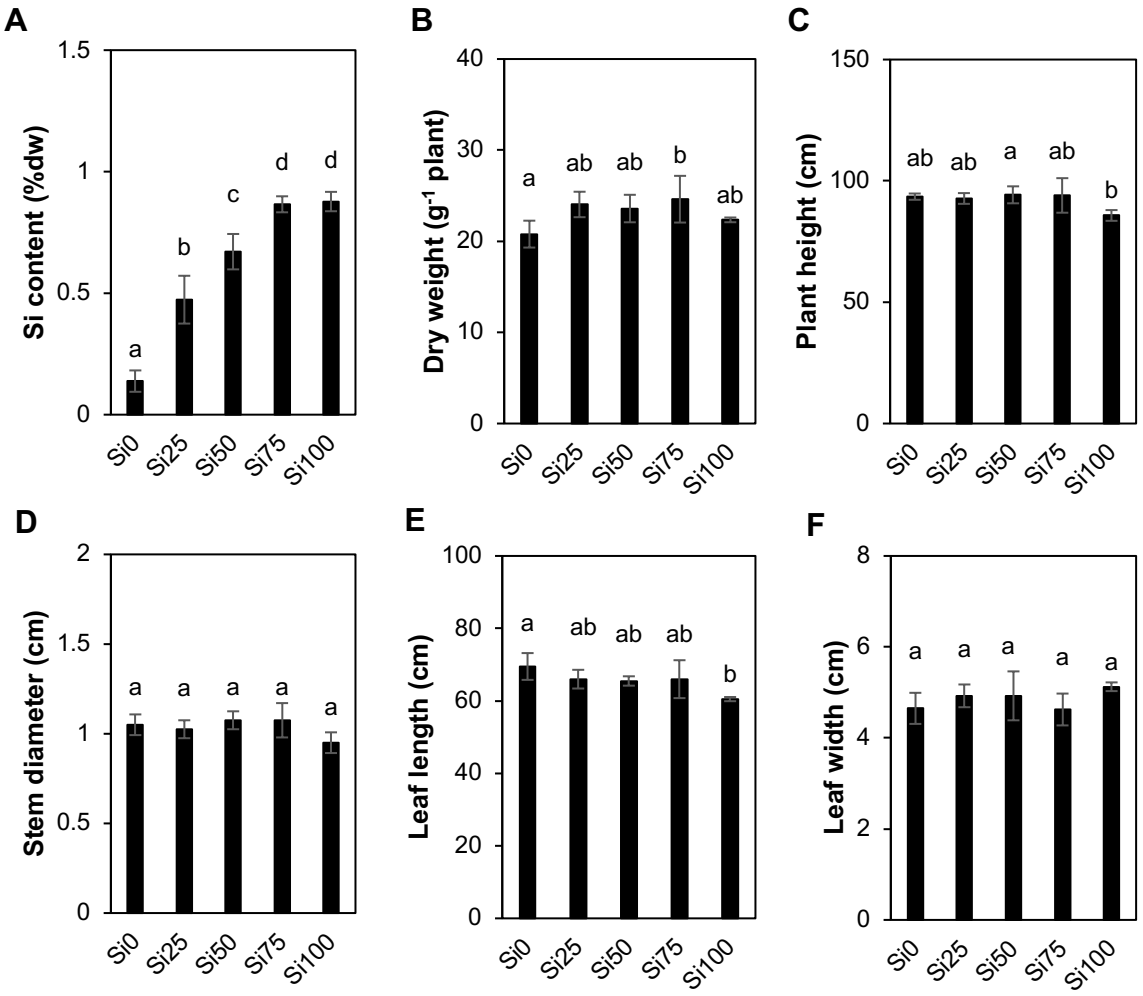

Figure 4.3. Effect of silicon (Si) application on growth of hydroponically grown mature sorghum plants at the heading stage (13-week-old) cultivated under high N supply. **(A)** Si content, **(B)** dry weight, **(C)** plant height, **(D)** stem diameter, **(E)** leaf length, and **(F)** leaf width of sorghum plants. Bars are means ± SD (n = 3 for A; n = 4 for B, C, D, E, and F). Different letters mean a significant difference (Tukey-Kramer test, $p < 0.05$).

In general, SPAD values, total N, and assimilated N contents were not obviously affected by Si application in mature sorghum plants, except in certain level of Si. Total and assimilated N of Si100-plants was higher than that of Si0 plants (**Figure 4.4A-C**). Consistent with the results in the seedling stage, the nitrate content was considerably reduced by applying 50 - 100 mg SiO_2 L^{-1} (**Figure 4.4D**). In addition, Si application increased K content in Si50- and Si100-plants but did not significantly alter the contents of other minerals, including, P, Ca, and Mg of mature sorghum plants under high-N supply (**Figure 4.5**). Taken together, these results suggest that Si has a beneficial effect to reduce nitrate content without affecting the biomass production of sorghum at both seedling and mature stage.

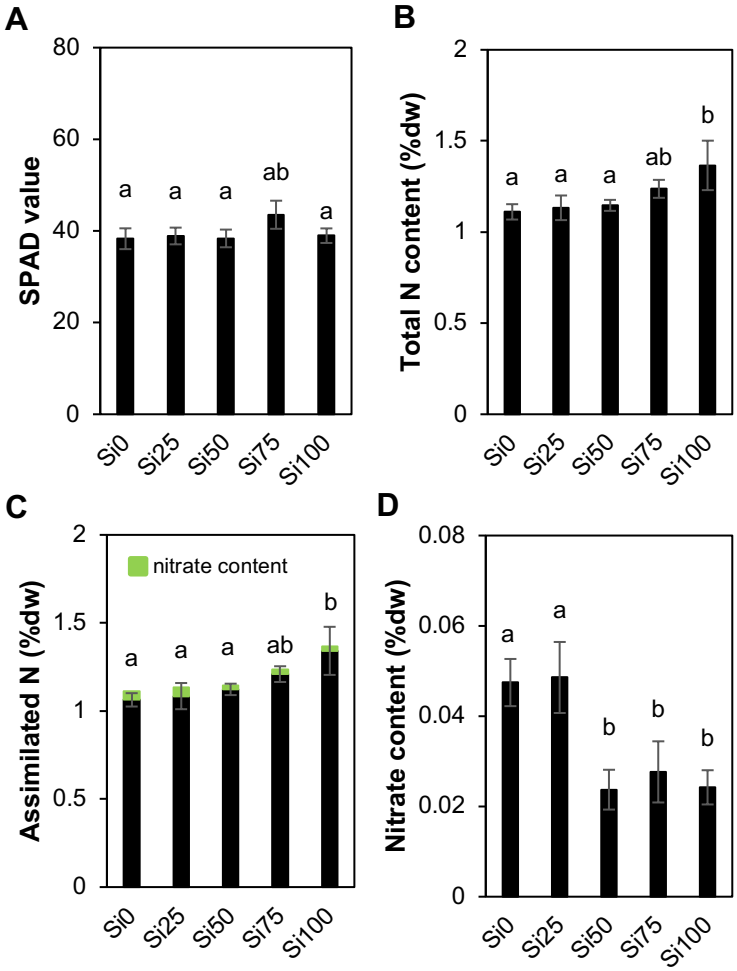

Figure 4.4. Effect of silicon (Si) application on nitrogen (N) status of hydroponically grown mature sorghum plants at the heading stage (13-week-old) cultivated under high N supply. **(A)** Soil-plant analysis development (SPAD) values, **(B)** total N content, **(C)** assimilated N, and **(D)** nitrate content of sorghum plants. Bars are means ± SD (n = 3). Different letters mean a significant difference (Tukey-Kramer test, $p < 0.05$).

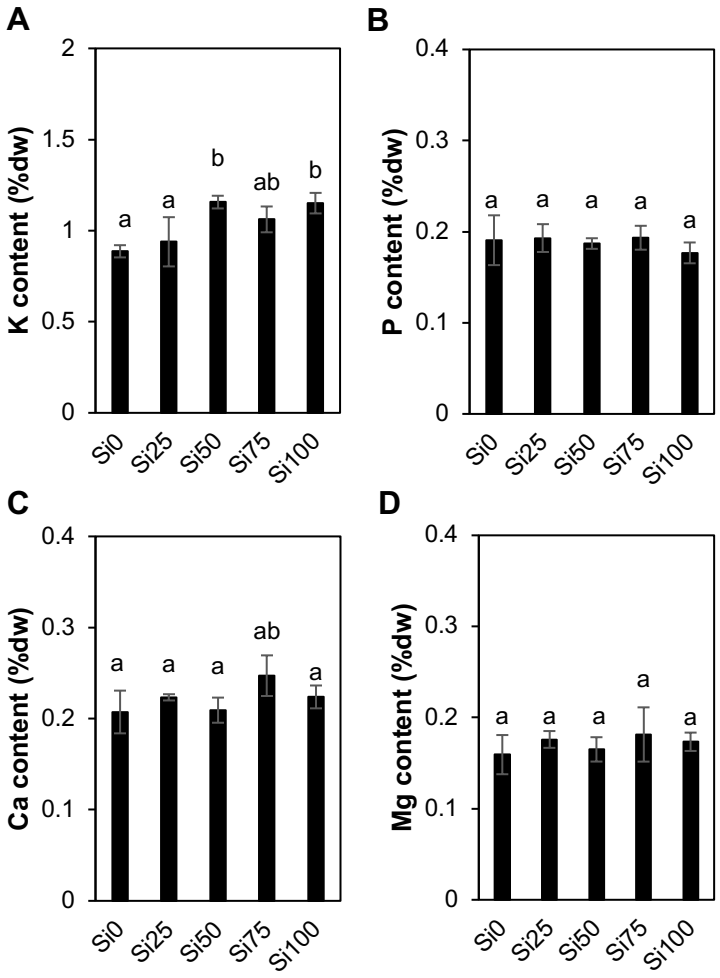

Figure 4.5. Effect of silicon (Si) application on mineral contents of hydroponically grown mature sorghum plants at the heading stage (13-week-old) cultivated under high N supply. **(A)** Potassium (K) content, **(B)** phosphorous (P) content, **(C)** calcium (Ca) content, and **(D)** magnesium (Mg) content of sorghum plants. Bars are means ± SD (n = 3). Different letters mean a significant difference (Tukey-Kramer test, $p < 0.05$).

4.3.3 Modulation of the expression of N metabolism related genes

In order to investigate how transcriptome were changed by the Si application, gene expression analysis was performed at the seedling stage. The transcriptomic analysis by RNA-sequencing followed by a gene ontology (GO) enrichment analysis of the DEGs under –Si and +Si condition is described in Chapter 3. The analysis revealed 50 or 69 biological processes overrepresented among the genes down- or up-regulated by Si application treatment, respectively, including the cellular N compound metabolic process (GO: 0034641). Within the

term, 85 or 80 genes were down- or up-regulated by Si application, then those exhibiting the $\log_2$ fold change ≥ 1 in expression either suppressed or induced by Si application were listed in **Table 4.2** or **Table 4.3**, respectively. The expression of gene encoding *nitrate reductase* (*NR*) was notably suppressed by Si application (**Table 4.2**). Additionally, the genes related to chlorophyll degradation activity including *red chlorophyll catabolite reductase* (*RCCR*) and *chlorophyllase 2* were suppressed by Si application (**Table 4.2**). In contrast, the expression of *glutamine synthase 2* (*GS2*), *ferredoxin-* and *NADH-dependent glutamate synthases* (*Fd-* and *NADH-GOGAT*) were induced by Si application (**Table 4.3**). A gene encoding *photosystem 1 subunit* G (*PS1G*), which related to photosynthesis was also found to be induced by Si application (**Table 4.3**). These results suggested a modulated expression of N metabolism and photosynthesis by Si application.

I also performed a reverse transcription-quantitative PCR (RT-qPCR) analysis to confirm the result from the RNA-sequencing analysis. As shown in **Figure 4.6**, the analysis confirmed the downregulated expression of *NR*, *RCCR*, and *chlorophyllase 2* under Si application treatment. The analysis also confirmed the upregulated expression of *PS1G* under Si application condition (**Figure 4.6**). A consistent tendency was observed in the expression of *Fd-* and *NADH-GOGAT* by applying Si treatment in the analysis, albeit with no statistical significance (**Figure 4.6**). Statistically significant change could not be seen with the expression of *GS2* (**Figure 4.6**). I also examined the expression of several genes that were suggested to be involved in N metabolism and chlorophyll degradation process in MOROKOSHI database (Makita et al. 2015). I found that the relative expression of *nitrate transporter 2.2* (*NRT2.2*), *nitrate transporter 2.5* (*NRT2.5*), *ammonium transporter 1.1* (*AMT1.1*), *nitrite reductase* (*NiR*), and *non yellow coloring1-like* (*NYC1-like*) were significantly suppressed by applying Si condition (**Figure 4.6**). A similar tendency of suppressed expression by Si application was observed with *nitrate transporter 1.1* (*NRT1.1*), *nitrate transporter 1.5* (*NRT1.5*), and *ammonium transporter 2* (*AMT2*) treatment, albeit with no statistical significance (**Figure 4.6**). In addition, I revealed that the relative expression of *chloride channel A* (*CLCa*), which is involved in vacuolar storage of nitrate, was induced by Si application (**Figure 4.6**).

Table 4.2. The suppressed expression of cellular nitrogen compound metabolic process related genes (GO: 0034641) in hydroponically grown sorghum seedlings in response to silicon (Si) application at three weeks after treatment. The log_2 values of the fold change (+Si/-Si) ≥ 1 are shown.

Gene ID	Functional annotation[a]	*p* value	*q* value	log_2 (fold change)
Sb04g034470	Nitrate reductase	1.E-14	0.E+00	-4.2
Sb01g009880	Glutamate decarboxylase	1.E-07	0.E+00	-2.5
Sb01g029900	Red chlorophyll catabolite reductase	9.E-06	0.E+00	-2.4
Sb01g041700	Glutamate decarboxylase	2.E-06	0.E+00	-2.3
Sb03g045940	Uridine 5-monophosphate synthase	5.E-09	0.E+00	-2.1
Sb03g036040	Homocysteine *S*-methyltransferase	2.E-07	0.E+00	-2.0
Sb05g017270	Red chlorophyll catabolite reductase	1.E-03	1.E-02	-2.0
Sb06g023110	Nicotinamidase 2	1.E-05	0.E+00	-2.0
Sb10g003510	Unknown	3.E-07	0.E+00	-2.0
Sb01g030270	Strictosidine synthase	1.E-07	0.E+00	-1.9
Sb03g026000	1-Aminocyclopropane-1-carboxylate oxidase	4.E-04	1.E-02	-1.9
Sb10g008320	Urea transmembrane transporters	5.E-06	0.E+00	-1.9
Sb02g012300	Chlorophyllase-2	2.E-03	2.E-02	-1.8
Sb02g025110	*S*-adenosylmethionine decarboxylase	1.E-07	0.E+00	-1.7
Sb02g036490	Alternative NAD(P)H dehydrogenase 1	5.E-03	3.E-02	-1.7
Sb03g039480	Triosephosphate isomerase	7.E-05	0.E+00	-1.7
Sb05g025240	Adenylyl-sulfate kinase	1.E-03	1.E-02	-1.7
Sb06g009610	NAD(P)-binding Rossmann-fold superfamily protein	3.E-03	2.E-02	-1.7
Sb08g022280	Cysteine synthase, *O*-acetylserine (thiol) lyase (OAS-TL)	4.E-13	0.E+00	-1.7
Sb01g000280	COP1-interacting protein	4.E-06	0.E+00	-1.6
Sb07g025080	6-phosphogluconolactonase, NagB/RpiA/CoA transferase-like	4.E-06	0.E+00	-1.6
Sb01g012960	5-Methyltetrahydropteroyltriglutamate-homocysteine methyltransferase	6.E-06	0.E+00	-1.5

Sb01g021240	Cationic amino acid transporter 2	5.E-04	1.E-02	-1.5
Sb03g009260	Cysteine synthase	2.E-11	0.E+00	-1.5
Sb05g021600	Aminotransferase	2.E-03	2.E-02	-1.5
Sb04g028610	Pyrimidine 1	5.E-06	0.E+00	-1.4
Sb02g003520	Tyrosine aminotransferase	1.E-03	1.E-02	-1.3
Sb02g029250	Ribulose-phosphate 3-epimerase	5.E-10	0.E+00	-1.3
Sb02g030830	Senescence-inducible chloroplast stay-green protein 1	2.E-03	2.E-02	-1.3
Sb04g026500	Adenosine kinase 2	4.E-12	0.E+00	-1.3
Sb09g027430	Threonine synthase	1.E-06	0.E+00	-1.3
Sb03g035480	Amino acid kinase	5.E-09	0.E+00	-1.2
Sb01g041240	Dihydrodipicolinate reductase	2.E-05	0.E+00	-1.1
Sb03g008050	Fructose-bisphospate aldolase isozyme	2.E-05	0.E+00	-1.1
Sb04g026510	Phenylalanine ammonia-lyase	2.E-03	2.E-02	-1.1
Sb06g033160	Allantoinase	9.E-03	5.E-02	-1.1
Sb01g046360	1,2-Dihydroxy-3-keto-5-methylthiopentene dioxygenase	1.E-04	0.E+00	-1.0
Sb01g046580	Aminotransferase	1.E-05	0.E+00	-1.0
Sb04g000580	Lactate/malate dehydrogenase	2.E-06	0.E+00	-1.0
Sb04g019020	Fructose-bisphospate aldolase isozyme	6.E-07	0.E+00	-1.0
Sb04g026940	Nitrilase 4	6.E-06	0.E+00	-1.0
Sb05g014880	Serine hydroxymethyltransferase	5.E-05	0.E+00	-1.0
Sb09g002470	Glutamate-cysteine ligase	3.E-03	3.E-02	-1.0

[a]According to the MOROKOSHI sorghum database.

Table 4.3. The induced expression of cellular nitrogen compound metabolic process related genes (GO: 0034641) in hydroponically grown sorghum seedlings in response to silicon (Si) application at three weeks after treatment. The $\log_2$ values of the fold change (+Si/-Si) ≥ 1 are shown.

Gene ID	Functional annotation[a]	*p* value	*q* value	$\log_2$ (fold change)
Sb08g016060	Ureide permease 2	9.E-06	0.E+00	2.3
Sb01g022730	Pyridoxal phosphate (PLP)-dependent transferase	6.E-04	1.E-02	2.1
Sb07g026100	ACT domain repeat 3	3.E-04	0.E+00	2.0
Sb02g031540	Phospholipase D delta	2.E-10	0.E+00	1.9
Sb01g042580	Homocysteine *S*-methyltransferase	8.E-07	0.E+00	1.8
Sb04g005360	Glutamine amidotransferase	2.E-03	2.E-02	1.8
Sb10g023850	Fructose-bisphospate aldolase isozyme	3.E-07	0.E+00	1.8
Sb04g035560	Trehalose-6-phosphate synthase	4.E-11	0.E+00	1.7
Sb03g035850	Polyphenol oxidase	3.E-03	2.E-02	1.6
Sb01g003540	Aromatic and neutral transporter 1	2.E-06	0.E+00	1.5
Sb01g044050	Serine acetyltransferase 2	8.E-05	0.E+00	1.5
Sb09g022310	Unknown	6.E-12	0.E+00	1.5
Sb02g033250	Pyridoxal-dependent decarboxylase	7.E-04	1.E-02	1.4
Sb06g030160	Shikimate/quinate 5-dehydrogenase	2.E-04	0.E+00	1.4
Sb10g020570	Spermidine synthase 3	3.E-09	0.E+00	1.4
Sb02g010470	Pyridoxal phosphate (PLP)-dependent transferase	2.E-04	0.E+00	1.3
Sb02g027900	Photosystem I subunit G	4.E-04	1.E-02	1.3
Sb03g003230	NADP-malic enzyme 4	1.E-08	0.E+00	1.3
Sb03g011270	Magnesium-protoporphyrin IX monomethyl ester cyclase	1.E-04	0.E+00	1.3
Sb03g031880	Threonine synthase	4.E-04	1.E-02	1.3
Sb03g035800	Pyridoxal phosphate (PLP)-dependent transferase	2.E-04	0.E+00	1.3
Sb06g031460	Glutamine synthetase 2 (GS2)	5.E-04	1.E-02	1.3
Sb09g022620	Riboflavin biosynthesis protein ribAB, GTP cyclohydrolase II	4.E-10	0.E+00	1.3

Sb01g004440	ACD1-like, pheophorbide a oxygenase	3.E-05	0.E+00	1.2
Sb01g010070	Histidine kinase	1.E-05	0.E+00	1.2
Sb03g041580	Amino acid permease 8, amino acid transporter	2.E-03	2.E-02	1.2
Sb06g032740	Magnesium-chelatase	1.E-04	0.E+00	1.2
Sb08g021000	Phytochrome interacting factor 4	9.E-05	0.E+00	1.2
Sb01g003860	ALBINA 1, magnesium-chelatase subunit chlD	1.E-05	0.E+00	1.1
Sb04g010210	Dynein light chain type 1, RHO guanyl-nucleotide exchange factor 11	2.E-04	0.E+00	1.1
Sb02g041740	Ferredoxin-dependent glutamate synthase (Fd-GOGAT)	2.E-05	0.E+00	1.0
Sb03g031310	NADH-dependent glutamate synthase 1 (NADH-GOGAT)	5.E-04	1.E-02	1.0
Sb03g033120	Serine acetyltransferase 1;1	6.E-04	1.E-02	1.0
Sb04g022140	Pyridoxal phosphate (PLP)-dependent transferase	2.E-08	0.E+00	1.0
Sb04g028050	Pyridine nucleotide-disulphide oxidoreductase	8.E-03	5.E-02	1.0
Sb08g003300	Enzyme binding;tetrapyrrole binding	7.E-04	1.E-02	1.0
Sb08g005210	Glycine cleavage system H protein	1.E-03	1.E-02	1.0
Sb09g025490	Cytochrome P450	5.E-03	3.E-02	1.0

[a]According to the MOROKOSHI sorghum database.

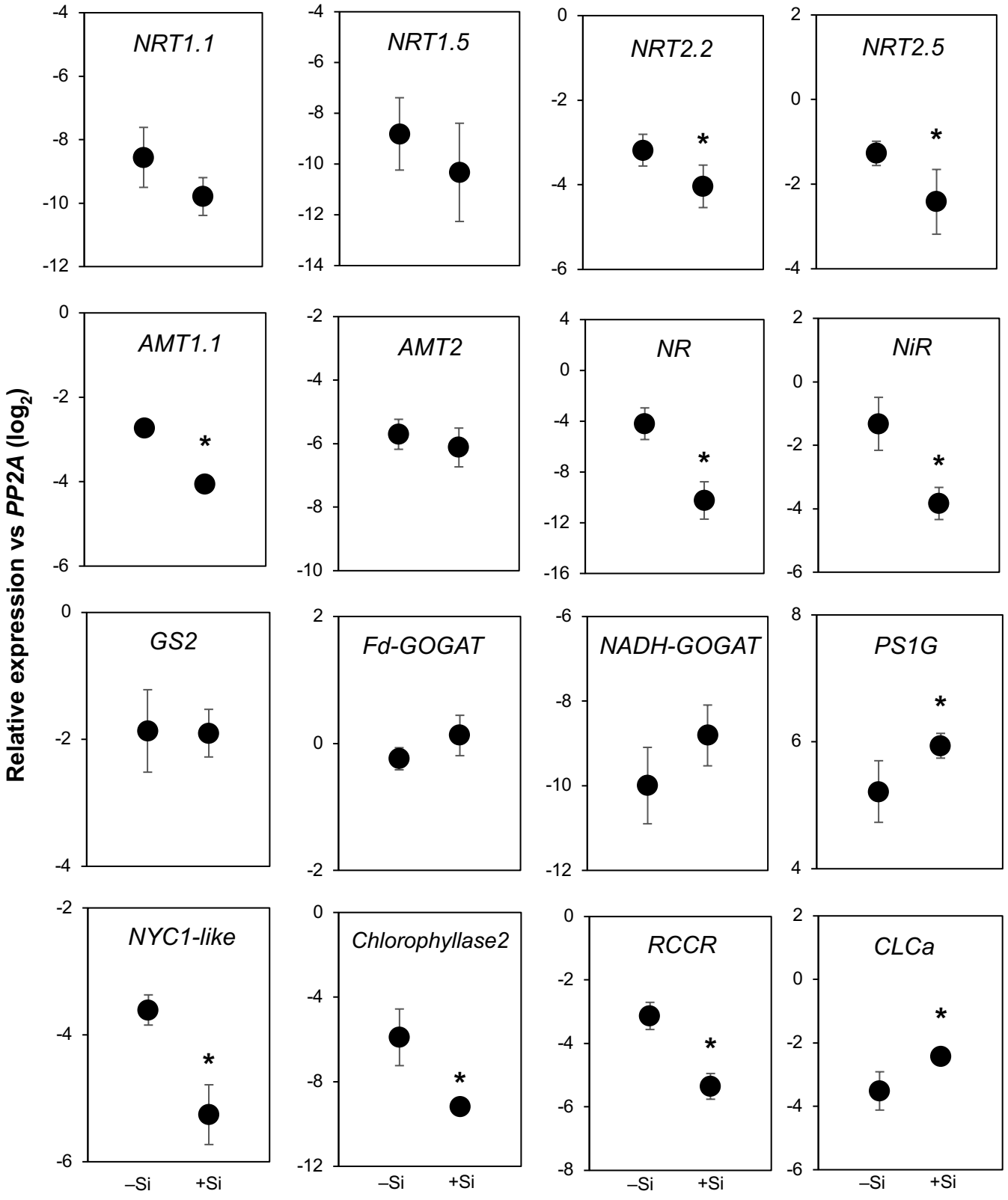

Figure 4.6. Reverse transcription-quantitative PCR analysis of the expression of nitrogen and photosynthesis metabolism related genes under Si application of hydroponically grown sorghum seedlings at 3 weeks after treatment. *NRT*: *nitrate transporter*, *AMT*: *ammonium transporter*, *NR*: *nitrate reductase*, *NiR*: *nitrite reductase*, *GS*: *glutamine synthase*, *Fd-* and *NADH-GOGAT*: *ferredoxin-* and *NADH-dependent glutamate synthases*, *CLCa*: *chloride channel A*, *PS1G*: *photosystem 1 subunit* G, *RCCR*: *red chlorophyll catabolite reductase*, *NYC1-like*: *non yellow coloring1-like*, and *PP2A*: *serine/threonine-protein phosphatase.* The expression of each gene was analyzed as transcript abundance relative to *PP2A* (XM_002453490). Values are given as mean ± SD (n = 3). Asterisks indicate significant differences between -Si and +Si plants. (Student's *t* test, $p < 0.05$).

4.3.4 Crude protein and *in vitro* digestibility of sorghum biomass

To consider the biomass utilization for animal fodder, the crude protein (CP) content and the *in vitro* digestibility rate of sorghum biomass under Si application were performed. The CP content was calculated from assimilated N content in dry weight basis (Jones 1941). In general, application of Si did not greatly affect the CP content of sorghum biomass both in seedling and mature stages, except for the increment of CP content in Si100-plants (**Figure 4.7A-B**). *In vitro* digestibility estimated as enzymatic saccharification performance did not significantly affect by Si application (**Figure 4.7C**). Also, the enzymatic saccharification efficiency, which was expressed as a relative proportion of the released glucose yield to total glucan (both crystalline and amorphous glucans), was not significantly changed by Si application condition (**Figure 4.7D**).

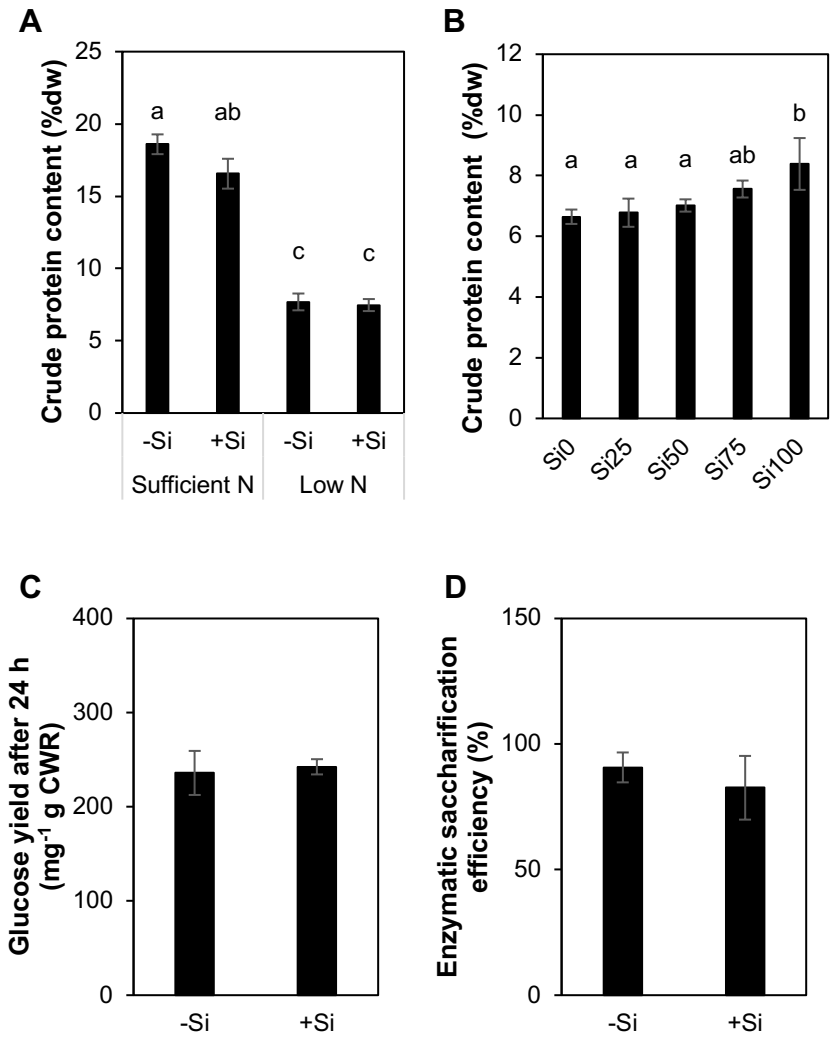

Figure 4.7. Effect of silicon (Si) application on biomass characteristics. **(A)** Crude protein content of hydroponically grown sorghum seedlings cultivated under sufficient or low nitrogen condition at 3 weeks after treatment, **(B)** crude protein content of hydroponically grown mature sorghum plants at heading stage (13-week-old) cultivated under high N supply, **(C)** enzymatic saccharification of cell walls after 24 h of enzymatic hydrolysis, and **(D)** the saccharification efficiency (glucose yield per total glucan) of hydroponically grown sorghum seedlings cultivated under -Si and +Si condition at 3 weeks after treatment. Bars are means ± SD (n = 6 for A; n = 3 for B, C, and D). Different letters mean a significant difference (Tukey-Kramer test, $p < 0.05$).

4.4 Discussion

In this chapter, I examined the impacts of Si application on the amount and quality of sorghum biomass as a fodder. First, I revealed that Si application did not significantly affect the growth and biomass accumulation of hydroponically grown sorghum plants both at seedling and mature stages under all N condition examined (**Figure 4.1**, **Figure 4.3**), which was

consistent with the previous results in Chapter 3. Positive effects of Si application on plant growth have been reported in multiple species such as rice (Ma et al., 1989), cucumber (Gou et al., 2020), tef (Ligaba-Osena et al., 2020), and maize (da Silva et al., 2021). On the other hand, the growth of soil-grown *Brachiaria brizantha*, a tropical forage grass, did not respond to Si application (de Melo et al., 2010). The response of growth to Si thus can be different among species.

Consistent with the unchanged biomass accumulation, in general, the Si treatment did not affect the level of assimilated N in plants, except for its increment in Si100-plants (**Figure 4.2C**, **Figure 4.4C**). On the other hand, nitrate content was considerably reduced in both sufficient-N seedling and high-N mature plant by Si application (**Figure 4.2D**, **Figure 4.4D**). The result suggests that Si application affected N uptake of sorghum plants. Several previous studies also suggested the interaction between Si and N in other species. The accumulation of N was negatively correlated with Si supply in rice (Wu et al., 2017). While, the increased N assimilation but decreased nitrate content was reported in cucumber by Si application under high-nitrate supply condition (Gou et al., 2020). Application of Si did not alter assimilated N but enhanced N use efficiency in winter wheat (Neu et al., 2017). In addition, the ammonium toxicity and/or deficiency was mitigated by Si supply in beet (Viciedo et al., 2019) and eucalyptus (de Souza et al., 2021). Taken together, the interaction between Si and N varies among the reports and depends on plant species, organ, developmental stage, and cultivation test condition.

Moreover, I propose a schematic model of the effect of Si on N metabolism in sorghum seedling under sufficient N condition as shown in **Figure 4.8**. First, the plant takes nitrate and ammonium up as inorganic N sources from the medium. Under +Si condition, N uptake as both nitrate and ammonium was likely to be decreased as suggested by the downregulated expression of nitrate and ammonium transporters, of both low- and high-affinity (**Figure 4.6**). Similar tendency was also found in rice, in which the expression level of nitrate and ammonium transporters was downregulated by Si application under high-N treatment (Wu et al., 2017). These findings suggest that, under +Si condition, plants sufficient with N then limit N uptake. The reduction of N uptake under Si application might be mediated by cytokinin signaling. Silicon is suggested to increase cytokinin biosynthesis as an indirect effect via a still unknown mechanism (Markovich et al., 2017). As Si presents in cell wall, one possible interaction between Si and cytokinin is in the apoplast where cytokinin and its catabolic enzymes actively occurred (Tameshige et al., 2015). In line with this notion, in this study, multiple genes annotated as cytokinin-related genes such as a sorghum putative *isopentenyltransferase 7*

(*SbIPT7*) (Markovich et al., 2017), *uridine diphosphate glycosyltransferases* (*UGTs*) and *cytokinin*-O-*glucosyltransferases* were modulated by Si application as shown in Chapter 3. Furthermore, the Si-induced cytokinin signaling alters N metabolism. Kiba et al. (2011) assumed that cytokinin synthesis is upregulated by N supply, and cytokinin thus synthesized downregulates the N uptake as a feedback to save the resources under sufficient N supply. Hence, the reduced nitrate content in this study might be due to a downregulated N uptake as the result of an enhanced cytokinin synthesis under Si-sufficient condition. However, other additional pathway would be involved in the transduction of Si effect before it modulates cytokinin metabolism. To get more insight into detail mechanism about this aspect, further study is needed in the near future.

Assimilation of N by plant needs the reduction of nitrate to nitrite, then nitrite to ammonium followed by ammonium assimilation into amino acid. Nitrate reduction into nitrite occurs in cytosol by NR activity. Meanwhile, nitrite reduction into ammonium is catalyzed by NiR activity in chloroplasts. In this study, the expression level of *NR* and *NiR* was downregulated by Si application (**Table 4.2**, **Figure 4.6**). It would be due to the reduction of nitrate uptake in +Si plants. In addition, I found that the expression level of *CLCa*, which is involved in nitrate transport from cytosol to vacuole (De Angeli et al., 2006), was upregulated under +Si condition (**Figure 4.6**). Although the transcripts of cytosolic NR and chloroplastic NiR were suggested to be declined under +Si condition, the N assimilation (**Figure 4.2C, Figure 4.4C**) and plant growth (**Figure 4.1, Figure 4.3**) were likely still maintained by elevating *GS/GOGAT* cycle as shown by the upregulated expression of *GS2* and *Fd*- and *NADH-GOGAT* which was suggested from RNA-sequencing analysis (**Table 4.3**), albeit no significant difference was observed in RT-qPCR analysis. Similar tendency of upregulation of *GS* and *GOGAT* expression under Si application has been reported in rice (Wu et al., 2017) and cucumber (Gou et al., 2020). These results suggest that +Si plants reduce nitrate uptake and accumulation without affecting the N assimilation and growth of hydroponically sorghum plants.

Under +Si condition, the photosynthesis process was well maintained by the plant as shown by upregulated expression of *PS1G* (**Table 4.2**, **Figure 4.6**) and the enrichment of GO terms associated with photosynthesis (GO: 0015979) in Chapter 3. The downregulated expression of some genes related to chlorophyll degradation activity, including *NYC1-like*, *chlorophyllase2* and *RCCR* in +Si plants suggests that the plants is under sufficient N status and the recycling of N compounds is not necessary in this condition (**Table 4.2**, **Figure 4.6**).

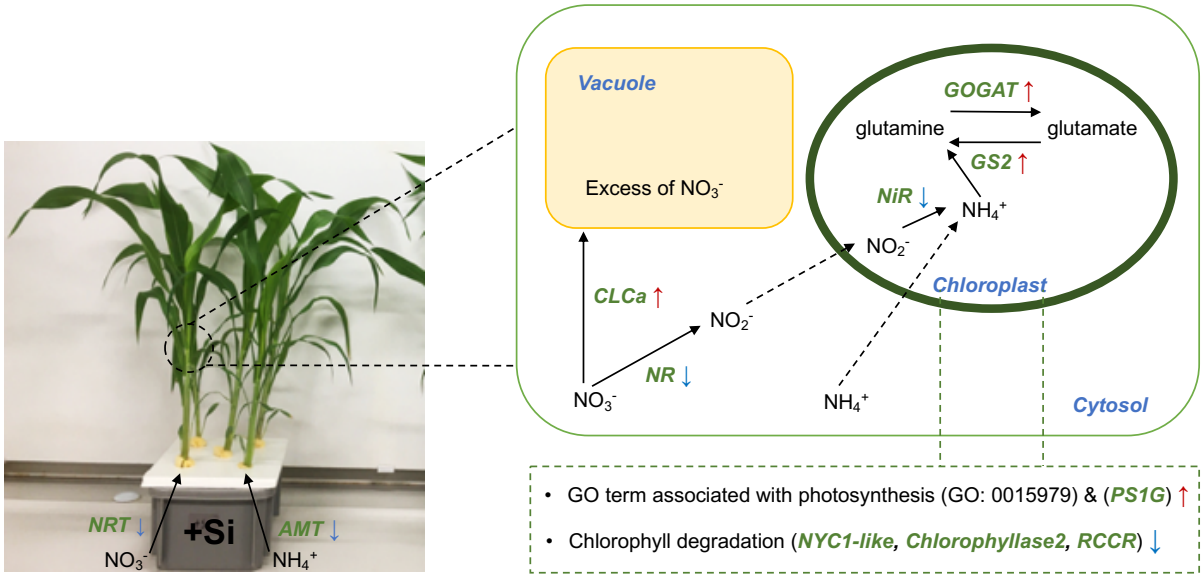

Figure 4.8. Schematic model of the effect of silicon (Si) application on nitrogen (N) metabolism of hydroponically grown sorghum seedlings at 3 weeks after treatment under sufficient N condition. *NRT*: *nitrate transporter*, *AMT*: *ammonium transporter*, *NR*: *nitrate reductase*, *NiR*: *nitrite reductase*, *GS*: *glutamine synthase*, *Fd-* and *NADH-GOGAT*: *ferredoxin-* and *NADH-dependent glutamate synthases*, *CLCa*: *chloride channel A*, *PS1G*: *photosystem 1 subunit* G, *RCCR*: *red chlorophyll catabolite reductase*, and *NYC1-like*: *non yellow coloring1-like*.

Silicon is known as essential element for normal animal growth and development (Carlisle, 1972). On the other hand, Si accumulated as silica can make the plant tissue stiffer, which may act as a feeding deterrant or increase recalcitrance against digestion. However, application of Si did not cause significant changes in feeding preference of sheep in several grass species (Massey et al., 2009). In addition, in this study, the crude protein content and *in vitro* digestibility rate of sorghum shoots were not significantly affected by Si application (**Figure 4.7**). Thus, maintaining sorghum under Si-sufficient condition can be a plausible way to minimize the accumulation of nitrate in the shoot without reducing its value as fodder. Since I performed this current experiment in hydroponic system which different with the real biomass production, further study with soil-grown plants is necessary. It is also needed to examine to what extent Si application can reduce the nitrate accumulation, taking the safety threshold of nitrate for livestock feeding into account.

Conclusions

Nitrogen often becomes a growth-limiting factor in crop production. Hence, to appropriately control the supply of N fertilizer in sorghum production, it would be significant to diagnose the N status of sorghum plants during their growth. In this study, biomarkers to diagnose the N nutrition status of sorghum were explored, and the leaf chlorophyll content measured as a soil plant analysis development (SPAD) value and the expression of low-N-responsive genes shown to respond to N status sensitively in hydroponically grown seedlings. The SPAD value is suggested to be useful under practical conditions as well, as it showed responses consistent with the applied N levels in multiple genotypes under field conditions.

In addition to biomass accumulation, the level of N supply also considerably affected the cell wall structure and composition of sorghum seedlings. Limitation of N led to a decrease in the S/G lignin unit ratio and an increase in the amount and alteration of tissue distribution of several hemicelluloses, including MLG and arabinoxylan. These cell wall alterations could affect the properties of biomass such as enzymatic saccharification performance. At least these cell wall alterations could be associated with changes in gene expression. Nitrogen status is thus one of the factors affecting the cell wall properties of sorghum seedlings.

The properties of sorghum cell walls were also altered by the level of Si supply. Limiting the Si supply significantly increased the thioglycolic acid lignin content and thioacidolysis-derived S/G lignin monomer ratio. At least part of the modification may be attributable to the change in gene expression, as suggested by the upregulation of phenylpropanoid biosynthesis-related genes under −Si conditions. The cell walls of the −Si plants had a higher mechanical strength and calorific value than those of the +Si plants. These results provide an insight into the enhancement of the value of sorghum biomass as a feedstock for energy production by limiting Si uptake.

Sorghum is also important as fodder crop. Content of nirate, which can be toxic to ruminants at high concentration, was found to be reduced by Si application in hydroponically grown sorghum plants both at seedling and mature stages. The reduction of nitrate content under Si-sufficient condition was due to a decreased nitrate uptake. The results suggest that maintaining sorghum under Si-sufficient condition can minimize the accumulation of nitrate in the shoot and therefore increase its value as fodder. Taken all together, I conclude that the value of sorghum as a biomass crop can evidentially be enhanced by managing nutrient supply.

References

Adams, C. B., Erickson, J. E., & Singh, M. P. (2015). Investigation and synthesis of sweet sorghum crop responses to nitrogen and potassium fertilization. *Field Crops Research*, *178*, 1–7. https://doi.org/10.1016/j.fcr.2015.03.014

Afgan, E., Baker, D., Batut, B., Van Den Beek, M., Bouvier, D., Ech, M., Chilton, J., Clements, D., Coraor, N., Grüning, B. A., Guerler, A., Hillman-Jackson, J., Hiltemann, S., Jalili, V., Rasche, H., Soranzo, N., Goecks, J., Taylor, J., Nekrutenko, A., & Blankenberg, D. (2018). The Galaxy platform for accessible, reproducible and collaborative biomedical analyses: 2018 update. *Nucleic Acids Research*, *46*, 537–544.

Agarwal, T., Grotewold, E., Doseff, A. I., & Gray, J. (2016). MYB31/MYB42 Syntelogs exhibit divergent regulation of phenylpropanoid genes in maize, sorghum and rice. *Scientific Reports*, *6*, 1–17. https://doi.org/10.1038/srep28502

Aglawe, S. B., Fakrudin, B., Patole, C .B., Bhairappanavar, S. B., Koti, R. V., & Krishnaraj, P. U. (2012). Quantitative RT-PCR analysis of 20 transcription factor genes of MADS, ARF, HAP2, MBF and HB families in moisture stressed shoot and root tissues of sorghum. *Physiology and Molecular Biology of Plants, 18*, 287–300.

Ali, N., Réthoré, E., Yvin, J. C., & Hosseini, S. A. (2020). The regulatory role of silicon in mitigating plant nutritional stresses. *Plants*, *9*(12), 1–18.

Arundale, R. A., Bauer, S., Haffner, F. B., Mitchell, V. D., Voigt, T. B., & Long, S. P. (2015). Environment has little effect on biomass biochemical composition of *Miscanthus* × *giganteus* across soil types, nitrogen fertilization, and times of harvest. *Bioenergy Research*, *8*(4), 1636–1646. https://doi.org/10.1007/s12155-015-9613-2

Barros, J., Escamilla-Trevino, L., Song, L., Rao, X., Serrani-Yarce, J. C., Palacios, M. D., Engle, N., Choudhury, F. K., Tschaplinski, T. J., Venables, B. J., Mittler, R., & Dixon, R. A. (2019). 4-Coumarate 3-hydroxylase in the lignin biosynthesis pathway is a cytosolic ascorbate peroxidase. *Nature Communications*, *10*(1), 1–11. https://doi.org/10.1038/s41467-019-10082-7

Barros, J., Serrani-Yarce, J. C., Chen, F., Baxter, D., Venables, B. J., & Dixon, R. A. (2016). Role of bifunctional ammonia-lyase in grass cell wall biosynthesis. *Nature Plants*, *2*(6), 16050. https://doi.org/10.1038/nplants.2016.50

Blumenkrantz, N., & Asboe-Hansen, G. (1973). New method for quantitative determination of uronic acids. *Analytical Biochemistry*, *54*(2), 484–489. https://doi.org/10.1016/0003-

2697(73)90377-1

Blümmel, M., Zerbini, E., Reddy, B. V. S., Hash, C. T., Bidinger, F., & Ravi, D. (2003). Improving the production and utilization of sorghum and pearl millet as livestock feed: Methodological problems and possible solutions. *Field Crops Research*, *84*(1–2), 123–142. https://doi.org/10.1016/S0378-4290(03)00145-X

Boerjan, W., Ralph, J., & Baucher, M. (2003). Lignin biosynthesis. *Annual Review of Plant Biology*, *54*, 519–546. https://doi.org/10.1146/annurev.arplant.54.031902.134938

Bout, S., & Vermerris, W. (2003). A candidate-gene approach to clone the sorghum *brown midrib* gene encoding caffeic acid *O*-methyltransferase. *Molecular Genetics and Genomics*, *269*(2), 205–214. https://doi.org/10.1007/s00438-003-0824-4

Bruning-Fann, C. S., & Kaneene, J. B. (1993). The effects of nitrate, nitrite, and N-nitroso compounds on animal health. *Veterinary and Human Toxicology*, *35*(3), 237–253. http://europepmc.org/abstract/MED/8351799

Buchelt, A. C., Teixeira, G. C. M., Oliveira, K. S., Rocha, A. M. S., de Mello Prado, R., & Caione, G. (2020). Silicon contribution via nutrient solution in forage plants to mitigate nitrogen, potassium, calcium, magnesium, and sulfur deficiency. *Journal of Soil Science and Plant Nutrition*, *20*(3), 1532–1548. https://doi.org/10.1007/s42729-020-00245-7

Camargo, E. L. O., Nascimento, L. C., Soler, M., Salazar, M. M., Lepikson-Neto, J., Marques, W. L., Alves, A., Teixeira, P. J. P. L., Mieczkowski, P., Carazzolle, M. F., Martinez, Y., Deckmann, A. C., Rodrigues, J. C., Grima-Pettenati, J., & Pereira, G. A. G. (2014). Contrasting nitrogen fertilization treatments impact xylem gene expression and secondary cell wall lignification in *Eucalyptus*. *BMC Plant Biology*, *14*(1), 1–9. https://doi.org/10.1186/s12870-014-0256-9

Carlisle, E. M. (1972). Silicon: an essential element for the chick. *Science*, *178*, 619 – 621. https://doi.org/10.1126/science.178.4061.619

Cesarino, I., Simões, M. S., dos Santos Brito, M., Fanelli, A., da Franca Silva, T., & Romanel, E. (2016). Building the wall: recent advances in understanding lignin metabolism in grasses. *Acta Physiologiae Plantarum*, *38*(11). https://doi.org/10.1007/s11738-016-2293-5

Chen, D., Cao, B., Wang, S., Liu, P., Deng, X., Yin, L., & Zhang, S. (2016). Silicon moderated the K deficiency by improving the plant-water status in sorghum. *Scientific Reports*, *6*, 1–14. https://doi.org/10.1038/srep22882

Cheng, M. H., Kadhum, H. J., Murthy, G. S., Dien, B. S., & Singh, V. (2020). High solids loading biorefinery for the production of cellulosic sugars from bioenergy sorghum.

Bioresource Technology, *318*, 124051. https://doi.org/10.1016/j.biortech.2020.124051

da Silva, E. S., de Mello Prado, R., Soares, A. de A. V. L., de Almeida, H. J., & dos Santos, D. M. M. (2021). Response of corn seedlings (*Zea mays* L.) to different concentrations of nitrogen in absence and presence of silicon. *Silicon*, *13*(3), 813–818. https://doi.org/10.1007/s12633-020-00480-8

Dahlberg, J. (2019). The role of sorghum in renewables and biofuels. *Methods in Molecular Biology*. *1931*, 269-277. https://doi.org/10.1007/978-1-4939-9039-9_19

De Angeli, A., Monachello, D., Ephritikhine, G., Frachisse, J. M., Thomine, S., Gambale, F., & Barbier-Brygoo, H. (2006). The nitrate/proton antiporter AtCLCa mediates nitrate accumulation in plant vacuoles. *Nature*, *442*, 939–942.

de Melo, S. P., Monteiro, F. A., & de Bona, F. D. (2010). Silicon distribution and accumulation in shoot tissue of the tropical forage grass *Brachiaria brizantha*. *Plant and Soil*, *336*(1), 241–249. https://doi.org/10.1007/s11104-010-0472-5

de Souza, J. P., de Mello Prado, R., de Morais, T. chagas B., Frazão, J. J., dos Santos Sarah, M. M., de Oliveira, K. R., & de Paula, R. C. (2021). Silicon fertigation and salicylic acid foliar spraying mitigate ammonium deficiency and toxicity in *Eucalyptus* spp. clonal seedlings. *PLoS ONE*, *16*, 1–11. https://doi.org/10.1371/journal.pone.0250436

Del Río, J. C., Rencoret, J., Gutiérrez, A., Elder, T., Kim, H., & Ralph, J. (2020). Lignin monomers from beyond the canonical monolignol biosynthetic pathway: another brick in the wall. *ACS Sustainable Chemistry and Engineering*, *8*(13), 4997–5012. https://doi.org/10.1021/acssuschemeng.0c01109

Demirbaş, A. (2001). Relationships between lignin contents and heating values of biomass. *Energy Conversion and Management*, *42*(2), 183–188.

Donaldson, L., Hague, J., & Snell, R. (2001). Lignin distribution in coppice poplar, linseed and wheat straw. *Holzforschung*, *55*(4), 379–385. https://doi.org/10.1515/HF.2001.063

Du, Y., Chu, H., Wang, M., Chu, I. K., & Lo, C. (2010). Identification of flavone phytoalexins and a pathogen-inducible flavone synthase II gene (*SbFNSII*) in sorghum. *Journal of Experimental Botany*, *61*(4), 983–994. https://doi.org/10.1093/jxb/erp364

Dumond, L., Lam, P. Y., van Erven, G., Kabel, M., Mounet, F., Grima-Pettenati, J., Tobimatsu, Y., & Hernandez-Raquet, G. (2021). Termite gut microbiota contribution to wheat straw delignification in anaerobic bioreactors. *ACS Sustainable Chemistry & Engineering*, *9*(5), 2191–2202. https://doi.org/10.1021/acssuschemeng.0c07817

Fernandes, J. C., García-Angulo, P., Goulao, L. F., Acebes, J. L., & Amâncio, S. (2013). Mineral stress affects the cell wall composition of grapevine (*Vitis vinifera* L.) callus.

Plant Science, *205–206*, 111–120. https://doi.org/10.1016/j.plantsci.2013.01.013

Ferreira, I. R., Santos, R. dos, Castro, R., Carneiro, A. de C. O., Castro, A. F., Santos, C. P. de S., Costa, S. E. de L., & Mairinck, K. (2019). Sorghum (*Sorghum bicolor*) pellet production and characterization. *Floresta e Ambiente*, *26*(3), 1–7. https://doi.org/10.1590/2179-8087.100117

Fornalé, S., Rencoret, J., Garcia-Calvo, L., Capellades, M., Encina, A., Santiago, R., Rigau, J., Gutiérrez, A., del Río, J. C., & Caparros-Ruiz, D. (2015). Cell wall modifications triggered by the down-regulation of *Coumarate 3-hydroxylase*-1 in maize. *Plant Science*, *236*, 272–282. https://doi.org/10.1016/j.plantsci.2015.04.007

Getachew, G., Putnam, D. H., De Ben, C. M., & De Peters, E. J. (2016). Potential of sorghum as an alternative to corn forage. *American Journal of Plant Sciences*, *7*, 1106–1121. https://doi.org/10.4236/ajps.2016.77106

Głazowska, S., Baldwin, L., Mravec, J., Bukh, C., Fangel, J. U., Willats, W. G., & Schjoerring, J. K. (2019). The source of inorganic nitrogen has distinct effects on cell wall composition in *Brachypodium distachyon*. *Journal of Experimental Botany*, *70*(21), 6461–6473. https://doi.org/10.1093/jxb/erz388

Głazowska, S., Baldwin, L., Mravec, J., Bukh, C., Hansen, T. H., Jensen, M. M., Fangel, J. U., Willats, W. G. T., Glasius, M., Felby, C., & Schjoerring, J. K. (2018). The impact of silicon on cell wall composition and enzymatic saccharification of *Brachypodium distachyon*. *Biotechnology for Biofuels*, *11*(1), 1–18. https://doi.org/10.1186/s13068-018-1166-0

Gleadow, R. M., Ottman, M. J., Kimball, B. A., Wall, G. W., Pinter Jr, P. J., LaMorte, R. L., & Leavitt, S. W. (2016). Drought-induced changes in nitrogen partitioning between cyanide and nitrate in leaves and stems of sorghum grown at elevated CO_2 are age-dependent. *Field Crops Research*, *185*, 97–102.

Global Bioenergy Statistics 2020 World Bioenergy Association. (2020). 3; 49. https://worldbioenergy.org/uploads/201210 WBA GBS 2020.pdf

Goto, M., Gordon, A. H., & Chesson, A. (1991). Changes in cell-wall composition and degradability of sorghum during growth and maturation. *Journal of the Science of Food and Agriculture*, *54*(1), 47–60. https://doi.org/10.1002/jsfa.2740540107

Gou, T., Yang, L., Hu, W., Chen, X., Zhu, Y., Guo, J., & Gong, H. (2020). Silicon improves the growth of cucumber under excess nitrate stress by enhancing nitrogen assimilation and chlorophyll synthesis. *Plant Physiology and Biochemistry*, *152*, 53–61.

https://doi.org/10.1016/j.plaphy.2020.04.031

Griggs, D., Stafford-Smith, M., Graffney, O., Rockstrom, J., Ohman, M.C., Shyamsunder, P., Steffen, W., Glaser, G., Kanie, N. and Noble, I. (2013). Sustainable developmnet goals for people and planet. *Nature*, *495*, 305–307.

Hatfield, R. D., Rancour, D. M., & Marita, J. M. (2017). Grass cell walls: a story of cross-linking. *Frontiers in Plant Science*, *7*. https://doi.org/10.3389/fpls.2016.02056

Hattori, T., Murakami, S., Mukai, M., Yamada, T., Hirochika, H., Ike, M., Tokuyasu, K., Suzuki, S., Sakamoto, M., & Umezawa, T. (2012). Rapid analysis of transgenic rice straw using near-infrared spectroscopy. *Plant Biotechnology*, *29*(4), 359–366. https://doi.org/10.5511/plantbiotechnology.12.0501a

Hayashi, T. (1989). Measuring β-glucan deposition in plant cell walls. In H.F. Linskens & J. F. Jackson (Eds.), *Plant Fibers* (pp. 138–160). Springer Berlin Heidelberg. https://doi.org/10.1007/978-3-642-83349-6_8

He, Y., Mouthier, T. M. B., Kabel, M. A., Dijkstra, J., Hendriks, W. H., Struik, P. C., & Cone, J. W. (2018). Lignin composition is more important than content for maize stem cell wall degradation. *Journal of the Science of Food and Agriculture*, *98*(1), 384–390. https://doi.org/10.1002/jsfa.8630

Hoch, G. (2007). Cell wall hemicelluloses as mobile carbon stores in non-reproductive plant tissues. *Functional Ecology*, *21*(5), 823–834. https://doi.org/10.1111/j.1365-2435.2007.01305.x

Hossain, M. T., Soga, K., Wakabayashi, K., Kamisaka, S., Fujii, S., Yamamoto, R., & Hoson, T. (2007). Modification of chemical properties of cell walls by silicon and its role in regulation of the cell wall extensibility in oat leaves. *Journal of Plant Physiology*, *164*(4), 385–393. https://doi.org/10.1016/j.jplph.2006.02.003

Jun, S. Y., Sattler, S. A., Cortez, G. S., Vermerris, W., Sattler, S. E., & Kang, C. H. (2018). Biochemical and structural analysis of substrate specificity of a phenylalanine ammonia-lyase. *Plant Physiology*, *176*(2), 1452–1468. https://doi.org/10.1104/pp.17.01608

Karlen, S. D., Free, H. C. A., Padmakshan, D., Smith, B. G., Ralph, J., & Harris, P. J. (2018). Commelinid monocotyledon lignins are acylated by *p*-coumarate. *Plant Physiology*, *177*(2), 513–521. https://doi.org/10.1104/pp.18.00298

Kiba, T., Kudo, T., Kojima, M., & Sakakibara, H. (2011). Hormonal control of nitrogen acquisition: roles of auxin, abscisic acid, and cytokinin. *Journal of Experimental Botany*, *62*(4), 1399–1409. https://doi.org/10.1093/jxb/erq410

Kim, D., Pertea, G., Trapnell, C., Pimentel, H., Kelley, R., & Salzberg, S. L. (2013). TopHat2:

accurate alignment of transcriptomes in the presence of insertions, deletions, and gene fusions. *Genome Biology*, *14*, 36. doi: https://doi.org/10.1186/gb-2013-14-4-r36

Kim, D., Langmead, B., & Salzberg, S. L. (2015). HISAT: A fast spliced aligner with low memory requirements. *Nature Methods*, *12*(4), 357–360.

Kim, H., Padmakshan, D., Li, Y., Rencoret, J., Hatfield, R. D., & Ralph, J. (2017). Characterization and elimination of undesirable protein residues in plant cell wall materials for enhancing lignin analysis by solution-state nuclear magnetic resonance spectroscopy. *Biomacromolecules*, *18*(12), 4184–4195.

Kim, H., & Ralph, J. (2010). Solution-state 2D NMR of ball-milled plant cell wall gels in DMSO-d_6/pyridine-d_5. *Organic & Biomolecular Chemistry*, *8*, 576–591.

Koshiba, T., Yamamoto, N., Tobimatsu, Y., Yamamura, M., Suzuki, S., Hattori, T., Mukai, M., Noda, S., Shibata, D., Sakamoto, M., & Umezawa, T. (2017). MYB-mediated upregulation of lignin biosynthesis in *Oryza sativa* towards biomass refinery. *Plant Biotechnology*, *34*(1), 7–15. https://doi.org/10.5511/plantbiotechnology.16.1201a

Kshirsagar, S. D., Bhalkar, B. N., Waghmare, P. R., Saratale, G. D., Saratale, R. G., & Govindwar, S. P. (2017). Sorghum husk biomass as a potential substrate for production of cellulolytic and xylanolytic enzymes by *Nocardiopsis* sp. KNU. *3 Biotech*, *7*(3), 1–10. https://doi.org/10.1007/s13205-017-0800-z

Lacey, J. A., Aston, J. E., & Thompson, V. S. (2018). Wear properties of ash minerals in biomass. *Frontiers in Energy Research*, *6*, 1–6. https://doi.org/10.3389/fenrg.2018.00119

Lam, P. Y., Lui, A. C. W., Wang, L., Liu, H., Umezawa, T., Tobimatsu, Y., & Lo, C. (2021). Tricin biosynthesis and bioengineering. *Frontiers in Plant Science*, *12*. https://doi.org/10.3389/fpls.2021.733198

Lam, P. Y., Lui, A. C. W., Yamamura, M., Wang, L., Takeda, Y., Suzuki, S., Liu, H., Zhu, F. Y., Chen, M. X., Zhang, J., Umezawa, T., Tobimatsu, Y., & Lo, C. (2019). Recruitment of specific flavonoid B-ring hydroxylases for two independent biosynthesis pathways of flavone-derived metabolites in grasses. *New Phytologist*, *223*(1), 204–219. https://doi.org/10.1111/nph.15795

Lam, P. Y., Tobimatsu, Y., Matsumoto, N., Suzuki, S., Lan, W., Takeda, Y., Yamamura, M., Sakamoto, M., Ralph, J., Lo, C., & Umezawa, T. (2019). *OsCAldOMT1* is a bifunctional *O*-methyltransferase involved in the biosynthesis of tricin-lignins in rice cell walls. *Scientific Reports*, *9*(1), 1–13. https://doi.org/10.1038/s41598-019-47957-0

Lam, P. Y., Tobimatsu, Y., Takeda, Y., Suzuki, S., Yamamura, M., Umezawa, T., & Lo, C. (2017). Disrupting flavone synthase II alters lignin and improves biomass digestibility.

Plant Physiology, *174*(2), 972–985. https://doi.org/10.1104/pp.16.01973

Lan, W., Lu, F., Regner, M., Zhu, Y., Rencoret, J., Ralph, S. A., Zakai, U. I., Morreel, K., Boerjan, W., & Ralph, J. (2015). Tricin, a flavonoid monomer in monocot lignification. *Plant Physiology*, *167*(4), 1284–1295. https://doi.org/10.1104/pp.114.253757

Lapierre, C., Monties, B., & Rolando, C. (1986). Preparative thioacidolysis of spruce lignin: isolation and identification of main monomeric products. *Holzforschung*, *40*, 47–50. https://doi.org/doi:10.1515/hfsg.1986.40.1.47.

Li, L., Popko, J. L., Umezawa, T., & Chiang, V. L. (2000). 5-Hydroxyconiferyl aldehyde modulates enzymatic methylation for syringyl monolignol formation, a new view of monolignol biosynthesis in angiosperms. *Journal of Biological Chemistry*, *275*(9), 6537–6545. https://doi.org/10.1074/jbc.275.9.6537

Li, Y., Tu, M., Feng, Y., Wang, W., & Messing, J. (2019). Common metabolic networks contribute to carbon sink strength of sorghum internodes: implications for bioenergy improvement. *Biotechnology for Biofuels*, *12*(1), 1–20. https://doi.org/10.1186/s13068-019-1612-7

Liao, Y., Smyth, G. K., & Shi, W. (2014). FeatureCounts: An efficient general purpose program for assigning sequence reads to genomic features. *Bioinformatics*, *30*(7), 923–930. https://doi.org/10.1093/bioinformatics/btt656

Ligaba-Osena, A., Guo, W., Choi, S. C., Limmer, M. A., Seyfferth, A. L., & Hankoua, B. B. (2020). Silicon enhances biomass and grain yield in an ancient crop tef [*Eragrostis tef* (Zucc.) Trotter]. *Frontiers in Plant Science*, *11*, 1–15.

Loh, F. C. W., Grabosky, J. C., & Bassuk, N. L. (2002). Using the SPAD-502 meter to assess chlorophyll and nitrogen content of benjamin fig and cottonwood leaves. *HortTechnology*, *12*(4), 682–686.

Love, M. I., Huber, W., & Anders, S. (2014). Moderated estimation of fold change and dispersion for RNA-seq data with DESeq2. *Genome Biology*, *15*(12), 1–21. https://doi.org/10.1186/s13059-014-0550-8

Ma, J. F., & Yamaji, N. (2008). Functions and transport of silicon in plants. *Cellular and Molecular Life Sciences*, *65*(19), 3049–3057. https://doi.org/10.1007/s00018-008-7580-x

Ma, J. F., Nishimura, K., & Takahashi, E. (1989). Effect of silicon on the growth of rice plant at different growth stages. *Soil Science and Plant Nutrition*, *35*(3), 347–356. https://doi.org/10.1080/00380768.1989.10434768

Ma, J. F., & Yamaji, N. (2006). Silicon uptake and accumulation in higher plants. *Trends in*

Plant Science, *11*(8), 392–397. https://doi.org/10.1016/j.tplants.2006.06.007

Majumdar, S., & Prakash, N. B. (2020). An overview on the potential of silicon in promoting defence against biotic and abiotic stresses in sugarcane. *Journal of Soil Science and Plant Nutrition*, *20*(4), 1969–1998. https://doi.org/10.1007/s42729-020-00269-z

Makino, A., & Osmond, B. (1991). Effects of nitrogen nutrition on nitrogen partitioning between chloroplasts and mitochondria in pea and wheat. *Plant Physiology*, *96*, 355–362. doi: https://doi.org/10.1104/pp.96.2.355

Makino, Y., & Ueno, O. (2018). Structural and physiological responses of the C4 grass *Sorghum bicolor* to nitrogen limitation. *Plant Production Science*, *21*(1), 39–50. https://doi.org/10.1080/1343943X.2018.1432290

Makita, Y., Shimada, S., Kawashima, M., Kondou-Kuriyama, T., Toyoda, T., & Matsui, M. (2015). MOROKOSHI: transcriptome database in *Sorghum bicolor*. *Plant and Cell Physiology*, *56*(1), e6. https://doi.org/10.1093/pcp/pcu187

Mansfield, S. D., Kim, H., Lu, F., & Ralph, J. (2012). Whole plant cell wall characterization using solution-state 2D NMR. *Nature Protocols*, *7*(9), 1579–1589. https://doi.org/10.1038/nprot.2012.064

Markovich, O., Kumar, S., Cohen, D., Addadi, S., Fridman, E., & Elbaum, R. (2019). Silicification in leaves of sorghum mutant with low silicon accumulation. *Silicon*, *11*(5), 2385–2391. https://doi.org/10.1007/s12633-015-9348-x

Markovich, O., Steiner, E., Kouřil, Š., Tarkowski, P., Aharoni, A., & Elbaum, R. (2017). Silicon promotes cytokinin biosynthesis and delays senescence in arabidopsis and sorghum. *Plant Cell and Environment*, *40*(7), 1189–1196.

Maranville, J. W., & Madhavan, S. (2002). Physiological adaptations for nitrogen use efficiency in sorghum. *Plant and Soil*, *245*, 25–34.

Massey, F. P., Massey, K., Roland Ennos, A., & Hartley, S. E. (2009). Impacts of silica-based defences in grasses on the feeding preferences of sheep. *Basic and Applied Ecology*, *10*(7), 622–630. https://doi.org/10.1016/j.baae.2009.04.004

Matsubara, K., Ochiai, K., & Matoh, T. (2016). Evaluation of the application of methane-fermentation waste fluid to paddy rice as basal nitrogen fertilizer *Japanese Journal of Soil Science and Plant Nutrition*, *87*, 110–119 [in Japanese].

Miyamoto, T., Takada, R., Tobimatsu, Y., Takeda, Y., Suzuki, S., Yamamura, M., Osakabe, K., Osakabe, Y., Sakamoto, M., & Umezawa, T. (2019). OsMYB108 loss-of-function enriches *p*-coumaroylated and tricin lignin units in rice cell walls. *Plant Journal*, *98*(6),

975–987. https://doi.org/10.1111/tpj.14290

Miyamoto, T., Tobimatsu, Y., & Umezawa, T. (2020). MYB-mediated regulation of lignin biosynthesis in grasses. *Current Plant Biology*, *24*, 100174. https://doi.org/10.1016/j.cpb.2020.100174

Morrison, A. J. (2007). Global demand projections for renewable energy resources. *2007 IEEE Canada Electrical Power Conference EPC 2007*, 537–542. https://doi.org/10.1109/EPC.2007.4520389

Moura, J. C. M. S., Bonine, C. A. V., de Oliveira Fernandes Viana, J., Dornelas, M. C., & Mazzafera, P. (2010). Abiotic and biotic stresses and changes in the lignin content and composition in plants. *Journal of Integrative Plant Biology*, *52*(4), 360–376. https://doi.org/10.1111/j.1744-7909.2010.00892.x

Naus, J., Prokopova, J., Rebicek, J., & Spundova, M. (2010). SPAD chlorophyll meter reading can be pronouncedly affected by chloroplast movement. *Photosynthesis Research*, 105, 265–271. doi: https://doi.org/10.1007/s11120-010-9587-z

Nazli, R. I., Tansi, V., Gulnaz, O., Kafkas, E., Kusvuran, A., Ozturk, H. H., & Budak, D. B. (2020). Interactive effects of nitrogen and humic substances applications on bioethanol production from sweet sorghum and combustion characteristics of its bagasse. *Agronomy*, *10*(9), 1–16. https://doi.org/10.3390/agronomy10091397

Nelson, D. R. (2009). The cytochrome P450 homepage. *Human Genomics*, *4*(1), 59–65. https://doi.org/10.1186/1479-7364-4-1-59

Neu, S., Schaller, J., & Dudel, E. G. (2017). Silicon availability modifies nutrient use efficiency and content, C:N:P stoichiometry, and productivity of winter wheat (*Triticum aestivum* L.). *Scientific Reports*, *7*, 3–10. https://doi.org/10.1038/srep40829

Parry, C., Blonquist Jr, J. M., & Bugbee, B. (2014). In situ measurement of leaf chlorophyll concentration: analysis of the optical/absolute relationship. *Plant, Cell and Environment 37*, 2508–2520. doi: https://doi.org/10.1111/pce.12324

Peng, F., Peng, P., Xu, F., & Sun, R. C. (2012). Fractional purification and bioconversion of hemicelluloses. *Biotechnology Advances*, *30*(4), 879–903. https://doi.org/10.1016/j.biotechadv.2012.01.018

Petrik, D. L., Karlen, S. D., Cass, C. L., Padmakshan, D., Lu, F., Liu, S., Le Bris, P., Antelme, S., Santoro, N., Wilkerson, C. G., Sibout, R., Lapierre, C., Ralph, J., & Sedbrook, J. C. (2014). *p*-Coumaroyl-CoA:monolignol transferase (PMT) acts specifically in the lignin biosynthetic pathway in *Brachypodium distachyon*. *Plant Journal*, *77*(5), 713–726.

https://doi.org/10.1111/tpj.12420

Pitre, F. E., Pollet, B., Lafarguette, F., Cooke, J. E. K., Mackay, J. J., & Lapierre, C. (2007). Effects of increased nitrogen supply on the lignification of poplar wood. *Journal of Agricultural and Food Chemistry*, *55*(25), 10306–10314. https://doi.org/10.1021/jf071611e

Pomar, F., Merino, F., & Barceló, A. R. (2002). *O*-4-linked coniferyl and sinapyl aldehydes in lignifying cell walls are the main targets of the Wiesner (phloroglucinol-HCl) reaction. *Protoplasma*, *220*(1–2), 17–28. https://doi.org/10.1007/s00709-002-0030-y

Poovaiah, C. R., Bewg, W. P., Lan, W., Ralph, J., & Coleman, H. D. (2016). Sugarcane transgenics expressing MYB transcription factors show improved glucose release. *Biotechnology for Biofuels*, *9*(1), 1–18. https://doi.org/10.1186/s13068-016-0559-1

Rai, K. M., Thu, S. W., Balasubramanian, V. K., Cobos, C. J., Disasa, T., & Mendu, V. (2016). Identification, characterization, and expression analysis of cell wall related genes in *Sorghum bicolor* (L.) Moench, a food, fodder, and biofuel crop. *Frontiers in Plant Science*, *7*, 1–19. https://doi.org/10.3389/fpls.2016.01287

Ralph, J. (2010). Hydroxycinnamates in lignification. *Phytochemistry Reviews*, *9*(1), 65–83. https://doi.org/10.1007/s11101-009-9141-9

Ralph, J., Lundquist, K., Brunow, G., Lu, F., Kim, H., Schatz, P. F., Marita, J. M., Hatfield, R. D., Ralph, S. A., Christensen, J. H., & Boerjan, W. (2004). Lignins: natural polymers from oxidative coupling of 4-hydroxyphenyl- propanoids. *Phytochemistry Reviews*, *3*(1), 29–60. https://doi.org/10.1023/B:PHYT.0000047809.65444.a4

Raun, W. R., & Johnson, GV. (1999). Review: Improving nitrogen use efficiency for cereal production. *Agronomy Journal*, *91*(3), 357–363. doi: https://doi.org/10.2134/agronj1999.00021962009100030001x

Reddy, N., & Yang, Y. (2015). Fibers from sorghum stems and leaves in. *Innovative Biofibers from Renewable Resources* (N. Reddy & Y. Yang (Eds.); pp. 11–12). Springer Berlin Heidelberg. https://doi.org/10.1007/978-3-662-45136-6_4

Reddy, S. P., Srinivas Reddy, D., Sivasakthi, K., Bhatnagar-Mathur, P., Vadez, V., & Sharma, K. K. (2016). Evaluation of sorghum [*Sorghum bicolor* (L.)] reference genes in various tissues and under abiotic stress conditions for quantitative real-time PCR data normalization. *Frontiers in Plant Science*, *7*, 1–14.

Roje, S. (2006). *S*-Adenosyl-*L*-methionine: beyond the universal methyl group donor. *Phytochemistry*, *67*(15), 1686–1698. https://doi.org/10.1016/j.phytochem.2006.04.019

Rooney, W. L., Blumenthal, J., Bean, B., & Mullet, J. E. (2007). Designing sorghum as a dedicated bioenergy feedstock. *Biofuels, Bioproducts and Biorefining*, *1*(2), 147–157. https://doi.org/https://doi.org/10.1002/bbb.15

Saballos, A., Sattler, S. E., Sanchez, E., Foster, T. P., Xin, Z., Kang, C., Pedersen, J. F., & Vermerris, W. (2012). *Brown midrib2* (*Bmr2*) encodes the major 4-coumarate:coenzyme A ligase involved in lignin biosynthesis in sorghum (*Sorghum bicolor* (L.) Moench). *Plant Journal*, *70*(5), 818–830. https://doi.org/10.1111/j.1365-313X.2012.04933.x

Saballos, A., Vermerris, W., Rivera, L., & Ejeta, G. (2008). Allelic association, chemical characterization and saccharification properties of *brown midrib* mutants of sorghum (*Sorghum bicolor* (L.) Moench). *BioEnergy Research*, *1*(3–4), 193–204. https://doi.org/10.1007/s12155-008-9025-7

Salvato, F., Wilson, R., Llerena, J. P. P., Kiyota, E., Reis, K. L., Boaretto, L. F., Balbuena, T. S., Azevado, R. A., Thelen, J. J., and Mazzafera, P. (2017). Luxurious nitrogen fertilization of two sugar cane genotypes contrasting for lignin composition causes changes in the stem proteome related to carbon, nitrogen, and oxidant metabolism but does not alter lignin content. *Journal of Proteome Research*, *16*, 3688–3703.

Schlüter, U., Mascher, M., Colmsee, C., Scholz, U., Bräutigam, A., Fahnenstich, H., & Sonnewald, U. (2012). Maize source leaf adaptation to nitrogen deficiency affects not only nitrogen and carbon metabolism but also control of phosphate homeostasis. *Plant Physiology*, *160*(3), 1384–1406. https://doi.org/10.1104/pp.112.204420

Scully, E. D., Gries, T., Funnell-Harris, D. L., Xin, Z., Kovacs, F. A., Vermerris, W., & Sattler, S. E. (2016). Characterization of novel *Brown midrib 6* mutations affecting lignin biosynthesis in sorghum. *Journal of Integrative Plant Biology*, *58*(2), 136–149. https://doi.org/10.1111/jipb.12375

Scully, E. D., Gries, T., Sarath, G., Palmer, N. A., Baird, L., Serapiglia, M. J., Dien, B. S., Boateng, A. A., Ge, Z., Funnell-Harris, D. L., Twigg, P., Clemente, T. E., & Sattler, S. E. (2016). Overexpression of *SbMyb60* impacts phenylpropanoid biosynthesis and alters secondary cell wall composition in *Sorghum bicolor*. *Plant Journal*, *85*(3), 378–395. https://doi.org/10.1111/tpj.13112

Sher, A., Hassan, F. U., Ali, H., Hussain, M., & Sattar, A. (2017). Enhancing forage quality through appropriate nitrogen dose, seed rate and harvest stage, in sorghum cultivars grown in Pakistan. *Grassland Science*, *63*(1), 15–22. https://doi.org/10.1111/grs.12137

Sidhu, P. K., Bedi, G. K., Mahajan, M. V., Sharma, S., Sandhu, K. S., & Gupta, M. P. (2011). Evaluation of factors contributing to excessive nitrate accumulation in fodder crops

leading to Ill-health in dairy animals. *Toxicology International*, *18*(1), 22–26. https://doi.org/10.4103/0971-6580.75848

Somegowda, V. K., Vemula, A., Naravula, J., Prasad, G., Rayaprolu, L., Rathore, A., Blümmel, M., & Deshpande, S. P. (2021). Evaluation of fodder yield and fodder quality in sorghum and its interaction with grain yield under different water availability regimes. *Current Plant Biology*, *25*, 100191. https://doi.org/10.1016/j.cpb.2020.100191

Soukup, M., Martinka, M., Bosnić, D., Čaplovičová, M., Elbaum, R., & Lux, A. (2017). Formation of silica aggregates in sorghum root endodermis is predetermined by cell wall architecture and development. *Annals of Botany*, *120*(5), 739–753. https://doi.org/10.1093/aob/mcx060

Soukup, M., Rodriguez Zancajo, V. M., Kneipp, J., & Elbaum, R. (2020). Formation of root silica aggregates in sorghum is an active process of the endodermis. *Journal of Experimental Botany*, *71*(21), 6807–6817. https://doi.org/10.1093/jxb/erz387

Sowiński, J., & Głąb, L. (2018). The effect of nitrogen fertilization management on yield and nitrate contents in sorghum biomass and bagasse. *Field Crops Research*, *227*, 132–143. https://doi.org/10.1016/j.fcr.2018.08.006

Stewart, J. J., Akiyama, T., Chapple, C., Ralph, J., & Mansfield, S. D. (2009). The effects on lignin structure of overexpression of ferulate 5-hydroxylase in hybrid poplar. *Plant Physiology*, *150*(2), 621–635. https://doi.org/10.1104/pp.109.137059

Sun, Q., Liu, X., Yang, J., Liu, W., Du, Q., Wang, H., Fu, C., & Li, W. X. (2018). MicroRNA528 affects lodging resistance of maize by regulating lignin biosynthesis under nitrogen-luxury conditions. *Molecular Plant*, *11*(6), 806–814. https://doi.org/10.1016/j.molp.2018.03.013

Susilowati, S. H., & Saliem, H. P. (2013). Sorghum trade in the World and Asian markets and its development prospect in Indonesia, *In* Sorghum: technology innovation and development (In Indonesian), Eds. Sumarno, Damardjati DS, Syam M, Hermanto, pp. 17–34. Agency for Agricultural Research and Development, Ministry of Agriculture, Republic of Indonesia.

Suzuki, S., Ma, J. F., Yamamoto, N., Hattori, T., Sakamoto, M., & Umezawa, T. (2012). Silicon deficiency promotes lignin accumulation in rice. *Plant Biotechnology*, *29*(4), 391–394. https://doi.org/10.5511/plantbiotechnology.12.0416a

Suzuki, S., Suzuki, Y., Yamamoto, N., Hattori, T., Sakamoto, M., & Umezawa, T. (2009). High-throughput determination of thioglycolic acid lignin from rice. *Plant Biotechnology*,

26(3), 337–340. https://doi.org/10.5511/plantbiotechnology.26.337

Sweet, D. P., Shapiro, R. H., & Albersheim, P. (1975). Quantitative analysis by various g.l.c. response-factor theories for partially methylated and partially ethylated alditol acetates. *Carbohydrate Research*, *40*(2), 217–225. https://doi.org/10.1016/S0008-6215(00)82604-X

Szydelko-Rabska, E., & Sowinski, J. (2014). Effect of nitrogen fertilization on the morphological traits of sweet sorghum cultivated on sandy soil. *Communications in Biometry and Crop Science*, *9*(2), 83–89.

Takeda, Y., Koshiba, T., Tobimatsu, Y., Suzuki, S., Murakami, S., Yamamura, M., Rahman, M. M., Takano, T., Hattori, T., Sakamoto, M., & Umezawa, T. (2017). Regulation of *CONIFERALDEHYDE 5- HYDROXYLASE* expression to modulate cell wall lignin structure in rice. *Planta*, *246*(2), 337–349. https://doi.org/10.1007/s00425-017-2692-x

Takeda, Y., Tobimatsu, Y., Karlen, S. D., Koshiba, T., Suzuki, S., Yamamura, M., Murakami, S., Mukai, M., Hattori, T., Osakabe, K., Ralph, J., Sakamoto, M., & Umezawa, T. (2018). Downregulation of p-*COUMAROYL ESTER 3-HYDROXYLASE* in rice leads to altered cell wall structures and improves biomass saccharification. *Plant Journal*, *95*(5), 796–811. https://doi.org/10.1111/tpj.13988

Takeda, Y., Tobimatsu, Y., Yamamura, M., Takano, T., Sakamoto, M., & Umezawa, T. (2019). Comparative evaluations of lignocellulose reactivity and usability in transgenic rice plants with altered lignin composition. *Journal of Wood Science*, *65*(1). https://doi.org/10.1186/s10086-019-1784-6

Tameshige, T., Hirakawa, Y., Torii, K. U., and Uchida, N. (2015). Cell walls as a stage for intercellular communication regulating shoot meristem development. *Frontiers in Plant Science*, *6*, 324.

Tang, C., Li, S., Li, M., & Xie, G. H. (2018). Bioethanol potential of energy sorghum grown on marginal and arable lands. *Frontiers in Plant Science*, *9*, 1–11. https://doi.org/10.3389/fpls.2018.00440

Tari, I., Laskay, G., Takács, Z., & Poór, P. (2013). Response of sorghum to abiotic stresses: a review. *Journal of Agronomy and Crop Science*, *199*(4), 264–274. https://doi.org/10.1111/jac.12017

Tarmadi, D., Tobimatsu, Y., Yamamura, M., Miyamoto, T., Miyagawa, Y., Umezawa, T., & Yoshimura, T. (2018). NMR studies on lignocellulose deconstructions in the digestive system of the lower termite *Coptotermes formosanus* Shiraki. *Scientific Reports*, *8*(1), 1–

9. https://doi.org/10.1038/s41598-018-19562-0

Teixeira, G. C. M., de Mello Prado, R., Oliveira, K. S., D'Amico-Damião, V., & da Silveira Sousa Junior, G. (2020). Silicon increases leaf chlorophyll content and iron nutritional efficiency and reduces iron deficiency in sorghum plants. *Journal of Soil Science and Plant Nutrition*, *20*(3), 1311–1320. https://doi.org/10.1007/s42729-020-00214-0

Tetreault, H. M., Gries, T., Palmer, N. A., Funnell-Harris, D. L., Sato, S., Ge, Z., Sarath, G., & Sattler, S. E. (2020). Overexpression of ferulate 5-hydroxylase increases syringyl units in *Sorghum bicolor*. *Plant Molecular Biology*, *103*(3), 269–285. https://doi.org/10.1007/s11103-020-00991-3

Thomas, L. H., Forsyth, V. T., Martel, A., Grillo, I., Altaner, C. M., & Jarvis, M. C. (2015). Diffraction evidence for the structure of cellulose microfibrils in bamboo, a model for grass and cereal celluloses. *BMC Plant Biology*, *15*(1), 1–7. https://doi.org/10.1186/s12870-015-0538-x

Tian, T., Liu, Y., Yan, H., You, Q., Yi, X., Du, Z., Xu, W., & Su, Z. (2017). AgriGO v2.0: a GO analysis toolkit for the agricultural community, 2017 update. *Nucleic Acids Research*, *45*, W122–W129. https://doi.org/10.1093/nar/gkx382

Timell, T. E. (1982). Recent progress in the chemistry and topochemistry of compression wood. *Wood Science and Technology*, *16*, 83–122.

Trapnell, C., Williams, B. A., Pertea, G., Mortazavi, A., Kwan, G., van Baren, M. J., Salzberg, S. L., Wold, B. J., & Pachter, L. (2010). Transcript assembly and quantification by RNA-Seq reveals unannotated transcripts and isoform switching during cell differentiation. *Nature Biotechnology, 28*, 511–515. doi: https://doi.org/10.1038/nbt.1621

Uchino, H., Watanabe, T., Ramu, K., Sahrawat, K. L., Marimuthu, S., Wani, S. P., & Ito, O. (2013). Calibrating chlorophyll meter (SPAD-502) reading by specific leaf area for estimating leaf nitrogen concentration in sweet sorghum. *Journal of Plant Nutrition* 36(10): 1640–1646. doi: https://doi.org/10.1080/01904167.2013.799190

Uddling, J., Gelang-Alfredsson, J., Piikki, K., & Pleijel, H. (2007). Evaluating the relationship between leaf chlorophyll concentration and SPAD-502 chlorophyll meter readings. *Photosynthesis Research*, *91*, 37–46. doi: https://doi.org/10.1007/s11120-006-9077-5

Umezawa T., Y. Tobimatsu, M. Yamamura, T. Miyamoto, Y. Takeda, T. Koshiba, R. Takada, P. Y. Lam, S. Suzuki, M. Sakamoto. (2020). lignin metabolic engineering in grasses for primary lignin valorization. *Lignin*, *1*, 30–41.

Umezawa, T. (2010). The cinnamate/monolignol pathway. *Phytochemistry Reviews*, *9*(1), 1–17. https://doi.org/10.1007/s11101-009-9155-3

Umezawa, T. (2018). Lignin modification in planta for valorization. *Phytochemistry Reviews*, *17*(6), 1305–1327. https://doi.org/10.1007/s11101-017-9545-x

Updegraff, D. M. (1969). Semimicro determination of cellulose inbiological materials. *Analytical Biochemistry*, *32*(3), 420–424. https://doi.org/10.1016/S0003-2697(69)80009-6

Vain, T., Crowell, E. F., Timpano, H., Biot, E., Desprez, T., Mansoori, N., Trindade, L. M., Pagant, S., Robert, S., Höfte, H., Gonneau, M., & Vernhettes, S. (2014). The cellulase KORRIGAN is part of the cellulose synthase complex. *Plant Physiology*, *165*(4), 1521–1532. https://doi.org/10.1104/pp.114.241216

Vicari, M., & Bazely, D. R. (1993). Do grasses fight back? The case for antiherbivore defences. *Trends in Ecology and Evolution*, *8*(4), 137–141. https://doi.org/10.1016/0169-5347(93)90026-L

Viciedo, D. O., de Mello Prado, R., Lizcano Toledo, R., dos Santos, L. C. N., Calero Hurtado, A., Nedd, L. L. T., & Castellanos Gonzalez, L. (2019). Silicon supplementation alleviates ammonium toxicity in sugar beet (*Beta vulgaris* L.). *Journal of Soil Science and Plant Nutrition*, *19*(2), 413–419. https://doi.org/10.1007/s42729-019-00043-w

Wahyuni, Y., Miyamoto, T., Hartati, H., Widjayantie, D., Windiastri, V. E., Sulistyowati, Y., Rachmat, A., Hartati, N. S., Ragamustari, S. K., Tobimatsu, Y., Nugroho, S., & Umezawa, T. (2019). Variation in lignocellulose characteristics of 30 Indonesian sorghum (*Sorghum bicolor*) accessions. *Industrial Crops and Products*, *142*, 111840. https://doi.org/10.1016/j.indcrop.2019.111840

Wang, D., Bean, S., McLaren, J., Seib, P., Madl, R., Tuinstra, M., Shi, Y., Lenz, M., Wu, X., & Zhao, R. (2008). Grain sorghum is a viable feedstock for ethanol production. *Journal of Industrial Microbiology and Biotechnology*, *35*(5), 313–320. https://doi.org/10.1007/s10295-008-0313-1

Wang, H., Sun, L., Glazebnik, S., & Zhao, K. (1995). Peralkylation of saccharides under aqueous conditions. *Tetrahedron Letters*, *36*(17), 2953–2956. https://doi.org/https://doi.org/10.1016/0040-4039(95)00446-J

Wiloso, E. I., Setiawan, A. A. R., Prasetia, H., Muryanto, Wiloso, A. R., Subyakto, Sudiana, I. M., Lestari, R., Nugroho, S., Hermawan, D., Fang, K., & Heijungs, R. (2020). Production of sorghum pellets for electricity generation in Indonesia: a life cycle assessment. *Biofuel Research Journal*, *7*(3), 1178–1194. https://doi.org/10.18331/BRJ2020.7.3.2

Withers, S., Lu, F., Kim, H., Zhu, Y., Ralph, J., & Wilkerson, C. G. (2012). Identification of grass-specific enzyme that acylates monolignols with *p*-coumarate. *Journal of Biological Chemistry*, *287*(11), 8347–8355. https://doi.org/10.1074/jbc.M111.284497

Worland, B., Robinson, N., Jordan, D., Schmidt, S., & Godwin, I. (2017). Post-anthesis nitrate uptake is critical to yield and grain protein content in *Sorghum bicolor*. *Journal of Plant Physiology*, *216*, 18–124. doi: https://doi.org/10.1016/j.jplph.2017.05.026

Wu, X., Yu, Y., Baerson, S. R., Song, Y., Liang, G., Ding, C., Niu, J., Pan, Z., & Zeng, R. (2017). Interactions between nitrogen and silicon in rice and their effects on resistance toward the brown planthopper *Nilaparvata lugens*. *Frontiers in Plant Science*, *8*, 1–11. https://doi.org/10.3389/fpls.2017.00028

Xiao, Y., Tholen, D., & Zhu, X. G. (2016). The influence of leaf anatomy on the internal light environment and photosynthetic electron transport rate: exploration with a new leaf ray tracing model. *Journal of Experimental Botany*, *67*(21), 6021–6035. doi: https://doi.org/10.1093/jxb/erw359

Xiong, D. L., Chen, J., Yu, T. T., Gao, W. L., Ling, X. X., Li, Y., Peng, S. B., & Huang, J. L. 2015. SPAD-based leaf nitrogen estimation is impacted by environmental factors and crop leaf characteristics. *Scientific Reports*, *5*, 13389 doi: https://doi.org/10.1038/srep13389

Xiong, Y., Zhang, P., Warner, R. D., & Fang, Z. (2019). Sorghum grain: from genotype, nutrition, and phenolic profile to its health benefits and food applications. *Comprehensive Reviews in Food Science and Food Safety*, *18*(6), 2025–2046.

Xu, D., Gao, T., Fang, X., Bu, H., Li, Q., Wang, X., & Zhang, R. (2020). Silicon addition improves plant productivity and soil nutrient availability without changing the grass:legume ratio response to N fertilization. *Scientific Reports*, *10*(1), 1–9. https://doi.org/10.1038/s41598-020-67333-7

Yamamoto, H., & Kojima, Y. (2002). Properties of cell wall constituents in relation to longitudinal elasticity of wood: Part 1. Formulation of the longitudinal elasticity of an isolated wood fiber. *Wood Science and Technology*, *36*(1), 55–74.

Yamamoto, T., Nakamura, A., Iwai, H., Ishii, T., Ma, J. F., Yokoyama, R., Nishitani, K., Satoh, S., & Furukawa, J. (2012). Effect of silicon deficiency on secondary cell wall synthesis in rice leaf. *Journal of Plant Research*, *125*(6), 771–779. https://doi.org/10.1007/s10265-012-0489-3

Yamamura, M., Hattori, T., Suzuki, S., Shibata, D., & Umezawa, T. (2012). Microscale

thioacidolysis method for the rapid analysis of *β-O*-4 substructures in lignin. *Plant Biotechnology*, *29*(4), 419–423. https://doi.org/10.5511/plantbiotechnology.12.0627a

Yamamura, M., Wada, S., Sakakibara, N., Nakatsubo, T., Suzuki, S., Hattori, T., Takeda, M., Sakurai, N., Suzuki, H., Shibata, D., & Umezawa, T. (2011). Occurrence of guaiacyl/*p*-hydroxyphenyl lignin in *Arabidopsis thaliana* T87 cells. *Plant Biotechnology*, *28*(1), 1–8. https://doi.org/10.5511/plantbiotechnology.10.0823c

Yang, X. S., Wu, J., Ziegler, T. E., Yang, X., Zayed, A, Rajani, M. S., Zhou, D., Basra, A. S., Schachtman, D. P., Peng, M., Amstrong, C. L., Caldo, R. A., Morrell, J. A., Lacy, M., & Staub, J. M. (2011). Gene expression biomarkers provide sensitive indicators of in planta nitrogen status in maize. *Plant Physiology*, *157*(4), 1841–1852. doi: https://doi.org/10.1104/pp.111.187898

Yang, H., Yang, J. P., Lv, Y., & He, J. J. (2014). SPAD values and nitrogen nutrition index for the evaluation of rice nitrogen status. *Plant Production Science*, *17*(1), 81–92. doi: https://doi.org/10.1626/pps.17.81

Yin, C.Y. (2011). Prediction of higher heating values of biomass from proximate and ultimate analyses. *Fuel*, *90*(3), 1128–1132.

Yuan, Z. F., Cao, Q., Zhang, K., Ata-Ul-Karim, S. T., Tian, Y. C., Zhu, Y., Cao, W. X., & Liu, X. J. 2016. Optimal leaf positions for SPAD meter measurement in rice. *Frontiers in Plant Science* 7: 719. doi: https://doi.org/10.3389/fpls.2016.00719

Yue, F., Lu, F., Sun, R. C., & Ralph, J. (2012). Syntheses of lignin-derived thioacidolysis monomers and their uses as quantitation standards. *Journal of Agricultural and Food Chemistry*, *60*(4), 922–928. https://doi.org/10.1021/jf204481x

Zexer, N., & Elbaum, R. (2020). Unique lignin modifications pattern the nucleation of silica in sorghum endodermis. *Journal of Experimental Botany*, *71*(21), 6818–6829.

Zhang, J., Zou, W., Li, Y., Feng, Y., Zhang, H., Wu, Z., Tu, Y., Wang, Y., Cai, X., & Peng, L. (2015). Silica distinctively affects cell wall features and lignocellulosic saccharification with large enhancement on biomass production in rice. *Plant Science*, *239*, 84–91.

Zhang, W., Wu, L., Ding, Y., Yao, X., Wu, X., Weng, F., Li, G., Liu, Z., Tang, S., Ding, C., & Wang, S. (2017). Nitrogen fertilizer application affects lodging resistance by altering secondary cell wall synthesis in japonica rice (*Oryza sativa*). *Journal of Plant Research*, *130* (5), 859–871.

Zhou, D., Zhou, X., Ling, Y., Zhang, Z., Su, Z. (2010). AgriGO: a GO analysis toolkit for the agricultural community. *Nucleic Acids Research* 38: 64-70.

Acknowledgements

The present thesis is based on the studies conducted at Laboratory of Plant Nutrition, Division of Applied Life Sciences, Graduate School of Agriculture, Kyoto University. This work was supported in part by the Science and Technology Research Partnership for Sustainable Development (SATREPS) project entitled "Producing biomass energy and material through revegetation of alang-alang (*Imperata cylindrica*) fields," which is supported by the Japan Science and Technology Agency and Japan International Cooperation Agency. I also acknowledge the Honjo International Scholarship Foundation for supporting my study at Kyoto University.

I would like to highly appreciate and fully acknowledge to my advisor Associate Prof. Masaru Kobayashi for his guidance and continuous support both in academic and daily lives. I am deeply grateful to Prof. Kentaro Ifuku and Assistant Prof. Kumiko Ochiai for their advice and encouragement. Thank you to all members of Laboratory of Plant Nutrition, Kyoto University for their help and friendship.

I sincerely admire to several colleagues (Prof. T. Umezawa, Associate Prof. Y. Tobimatsu, Dr. T. Miyamoto, and all members of Laboratory of Metabolic Sciences of Forest Plants and Microorganisms, Kyoto University; Assistant Prof. T. Awano, Associate Prof. A. Yoshinaga, Prof. J. Sugiyama, and all members of Laboratory of Tree Cell Biology, Kyoto University; Prof. Daisuke Shibata and Dr. Shigeru Hanano from Kazusa DNA Research Institute; Assist. Prof. K. Ohdoi & Mr. T. Iguchi from Laboratory of Agricultural Systems Engineering, Kyoto University; and the EARTHNOTE Co. Ltd.) for their nice help and cooperation.

A part of this study was conducted using the facilities in the DASH/FBAS at the Research Institute for Sustainable Humanosphere, Kyoto University, and the NMR spectrometer at the Joint Usage/Research Center at the Institute for Chemical Research, Kyoto University.

Finally, I would like to deliver the special acknowledgement to my beloved family and Indonesian friends (LIPI and PPI Kyoto-Shiga) for their love and unlimited support.

Kyoto, January 2022

Reza Ramdan Rivai

Publications

1. **Reza Ramdan Rivai**, Rie Takada, Takuji Miyamoto, Shigeru Hanano, Daisuke Shibata, Katsuaki Ohdoi, Masaru Kobayashi (2021) Examination of the usability of leaf chlorophyll content and gene expression analyses as nitrogen status biomarkers in *Sorghum bicolor*. *Journal of Plant Nutrition*, 44, 773-790.

2. **Reza Ramdan Rivai**, Takuji Miyamoto, Tatsuya Awano, Rie Takada, Yuki Tobimatsu, Toshiaki Umezawa, Masaru Kobayashi (2021) Nitrogen deficiency results in changes to cell wall composition of sorghum seedlings. *Scientific Reports*, 11, 23309.

3. **Reza Ramdan Rivai**, Takuji Miyamoto, Tatsuya Awano, Arata Yoshinaga, Shuoye Chen, Junji Sugiyama, Yuki Tobimatsu, Toshiaki Umezawa, Masaru Kobayashi: Limiting silicon supply alters lignin content and structures of sorghum seedling cell walls. *Plant Science*. (submitted)

4. **Reza Ramdan Rivai**, Masaru Kobayashi: The beneficial effect of silicon to reduce nitrate content in *Sorghum bicolor*. (in preparation)